EARTHQUAKE GROUND MOTION STUDY
IN THE VICINITY OF
THE SEQUOYAH NUCLEAR POWER PLANT

A Supplemental Report:

prepared for

TENNESSEE VALLEY AUTHORITY

in the context of

JUSTIFICATION OF THE SEISMIC DESIGN CRITERIA
USED FOR THE SEQUOYAH, WATTS BAR, AND
BELLEFONTE NUCLEAR POWER PLANTS

PHASE II

February 1979

Weston Geophysical
CORPORATION

TABLE OF CONTENTS

LIST OF TABLES

LIST OF FIGURES

RESPONSES OF SITES RELATIVE TO THE
MEAN AND MEAN PLUS 1 S.D. SPECTRA (Continued)

RESPONSES OF SITES RELATIVE TO THE
SEQ SITE RESPONSE

ABSTRACT

In the context of justification of the seismic design criteria used, particularly for the Sequoyah Nuclear Plant, an earthquake ground motion study was conducted using portable seismographic instruments at six competent rock sites located at and in the vicinity of the Sequoyah facility. Spectral analysis, in the frequency band of 0.3 to 7 Hz, of recordings from three regional and two distant earthquakes suggests a large variation in absolute site response. Typically, sites located on the Cumberland Plateau experienced the largest ground motion for all events. Amplification ratios of these sites to sites located in the adjacent Tennessee River Valley ranged from two to six over broad frequency bands, and in excess of an order of magnitude over narrow bands. The site occupied near the Sequoyah Nuclear Plant, typically responded very close or below the mean and well below the mean plus one standard deviation response.

PREFACE

At present, the computation of design response spectra for specific sites, proceeds from analysis of strong motion data that have been classified according to their site foundations. These several groups of data are described as being either "soft", "intermediate", or "hard" (Trifunac, 1976); or as sites founded on "rock", "stiff soils", "deep cohesionless soils", or "medium clays and sands" (Seed et al, 1976). Statistical analyses of these strong motion data indicate that large deviations in recorded ground motion still exist within groups of records taken from sites assumed to be similar. These large differences suggest strongly that some important effects influencing the seismic signal have not been accounted for by the types of classification presently used. These effects can be related either to the differences in source mechanism and travel paths, or most likely to individual site conditions, since it is well known that the local structure and the rock properties within the crustal column of each site affect the transmission of seismic waves.

An estimation of these local effects, in terms of relative ground motion amplification as a function of frequency, can only be done through on-site monitoring.

Such an estimation should be a prerequisite to the extrapolation of any empirical ground motion relations into regions devoid of strong motion recordings.

In an effort to characterize the observable local site response at the Sequoyah nuclear power plant site, relative to other rock sites in the immediate region, a six-element portable seismograph network was installed in eastern Tennessee during the summer of 1978.

Through this seismic monitoring at six sites including Sequoyah, the relative spectral response of the six sites to regional and teleseismic earthquake input, in the band-width of 0.3 to 7.0 Hz, was studied. The results of this investigation are presented in the following report entitled "Earthquake Ground Motion Study in Eastern Tennessee".

EARTHQUAKE GROUND MOTION STUDY
IN EASTERN TENNESSEE

INTRODUCTION

Within the framework of the present task objective, which is to demonstrate the adequacy of the seismic design spectra of three Tennessee Valley Authority (TVA) nuclear plants currently under review by the Nuclear Regulatory Commission (NRC) (i.e., Sequoyah, Watts Bar, and Bellefonte), a brief experimental study of the local crustal amplification in southeastern Tennessee was undertaken with a particular emphasis on the Sequoyah site.

The main purpose of the study was to obtain, in the short time available, experimental data which would permit an evaluation of the Sequoyah crustal response to various seismic inputs.

Seismic design spectra are usually based on statistical mean values of strong motion data. The inhomogeneity of the present intensity-acceleration data base results in large standard deviations which, for the sake of safety, are conservatively accepted in the final design. A first step to avoid undue and costly conservatism in structural design consists in sorting more carefully the various elements of a strong motion data set, either by defining more specifically the distance and magnitude ranges of data accepted in the set or by tightening the criteria for foundation similarity on the basis of geological and geophysical parameters (e.g., shear wave velocities). Such an effort has already been made in a previous study prepared by TVA. A second step consists in using experimental guidelines to specify the amount of conservatism needed. These guidelines can be obtained from experimental studies of local crustal responses, both at the site and at neighboring sites. By defining these local crustal responses and their relative differences, an insight on intensity distribution can be obtained, since intensity reports are certainly a function of the site responses.

The present experiment was devised to gather information on the crustal response of the Sequoyah site relative to some adjacent sites with the objective of establishing experimentally the qualitative and, if possible, quantitative response level of the Sequoyah site relative to others. Such information should define the need for using either the mean or the mean plus one standard deviation in the selection of the response spectrum.

THEORETICAL BACKGROUND

It is well known, since the early 1930's with the rise of seismographic instrumentation, that a seismic signal can be substantially affected by the crustal structure at a recording site. In Japan, Imamura (1929), Ishimoto (1931, 1932, 1934), and Takahasi and Hirano (1941) studied crustal effects, both theoretically and experimentally. Basically, they had noticed that certain events produced substantially different recordings at stations located relatively close and using similar instrumentation. In the United States, Gutenberg (1934, 1957) reported that certain stations appeared to have a "preferential frequency band". Eventually, numerous researchers (e.g., Nuttli and Whitmore (1961), Fernandez (1963), Nuttli (1964), Phinney (1964), Leblanc (1967), Hasegawa (1971), Kurita (1973), and many others), have shown the influence of the local crust on the amplitude levels of various phases. The resulting signal amplification (or attenuation) is a function of frequency. The crustal transfer function can be derived analytically with the Haskell matrix formulation using the density, longitudinal and shear wave velocities, and thickness of each crustal layer. It can also be observed directly (Leblanc, 1967; Leblanc and Howell, 1967) in the frequency domain through spectral analysis.

Schematically, a recorded seismogram obtained at a given site can be considered as the output of a series of filters into which an original seismic input is fed. In the time domain, the source function, b(t), and other influencing factors such as the azimuthal effects related to source mechanism, az(t), the attenuation, d(t), the crustal effects, h(t), and the instrumental response, s(t), can be considered in terms of filters:

$$\boxed{b(t)} \rightarrow \boxed{az(t)} \rightarrow \boxed{d(t)} \rightarrow \boxed{h(t)} \rightarrow \boxed{s(t)} = \boxed{r(t)} \qquad (1)$$

where r(t) is the recorded seismogram.

the excessive noise level resulting from construction activity, the Sequoyah site (SEQ) station was deployed in an abandoned quarry, 3 km from the power plant site, in the Ordovician Age Chicamauya L.S., which stratigraphically overlies the Cambrian Age Conasauga group rocks of the power plant foundation.

The Watts Bar (WAT) site station was selected in a roadcut located 1.5 km from the plant, in the Cambrian Age Rome formation, which stratigraphically underlies the Cambrian Age Conasauga group foundation rocks at the power plant site. The concern for vandalism influenced the selection of a site within the fenced-in area of the plant. Sparcity of outcrops further limited the quality of the site. The WAT site was located on a vertical bed of sandy siltstone, 3 to 4 feet thick, included in a sequence of weathered shales and thinly-bedded siltstone. The poor quality of the rock site and its close proximity to construction activity resulted in a very low signal-to-noise ratio. The noise level was so high that most of the WAT recordings could not be used in the study.

The remaining four seismic stations were deployed to sample competent rock sites, both on the Cumberland Plateau and along the Tennessee River Valley. It should be remembered that the Huckleberry (HUC, HUK) and Grandview (GNV) stations are both located west of the Cumberland escarpment at approximately the same elevation (500 M) in Pennsylvanian age sandstone formations. The Cleveland (CLE) and Sweetwater (SWT) stations are both located in the Tennessee River Valley, also at similar elevation (270 M), in Ordovician age limestones.

Table 1 lists the names, codes, coordinates, elevations, and geologic formation names and ages of the six sites occupied during the ground motion experimental study. The site locations and distances between sites are shown in Figure 1.

EVENTS SELECTED FOR GROUND MOTION STUDY

During the 56-day study period, approximately 25 events originating from sources at regional and teleseismic distances, were recorded by the portable network. Of these, three regional events located in the central and south-central United States with m_{bLg} magnitudes of 2.6, 3.8, and 3.9, were retained for analysis. Two teleseisms, both with m_b magnitudes of 5.7, one located in Venezuela, the other off the coast of Nicaragua, were also used in the study. Table 2 lists the parameters of these events, while Figures A-1 through A-5 in Appendix A illustrate their time histories as recorded by the six-station network.

By using both regional and distant events, a broader spectrum of excitation pulses are considered. The Lg phase of regional events tends to favor higher frequencies, while the P phase of distant earthquakes is richer in lower frequencies.

DATA PROCESSING

All recordings of the five events listed in Table 2 were photographically enlarged by a factor of 3 to 5. The enlarged photocopies were then manually digitized using a sampling rate varying between 30 and 50 counts per second depending on the scale of the enlarged copies. For some events, two independent digitizations of the same records by two analysts were made and compared to evaluate any digitizing error. By comparing a plot of the digitized records with the recorded time histories, spurious points were identified and corrected. A final visual check of all digitized time histories was made to confirm their equivalence in time and amplitude to the recorded seismograms.

Once the recorded seismograms were digitized, the following steps were followed to obtain the relative spectral responses from the time series.

First, a correction was made to remove the effect of curvature always present on visual recorders obtained with a pivoting pen. The corrected traces are shown in Appendix B, while the original curved traces are presented in Appendix A. It should be noted that the time series of the uncurved traces have varying time increments. A new time series with regular time increments was obtained before proceeding with the Fourier analysis.

Secondly, the Fourier Amplitude Spectrum was determined for each curvature-corrected trace, using a rectangular-shaped time window of approximately 15 seconds for the P phase.

of the two teleseism, and of approximately 14, 17, and 20 seconds for the Lg phase of the three regional events.

In a third step, the calculated amplitude spectra were corrected for the displacement sensitivity of the seismograph systems. The magnification curve used in this correction is shown in Figure 2. After this stage of processing, the computed amplitude spectra correspond to true ground displacement over the frequency band of 0.3 to 7.0 Hz. All of the spectra for the five selected events are shown in Appendix B, along with the corresponding uncurved time histories.

The next step was to correct the spectra of the three regional events for the effects of attenuation. Distances to the earthquake epicenters were calculated and the spectra were corrected for the combined effects of geometrical spreading and anelastic attenuation, using the shortest epicentral distance as a datum. This correction was made by assuming that the Lg-phase amplitudes obey the relationship:

$$A \simeq \Delta^{-1/3}(\sin \Delta)^{-1/2}\exp(-\gamma\Delta) \qquad (5)$$

(Ewing et al, 1957)

where

A is the ground amplitude

Δ the epicentral distance in degree

γ the coefficient of anelastic attenuation

Values of the coefficients of anelastic attenuation (γ) of Lg waves, used in this correction, were linearly interpolated from the values of 0.0006 km^{-1} at 1 Hz and 0.006 km^{-1} at 10 Hz, observed by Nuttli (1978).

After these corrections for instrumental response and for attenuation were made, and assuming that the azimuthal effect is small, less than 10° for all events, the remaining spectra were considered to be site dependent, according to Equation 4. The final phase of the processing was to determine the relative responses of each site.

This was accomplished first by determining the mean of all site response spectra and the mean plus one standard deviation site response spectra for all five events. Secondly, the responses of each site relative to these statistically-determined spectra were calculated. Finally, the responses of each site relative to the SEQ site response were determined.

Figure 3 shows the flow diagram of the entire procedure used in analyzing the data.

It should be kept in mind that velocity and acceleration spectra would only enhance the displacement spectra by a factor of ω and ω^2, without changing the overall characteristics of the crustal response.

RESULTS

To facilitate the comparison of the site responses, the spectral data calculated for the five events were displayed in three ways. The first method was to plot the SEQ site spectra versus the mean and the mean plus one S.D. spectra, calculated from the responses of five sites for four events, and from all six sites for the teleseism of May 30. Figures 4 through 8 show these plots. From these figures, it can be seen that the variations in site responses are more pronounced for the regional events of May 23, June 1, and June 9 than for the teleseisms of May 30 and July 11. (Note: the mean spectra are plotted as disconnected squares; the mean plus one S.D. spectra are plotted as disconnected plus signs; the SEQ spectra are in solid lines.) It is also clear from these figures that the SEQ spectra have fewer peaks above the mean spectra than below, and very seldom reach or peak over the mean plus one S.D. spectra; this is true for the three regional events and for the teleseism of July 11. For the teleseism of May 30, the SEQ spectrum shows points equally distributed below and above the mean; it also has some points above the mean plus one S.D. spectrum. It should be noted, however, that for this event, all of the sites had an approximately equivalent response as shown by the small scatter in the data plotted in Figure 6.

The second method used to display the data shows the relative responses of all of the sites plotted as a percentage of the mean spectra and also of the mean plus one S.D. spectra. Figures 9 through 20 illustrate these relative responses of the sites. For the sake of clarity, the SEQ site response is displayed twice in each figure: once with the CLE and SWT stations; and once with the HUC and GNV stations (and with the WAT station for the event of May 30). The traces in these figures, except for Figures 17 and 18, were smoothed before display with a 3-point digital filter, (¼, ½, ¼) to enhance the major features.

Figures 17 and 18 show the unsmoothed versions of the two previous figures (15 and 16); by comparison of these four figures, the effects of filtering can be assessed. Several observations can be drawn from this second series of plots (Figures 9 through 20). First, in terms of site responses relative to the mean and the mean plus one standard deviation responses, two stations located in the valley, SWT and CLE have, in general, the lowest (and best) responses for all events. The SEQ site, also in the valley, tends to be slightly higher than CLE and SWT, as in Figures 11, 12, 13, 14, 15, 16, 17, and 18, although it compares favorably with CLE in Figures 9, 10, 19, and 20. In Figures 9 and 10, 13 and 14, 15 and 16, and 18 and 19, SEQ remains, in general, below the mean and the mean plus one standard deviation, with only occasional and narrow peaks above, and never in excess of 30 percent.

The stations located on the ridge, HUK and GNV, show relative responses that are considerably higher than the SEQ responses. HUK has the highest responses of all, over most of the entire frequency band. Thus, this second series of plots demonstrates that SEQ has a better crustal response than stations on the ridge, and compares well with stations in the valley.

The third series of figures (21, 22, and 23) display the responses of other sites as a percent of the SEQ site response for the three regional events. Some of the conclusions already made are once again emphasized by these figures; namely, the low relative response of the SWT and CLE sites and the high relative response of the GNV and HUC sites. Futhermore, these figures show that the SWT and CLE sites do not underlie the SEQ response by more than 100 percent, and that the HUC and GNV sites, and in some instances the CLE site, generally exceed the SEQ response by a factor of 2 to 6, and over some narrow frequency bands, exceed it by more than one order of magnitude.

In these three figures where positive and negative ordinates represent positive and negative signal ratios at various stations with respect to SEQ, the predominance of positive responses demonstrates clearly that the SEQ site response compares very favorably with the responses of other sites in southeastern Tennessee.

CONCLUSIONS

The preceeding analysis illustrates a large range of variations in the site response of six competent rock sites located in a small area of southeastern Tennessee to regional and distant seismic inputs. Over some narrow frequency bands, the variations in crustal response can exceed one order of magnitude, and over broad bands, some sites can respond higher by factors ranging from 2 to 6. This variation in crustal response of rock sites, coupled with the additional ground motion amplification of an overlying soil layer, can account for the large scatter of reported intensities within a restricted epicentral region. Typically, in eastern United States, earthquakes are often characterized by the highest intensity reported, regardless of the fact that this intensity may be reported in only one or few instances and that a lower intensity level clearly prevailed in the epicentral region.

When such a characterization is applied to the design earthquake used in safety analysis, a large amount of conservatism is imposed. All sites are assumed to have a high crustal amplification equivalent to the maximum intensity of the design earthquake, when experimental data show that, for many sites in the immediate vicinity, such a high intensity value should not be generalized. Based on the results of the preceeding section, namely the low response of the SEQ, CLE, SWT sites relative to that of the nearby sites on the Cumberland Plateau (i.e., HUC and GNV), it becomes obvious that applying the same rigid safety guidelines to all sites would be overly conservative in the case of the lower responding sites. It is, therefore, recommended that, as a reasonable relaxation, the 84 percentile site specific response spectrum, developed by the TVA, based on a suite of United States, West Coast, and Italian strong motion records, need not be applied in the case of the SEQ site. The application of the mean design spectrum appears to be more realistic and fully adequate for the relatively quiet SEQ site.

TABLE 1

EASTERN TENNESSEE GROUND MOTION STUDY NETWORK

STATION	CODE	LATITUDE N.	LONGITUDE W.	ELEVATION M.	GEOLOGIC FORMATION	AGE
CLEVELAND	CLE	$35^{\circ}09.94'$	$84^{\circ}46.75'$	262	Mosheim L.S.	Ord.
GRANDVIEW	GNV	$35^{\circ}49.365'$	$84^{\circ}50.081'$	494	Crossville S.S.	Penn.
HUCKLEBERRY	HUC	$35^{\circ}16.277'$	$85^{\circ}12.169'$	518	Vandever S.S.	Penn.
	HUK	$35^{\circ}16.272'$	$85^{\circ}12.193'$	520		
SEQUOYAH	SEQ	$35^{\circ}14.964'$	$85^{\circ}05.793'$	210	Chickamauga L.S.	Ord.
SWEETWATER	SWT	$35^{\circ}37.354'$	$84^{\circ}20.165'$	280	Newala L.S.	Ord.
WATTS BAR	WAT	$35^{\circ}36.449'$	$84^{\circ}48.226'$	238	Rome Fm.	Camb.

TABLE 2

EVENTS USED IN THE GROUND MOTION STUDY

DATE 1978	ORIGIN TIME HR:MM:SEC(EDT)	LATITUDE N.	LONGITUDE W.	MAGNTIDUE M_{bLg}	M_b	REMARKS
REGIONAL EVENTS						
23 MAY	06:16:01.8	37°16.7'	87°25.3'	2.6		W. Kentucky[1]
01 JUNE	22:07:09.0	38°17.8'	88°41.8'	3.9		S. Illinois[1]
09 JUNE	19:14:58.1	31°58.6'	88°39.7'	3.8		S. Miss.-Ala. Border[1]
TELESEISMIC EVENTS						
30 MAY	21:12:	12°42.6'	87°38.4'		5.7	Nicaragua Coast[2]
11 JULY	08:24	9°46.8'(S.)	70°32.4'		5.7	Venezuela[2]

---

[1] Locations determined using Ground Motion Network Data, Standard errors in Lat. 6.6' to 8.2'; Standard errors in Long. 7.5' to 11.0'.

[2] Location by U.S.G.S. using WWSSN data.

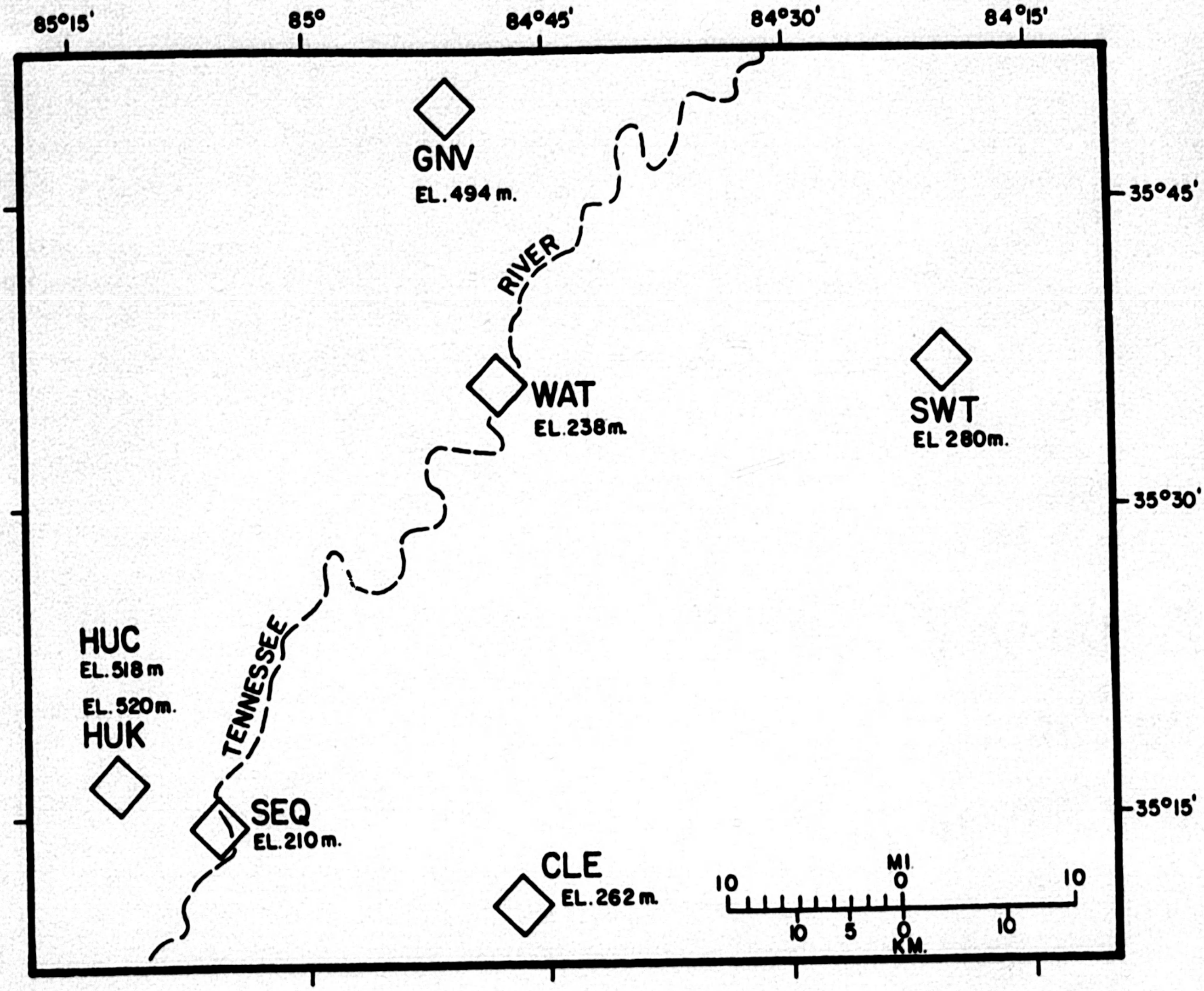

DISTANCES BETWEEN STATIONS (K M.)

	SEQ	HUC	CLE	WAT	GNV	SWT
SEQ	—					
HUC	9.9	—				
CLE	30.4	40.3	—			
WAT	47.8	52.0	49.1	—		
GNV	67.9	69.7	73.1	24.1	—	
SWT	80.5	87.8	64.7	42.4	50.3	

Figure 1

Weston Geophysical

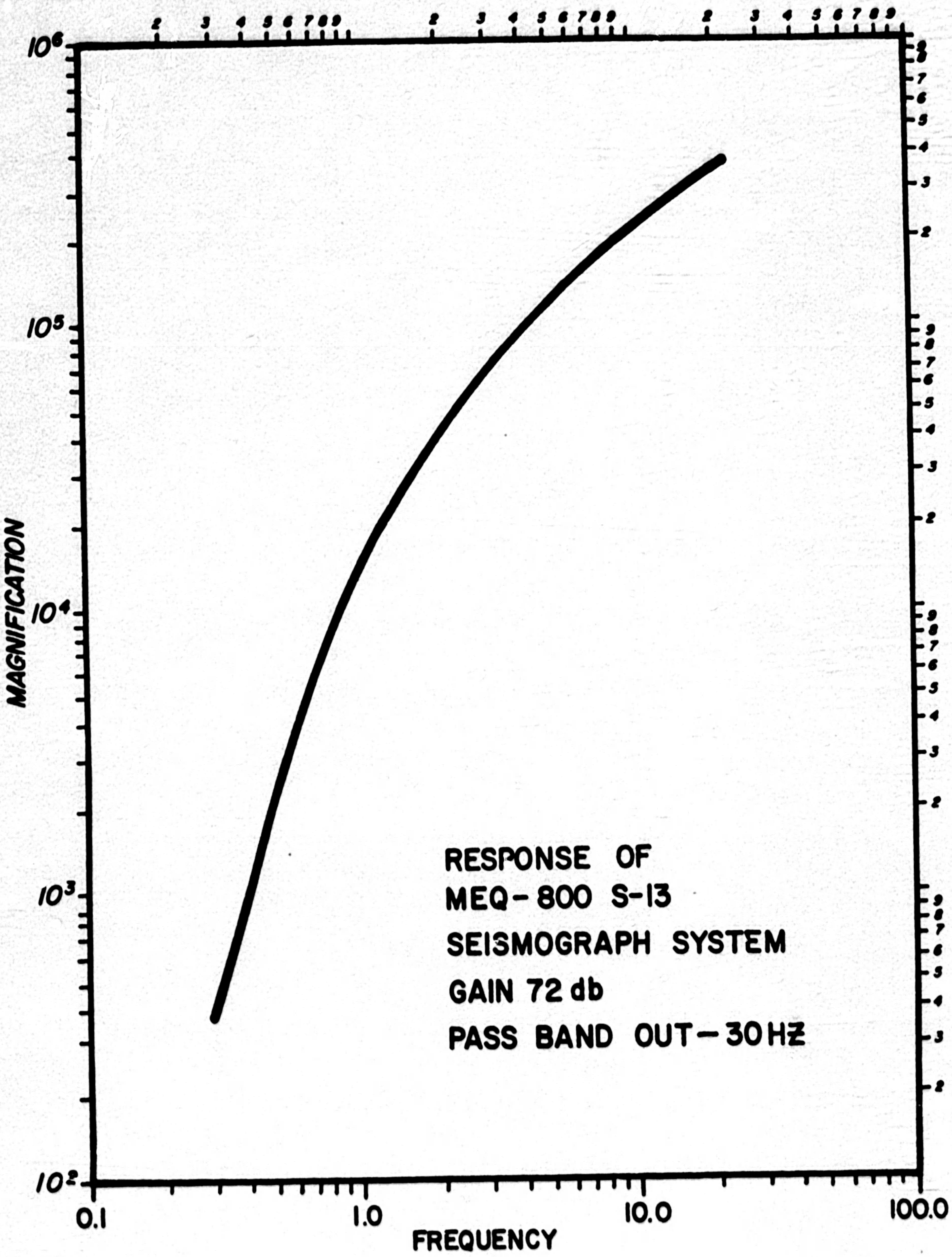

10⁶
10⁵
10⁴
10³
10²
MAGNIFICATION
0.1
1.0
10.0
100.0
FREQUENCY
RESPONSE OF
MEQ- 800 S-13
SEISMOGRAPH SYSTEM
GAIN 72 db
PASS BAND OUT-30 HZ

Figure 2

EASTERN TENNESSEE GROUND MOTION STUDY

DATA PROCESSING FLOW DIAGRAM

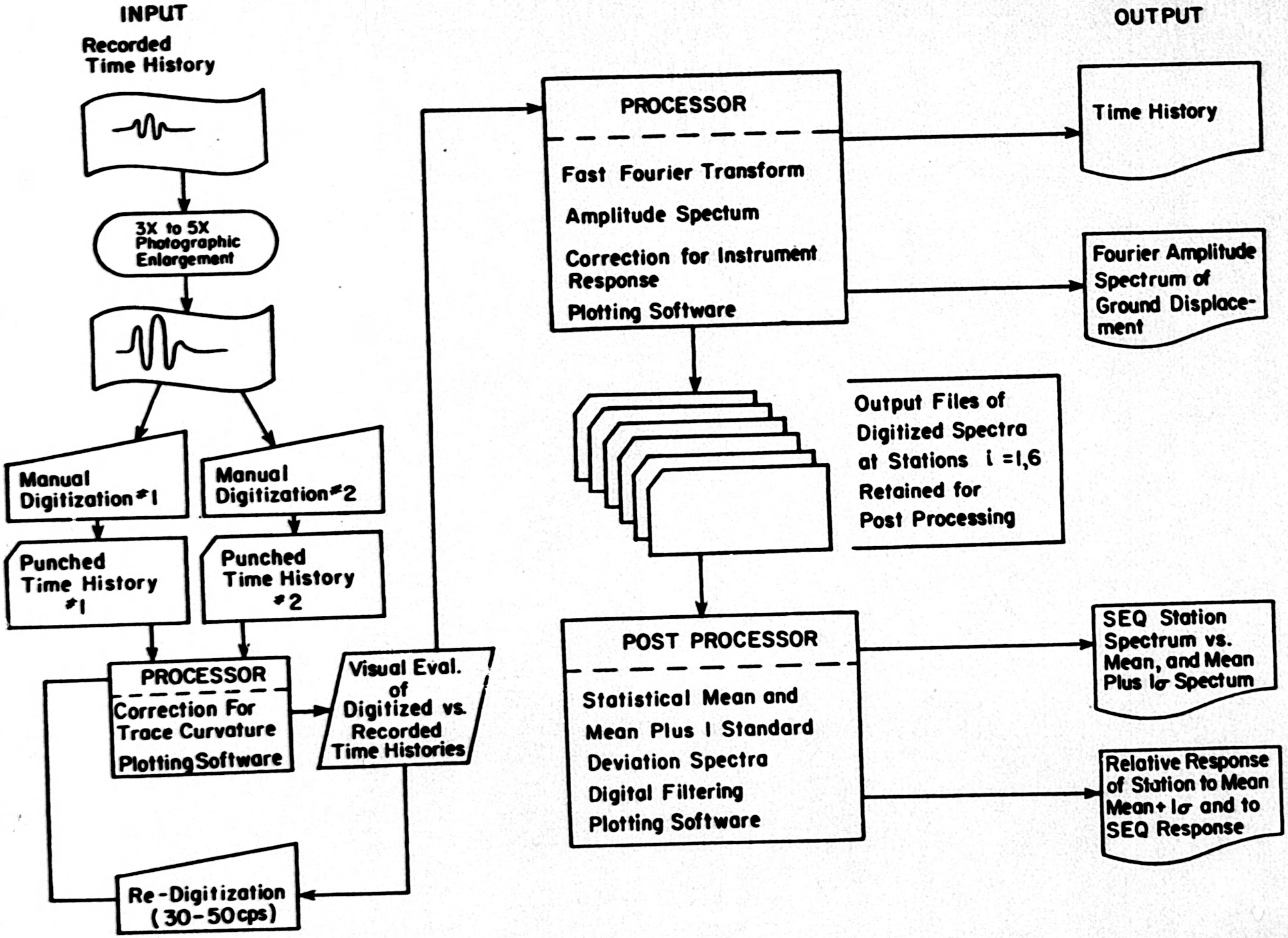

Figure 3

Weston Geophysical

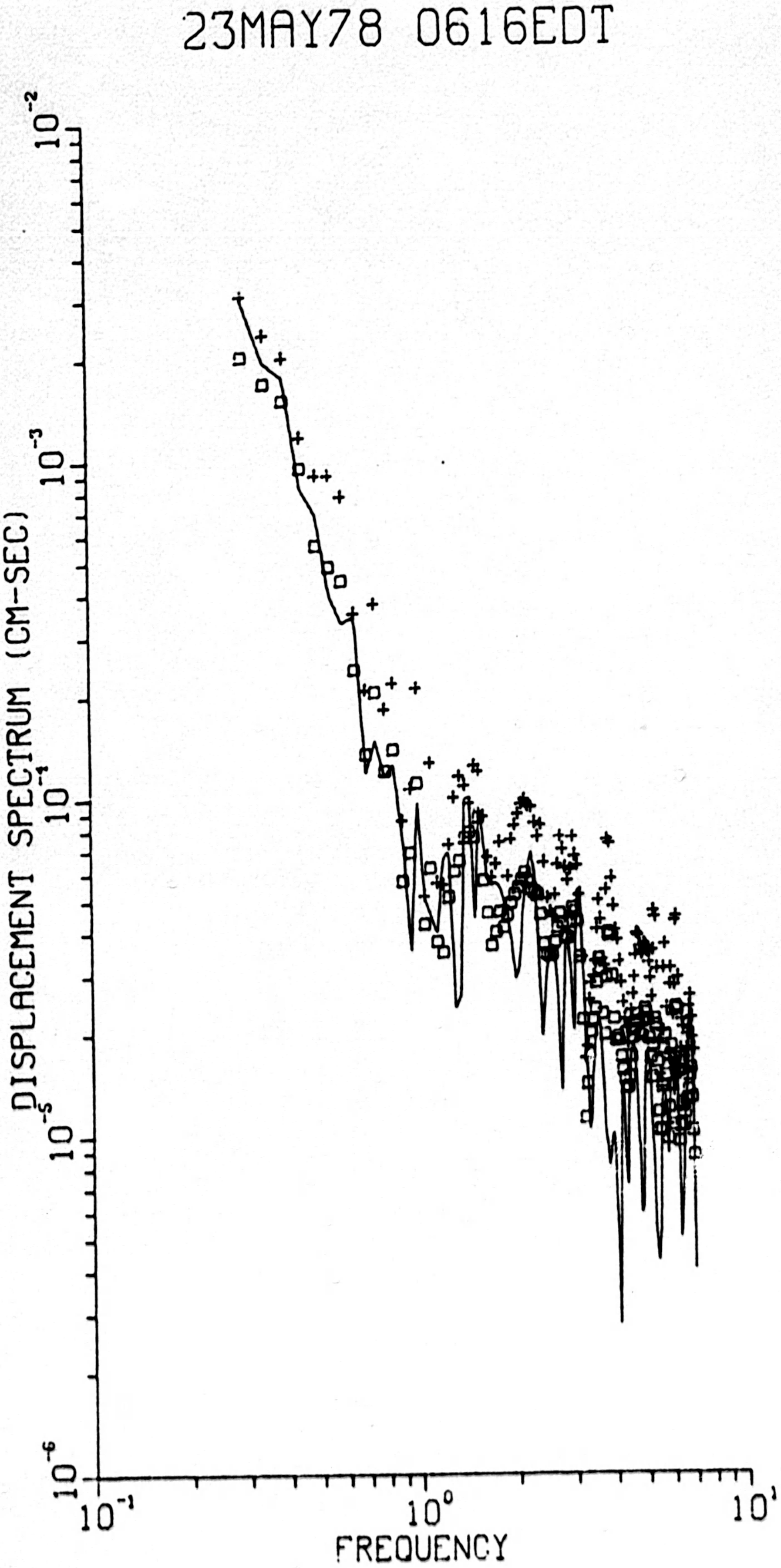

Figure 4

Weston Geophysical

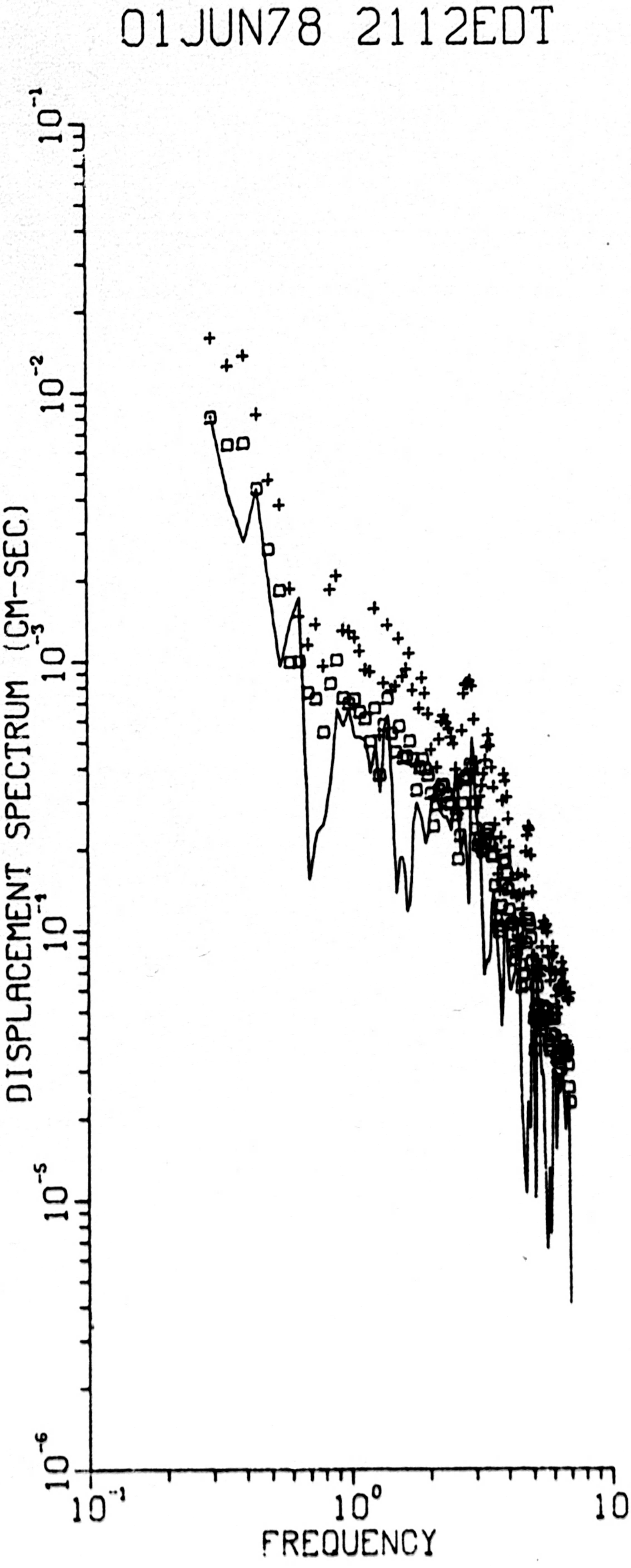

Figure 5

Weston Geophysical

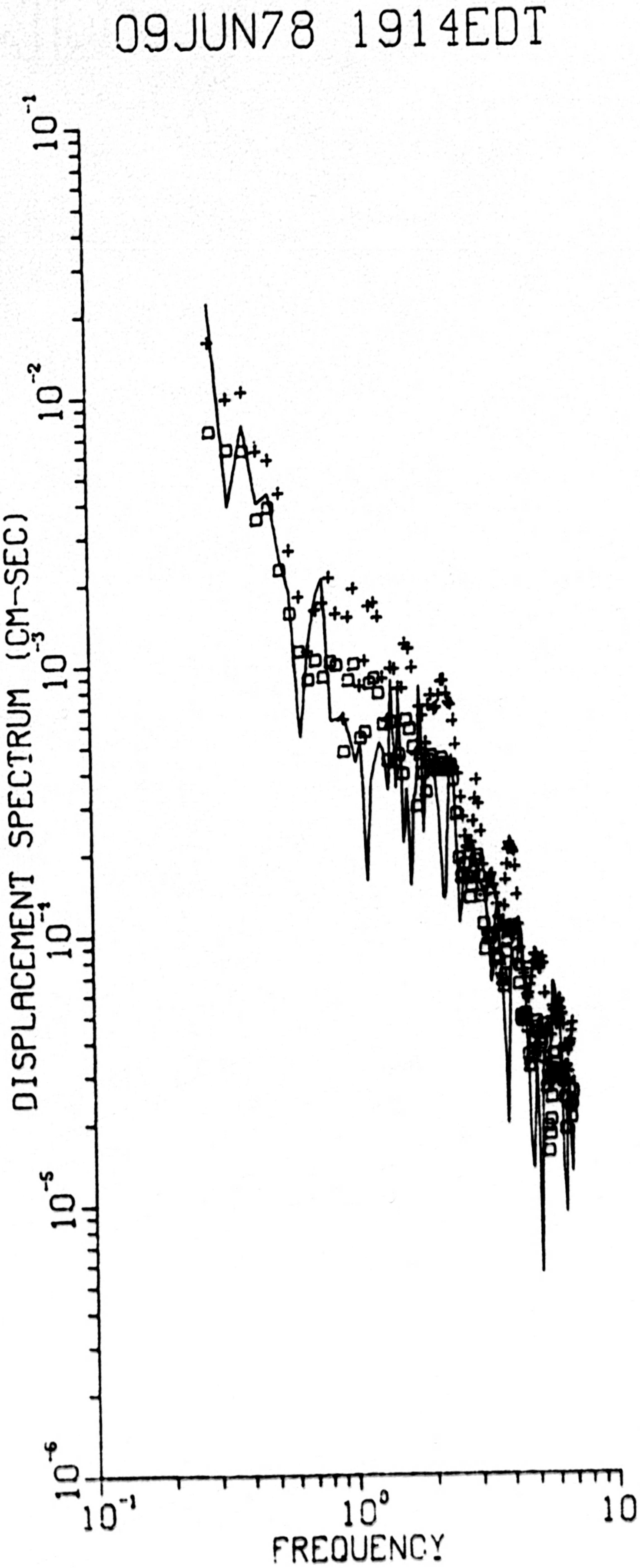

Figure 6

Weston Geophysical

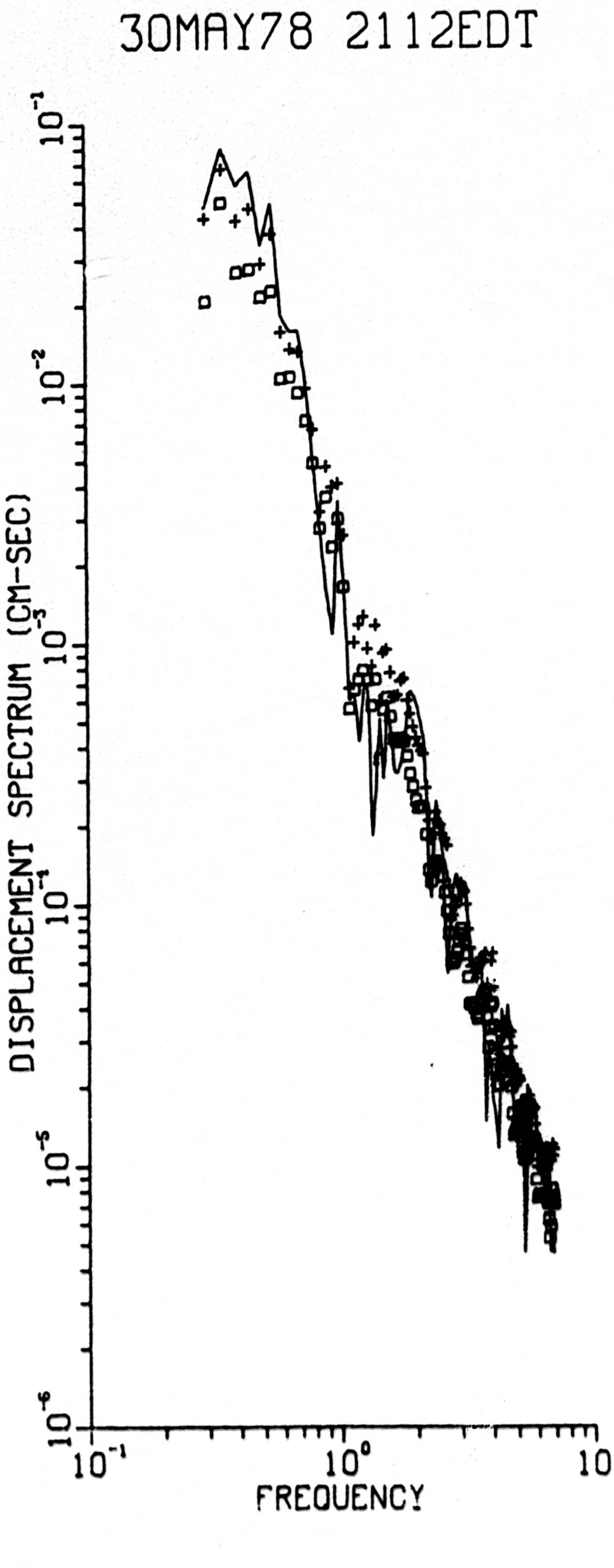

Figure 7

Weston Geophysical

11JUL78 0824EDT

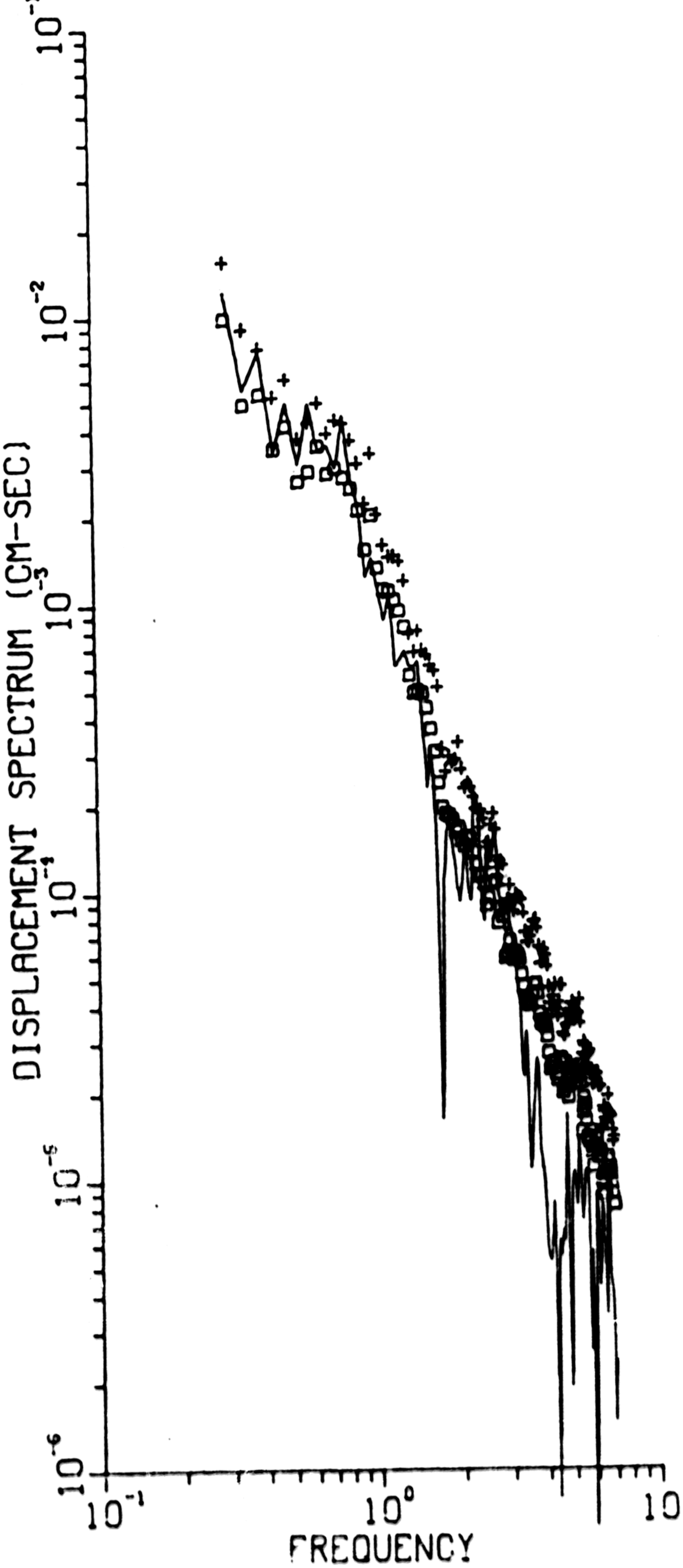

Figure 8

Weston Geophysical

23 MAY 1978 06 16 (EDT)

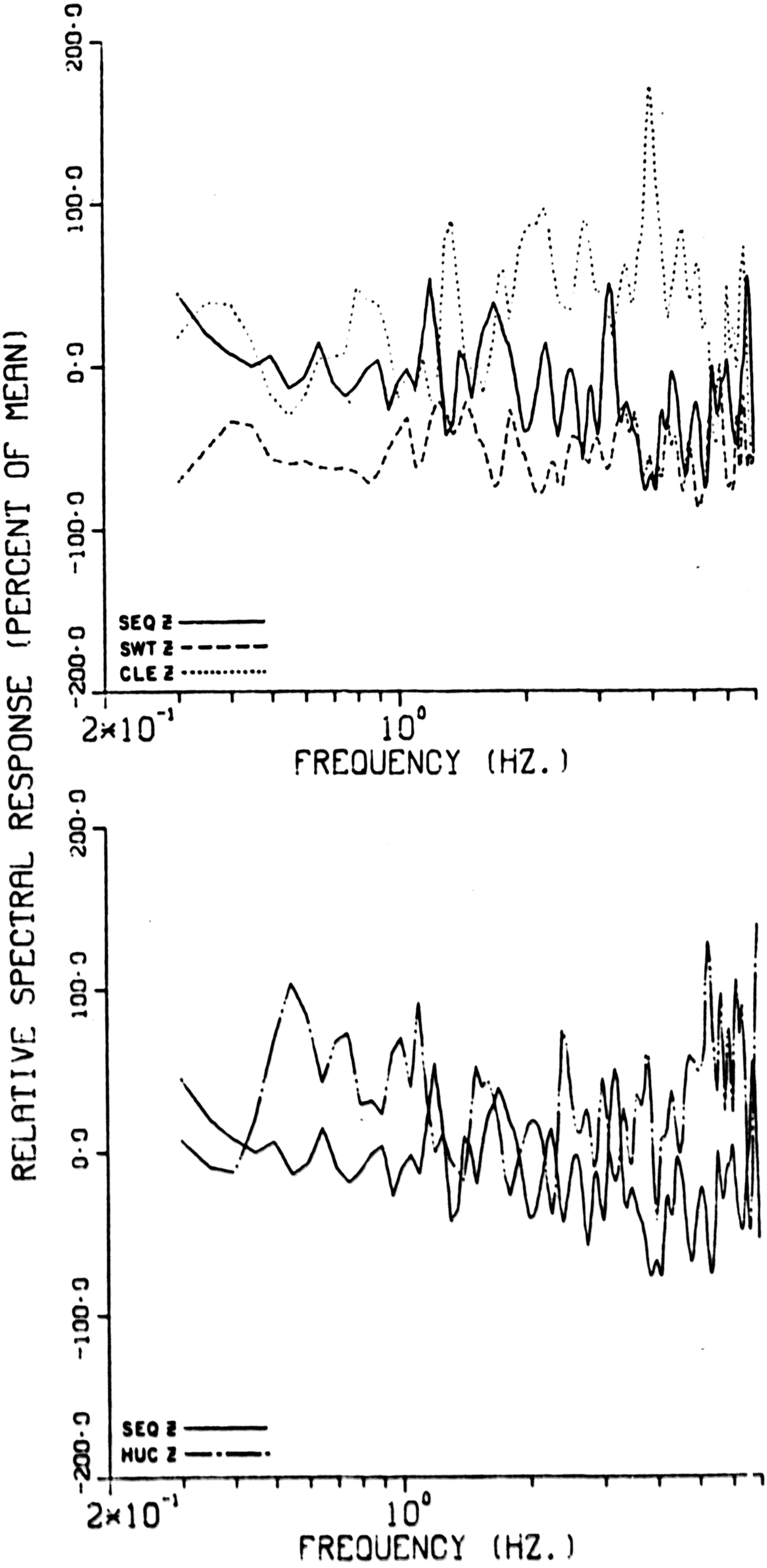

Figure 9

Weston Geophysical

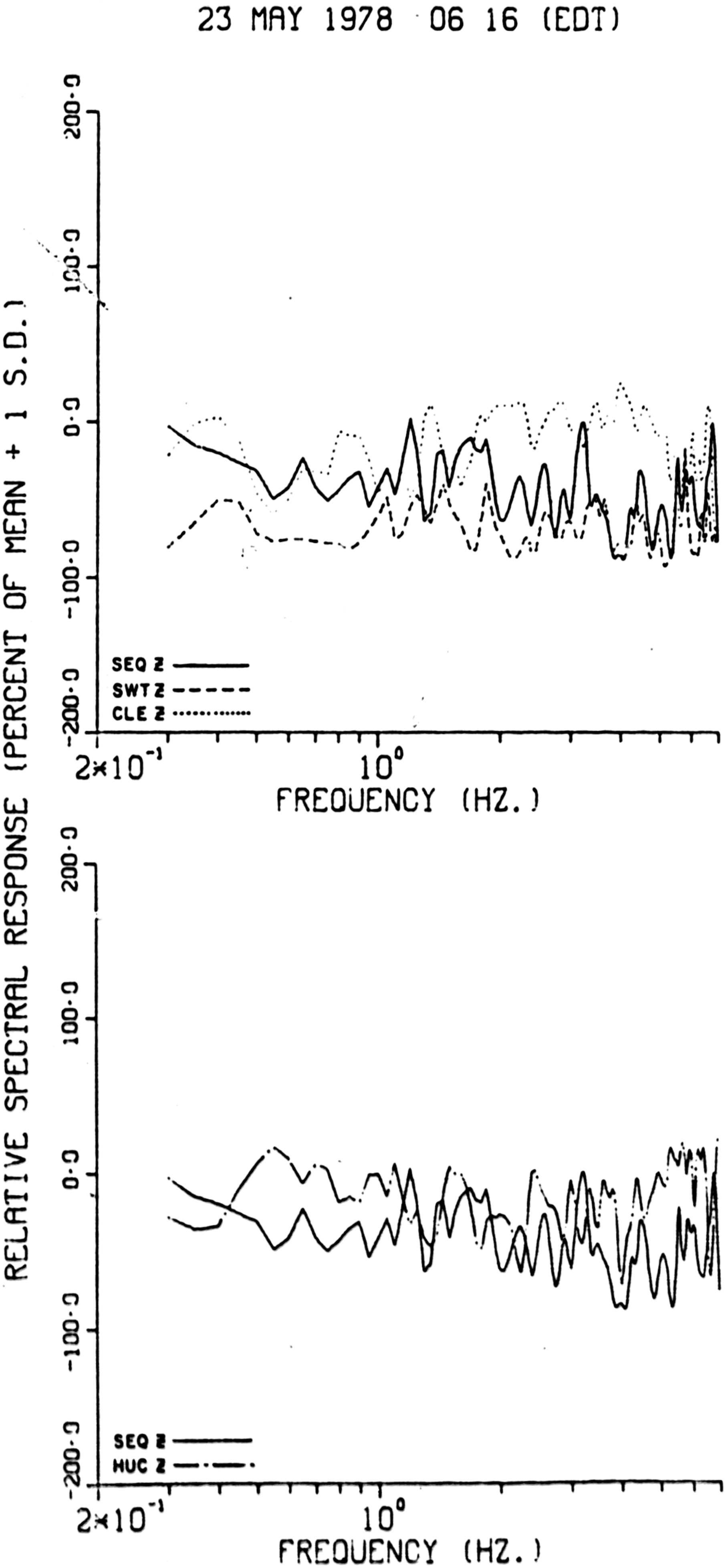

Figure 10

Weston Geophysical

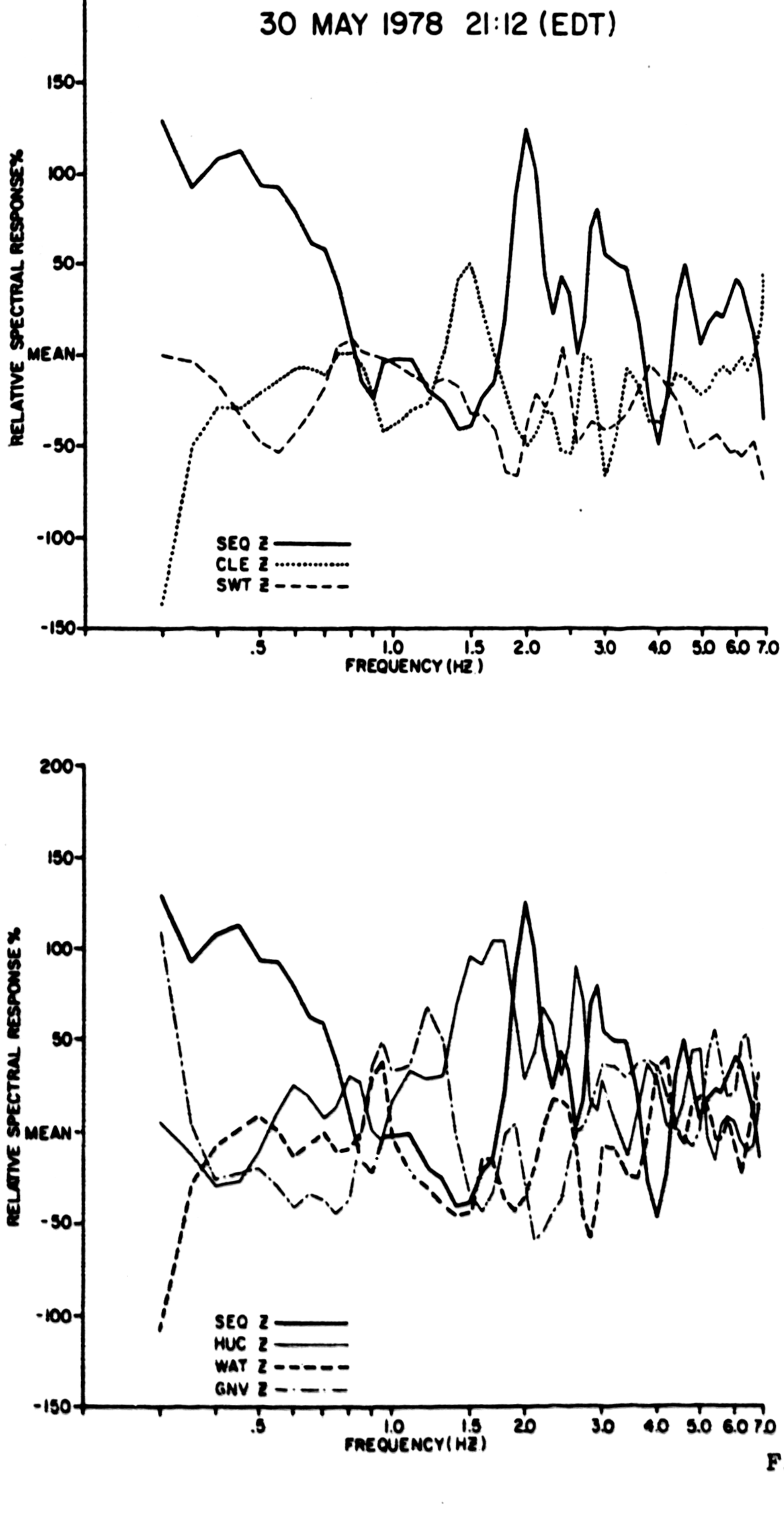

Figure 11

Weston Geophysical

30 MAY 1978 21:12 (EDT)

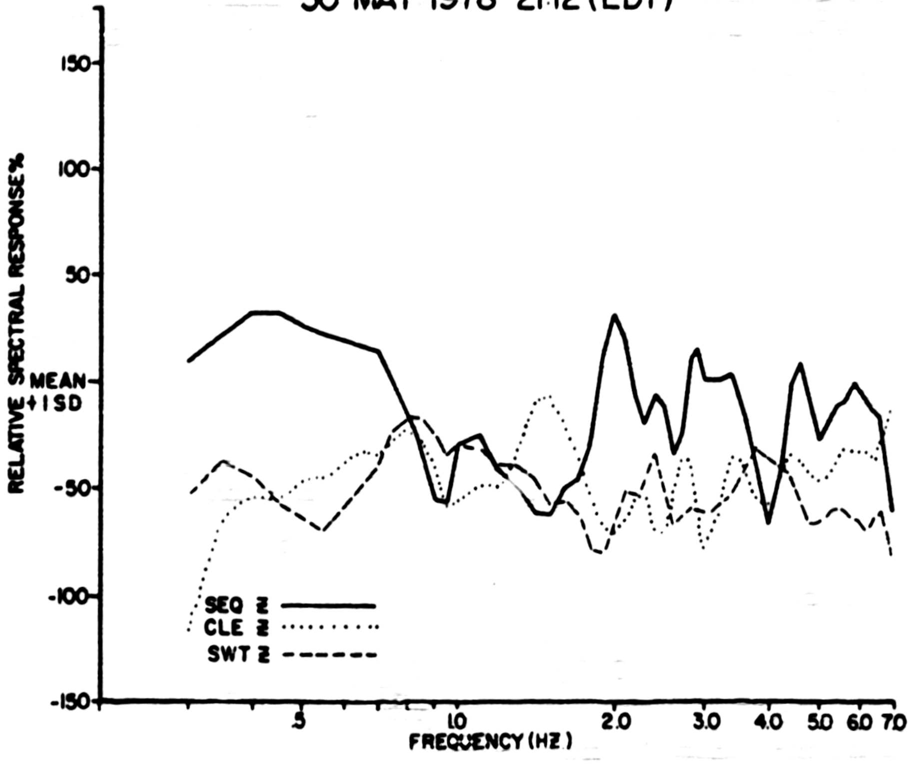

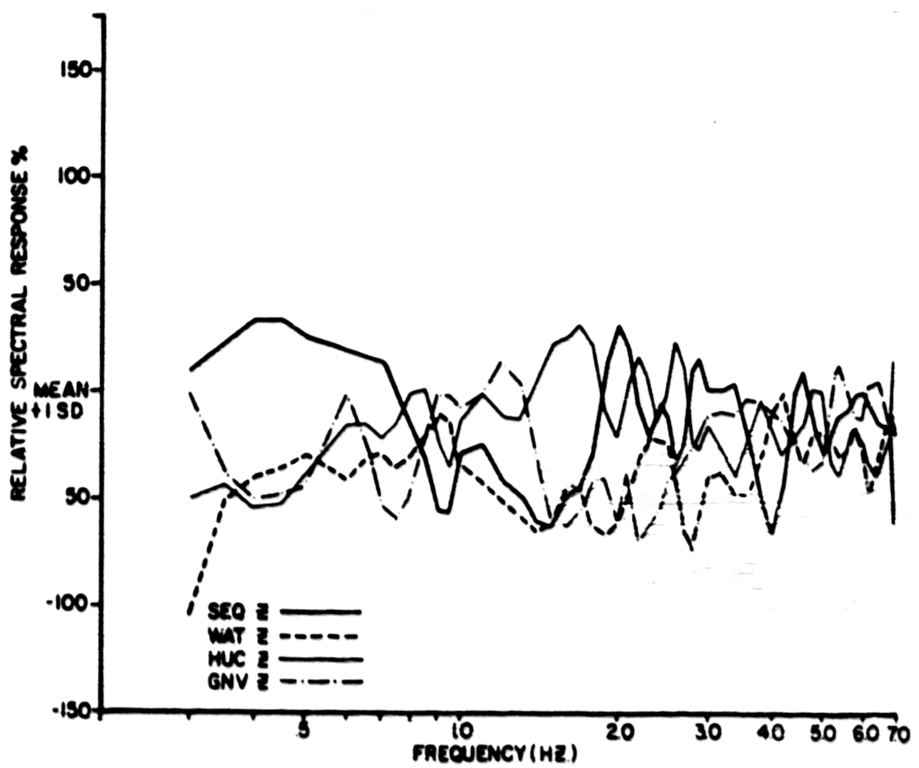

Figure 12

Weston Geophysical

01 JUNE 1978 21 12 (EDT)

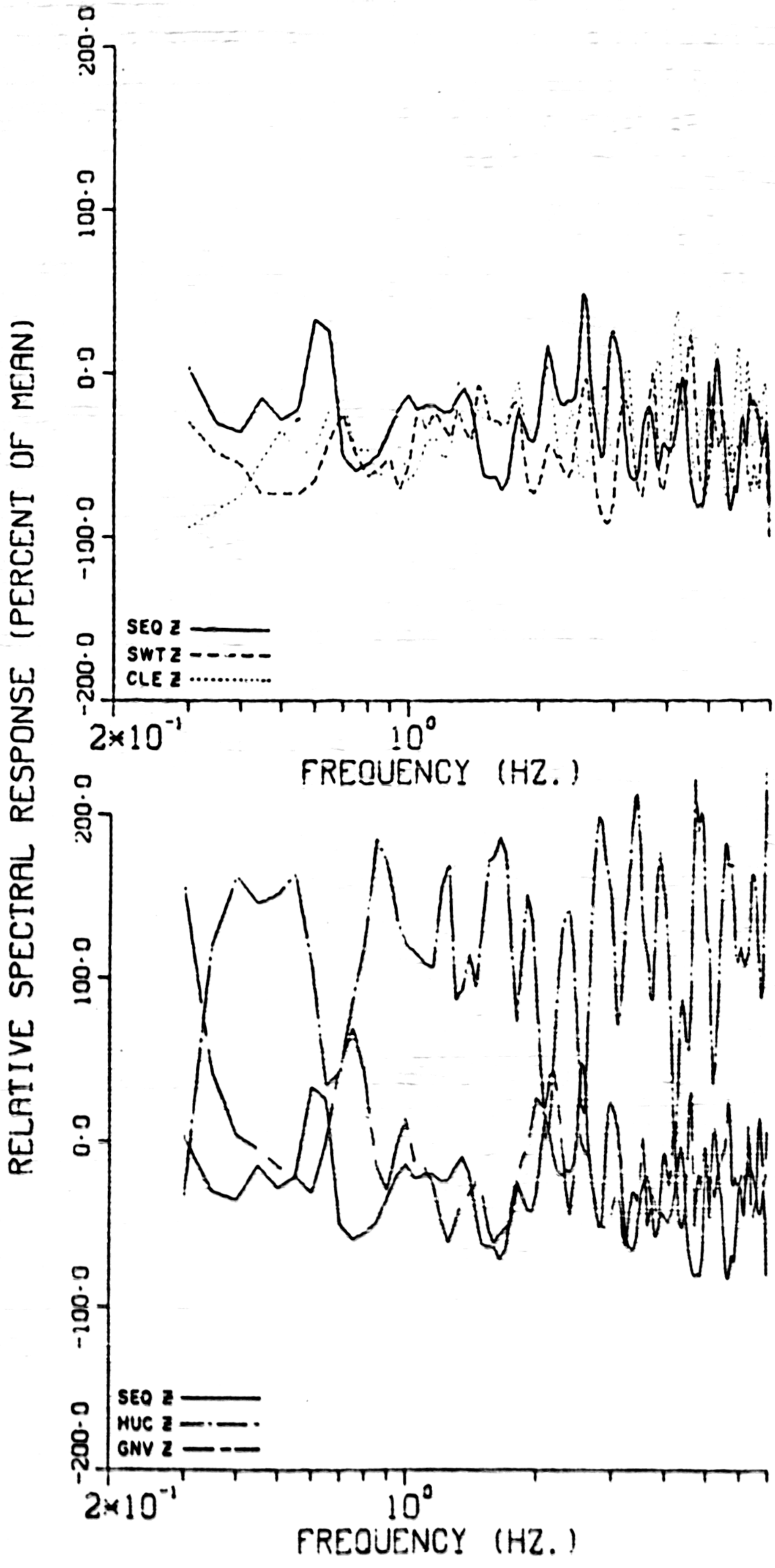

Figure 13

Weston Geophysical

01 JUNE 1978 21 12 (EDT)

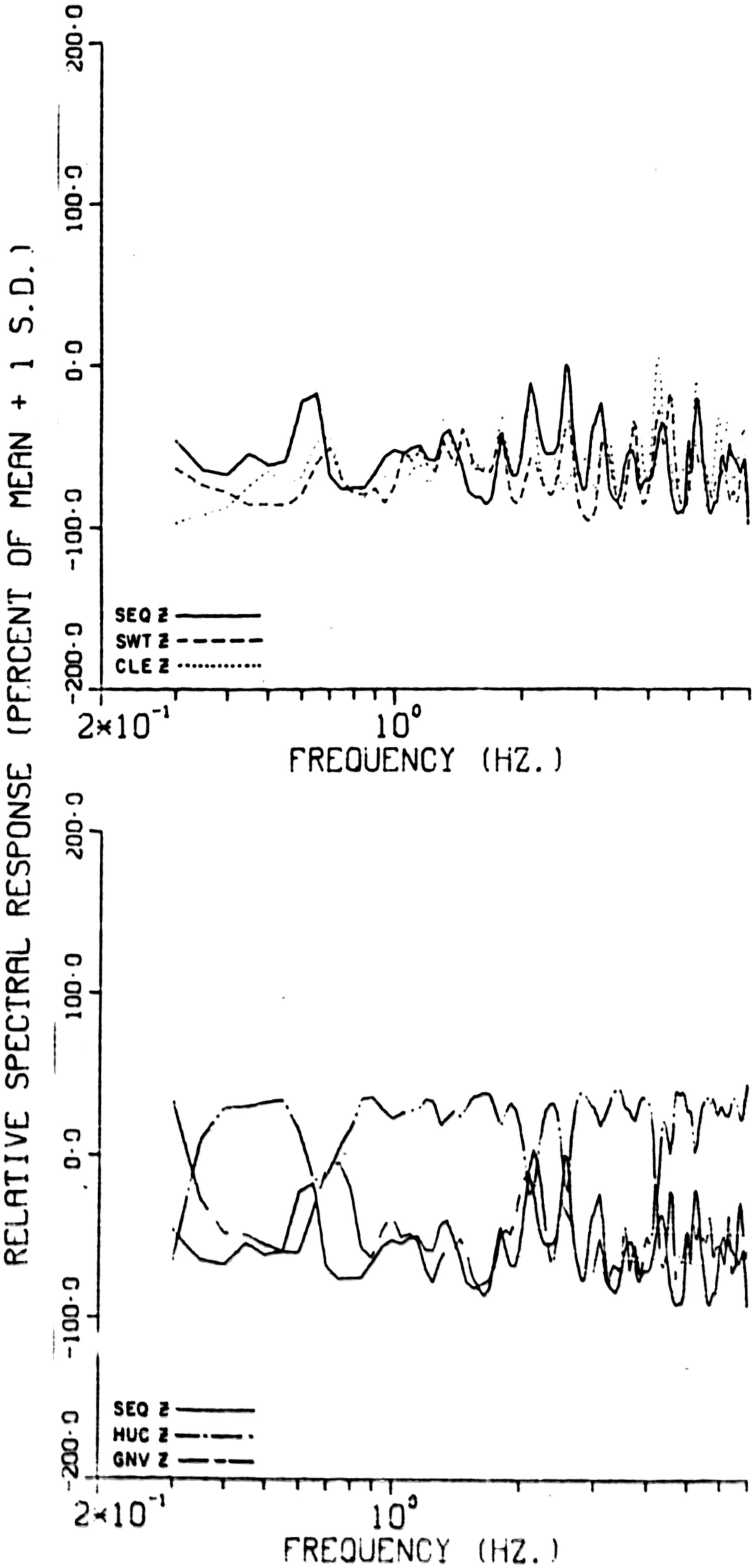

Figure 14

Weston Geophysical

09 JUNE 1978 19 14 (EDT)

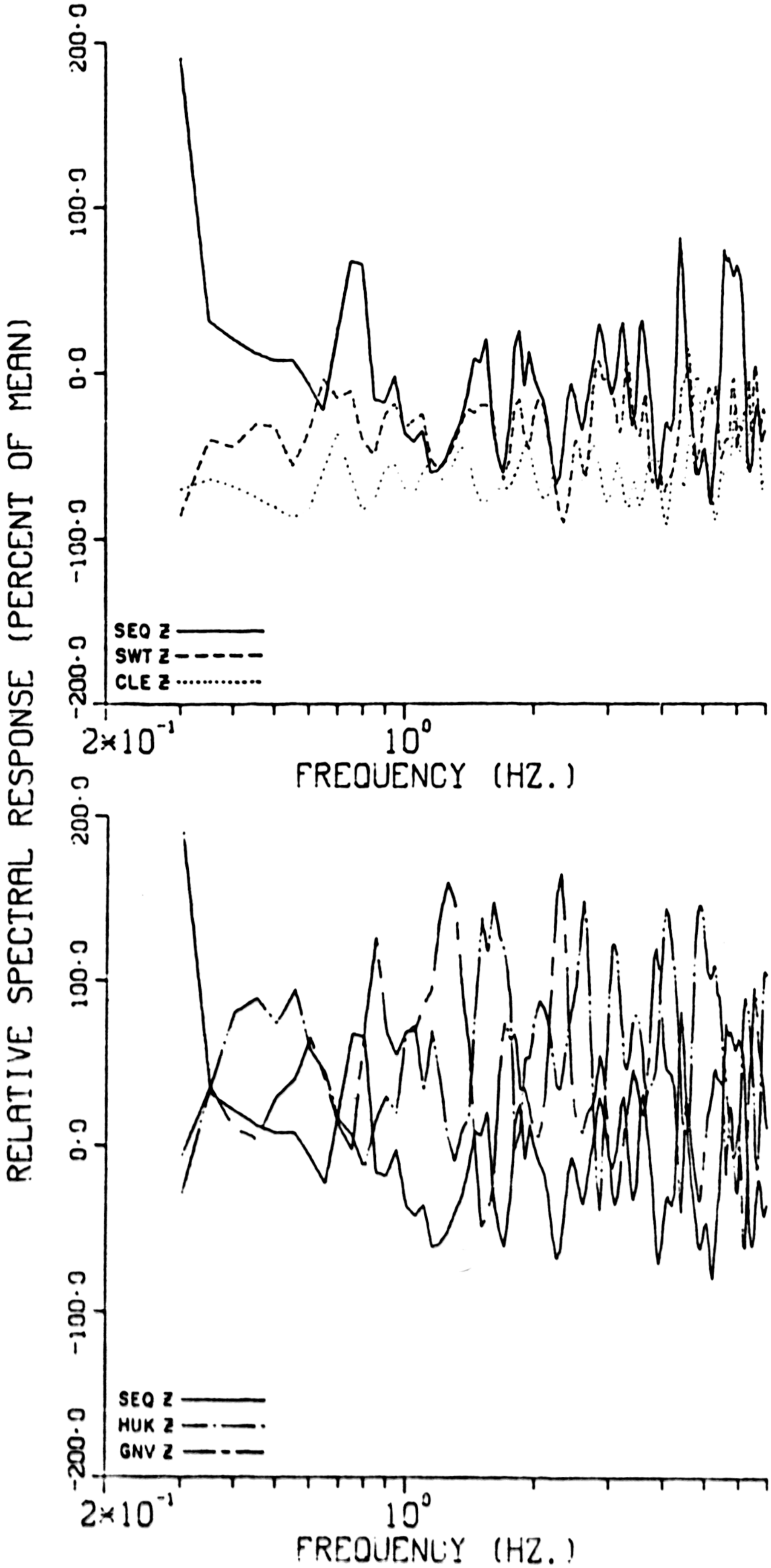

Figure 15

Weston Geophysical

09 JUNE 1978 19 14 (EDT)

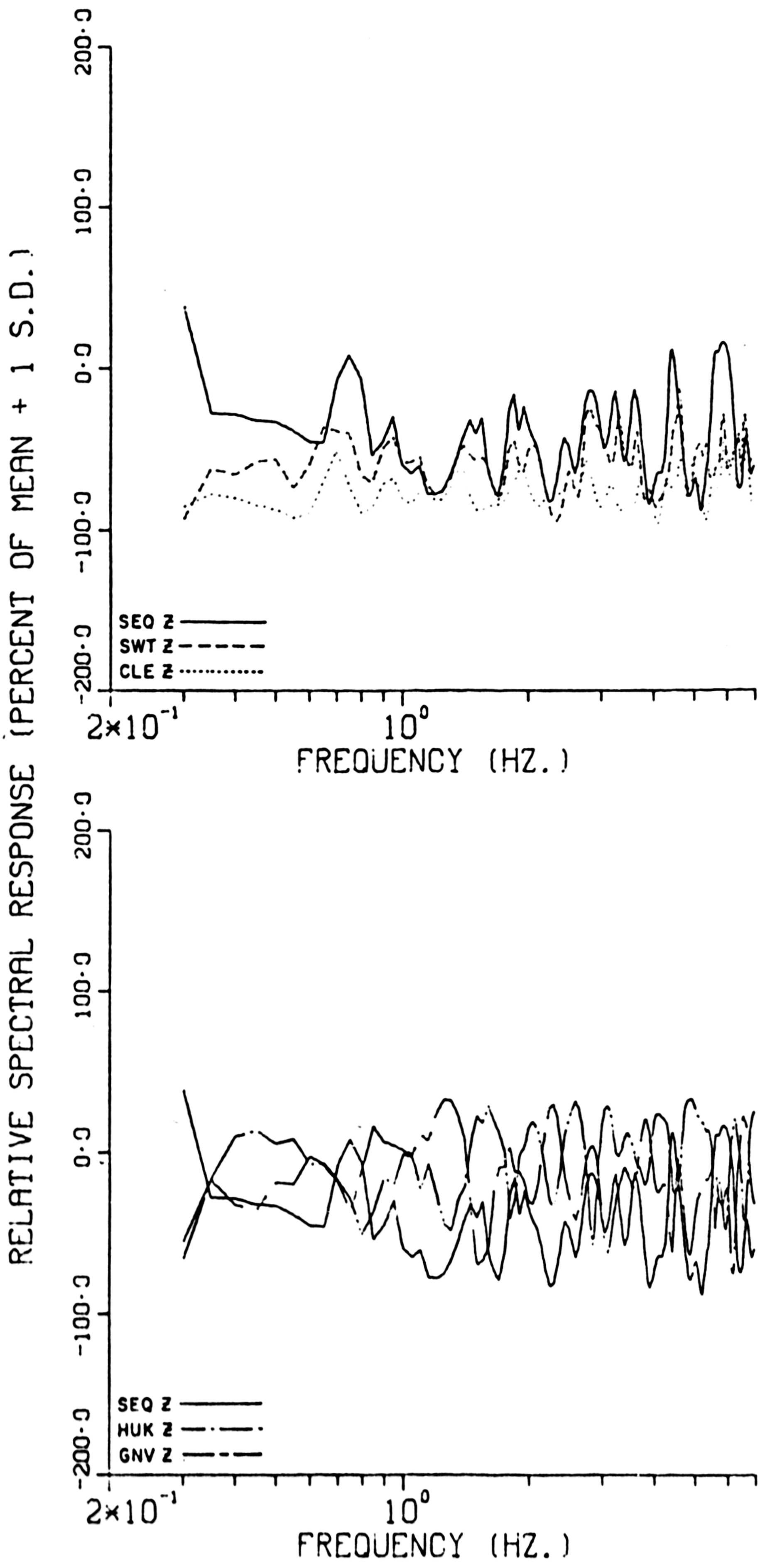

Figure 16

Weston Geophysical

09 JUNE 1978 19 14 (EDT)

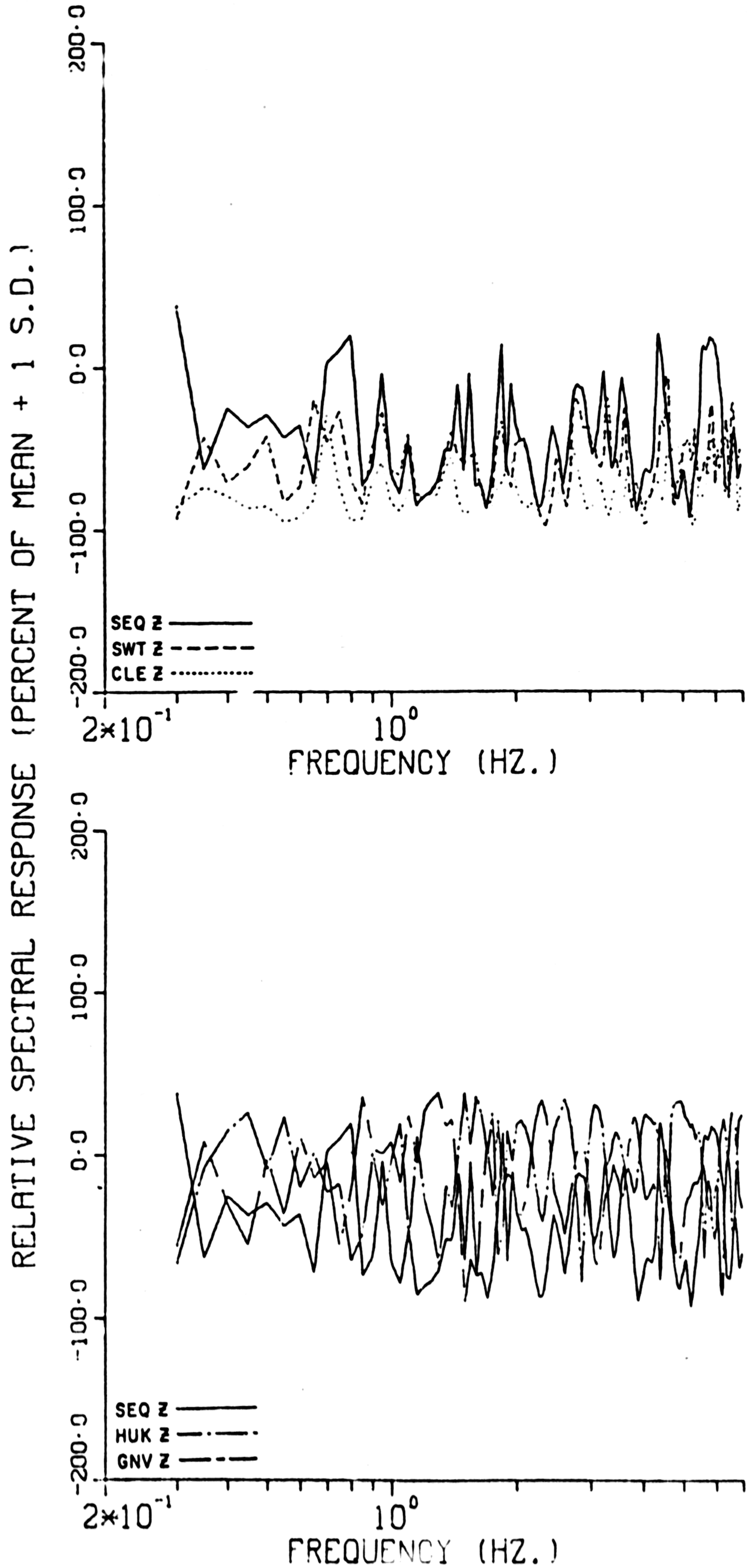

Figure 18

Weston Geophysical

11 JULY 1978 08:24 (EDT)

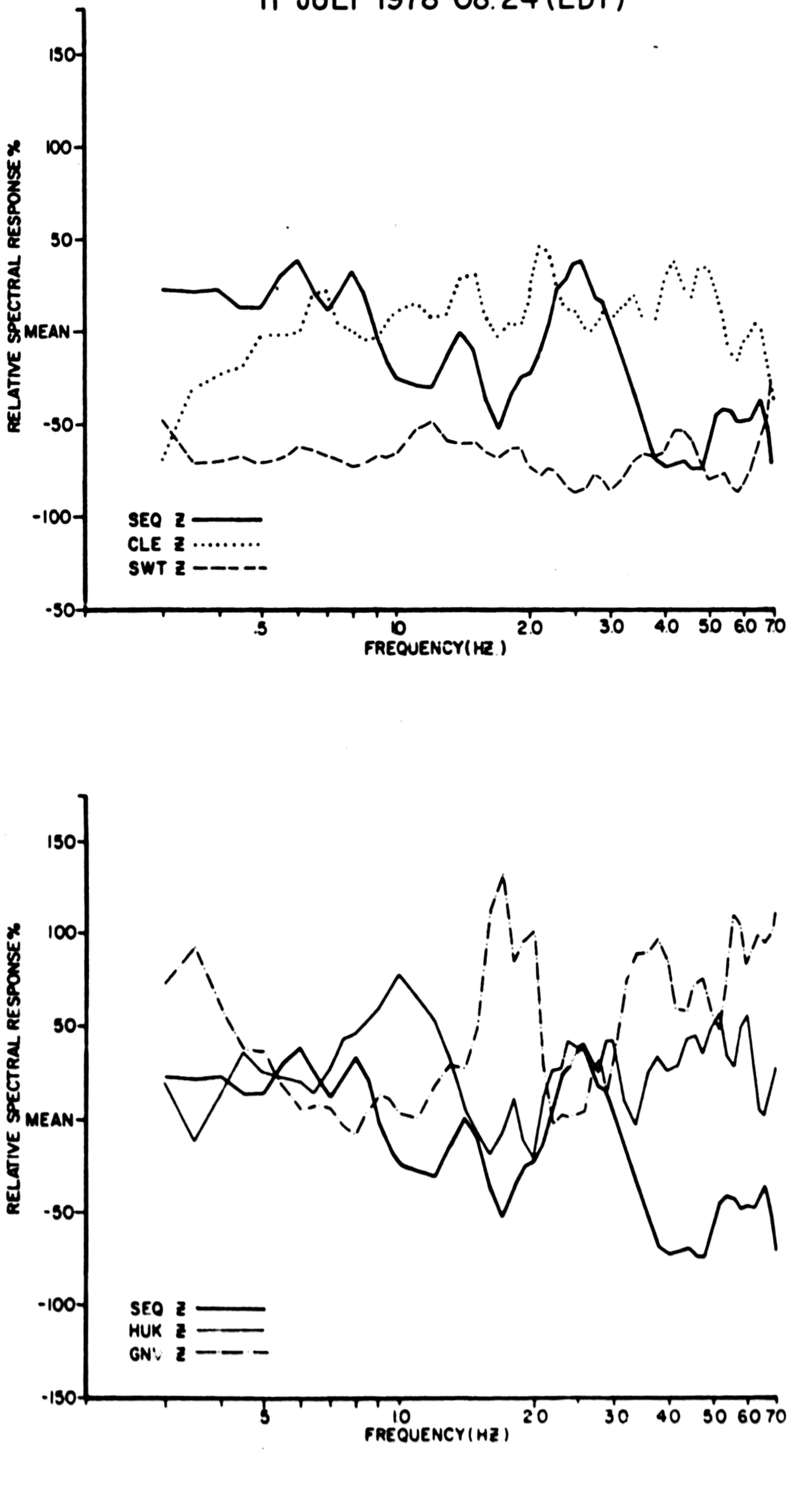

Figure 19

Weston Geophysical

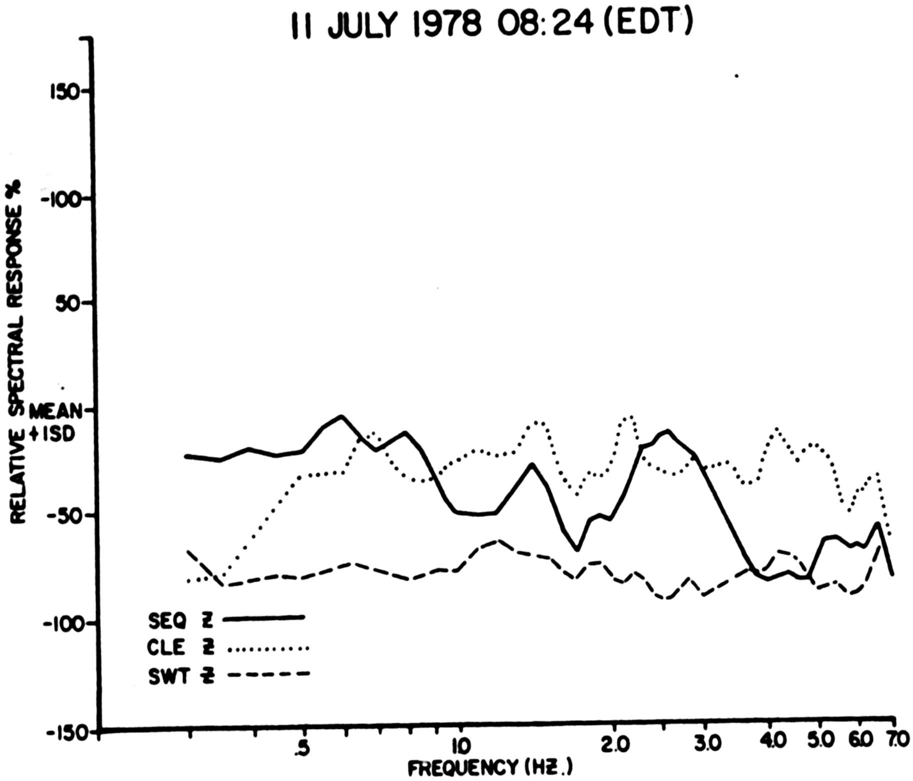
11 JULY 1978 08:24 (EDT)
RELATIVE SPECTRAL RESPONSE %
150
-100
50
MEAN+1SD
-50
-100
-150
SEQ Z
CLE Z
SWT Z
.5
10
2.0
3.0
4.0
5.0
6.0
7.0
FREQUENCY (HZ.)

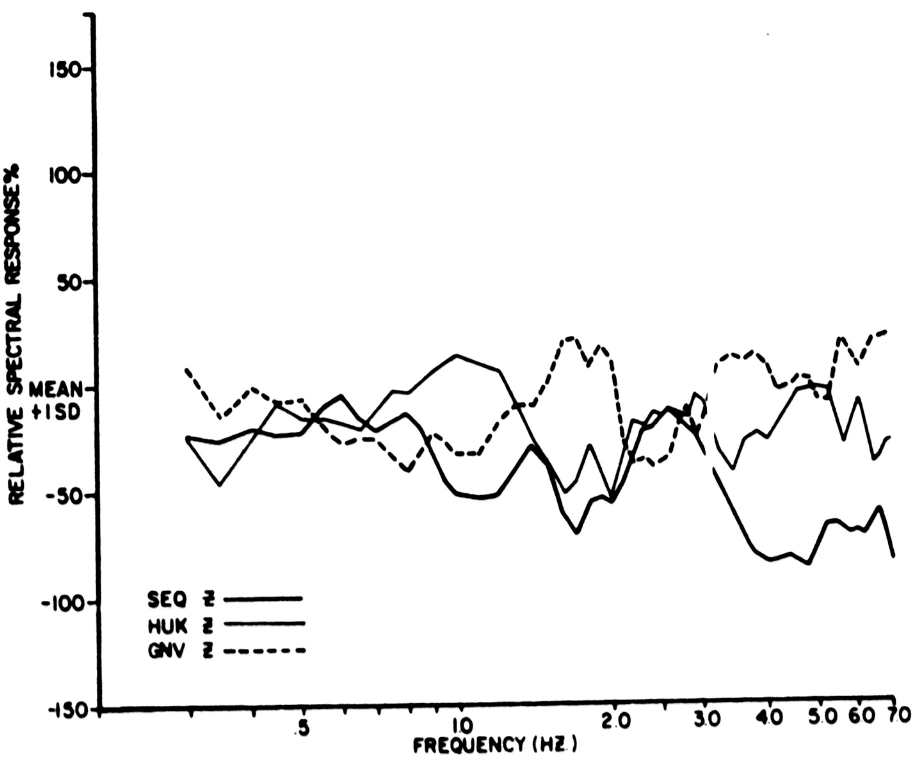
RELATIVE SPECTRAL RESPONSE%
150
100
50
MEAN+1SD
-50
-100
-150
SEQ Z
HUK Z
GNV Z
.5
10
2.0
3.0
40
5.0
60
70
FREQUENCY (HZ.)

Figure 20

23 MAY 1978 06 16 (EDT)

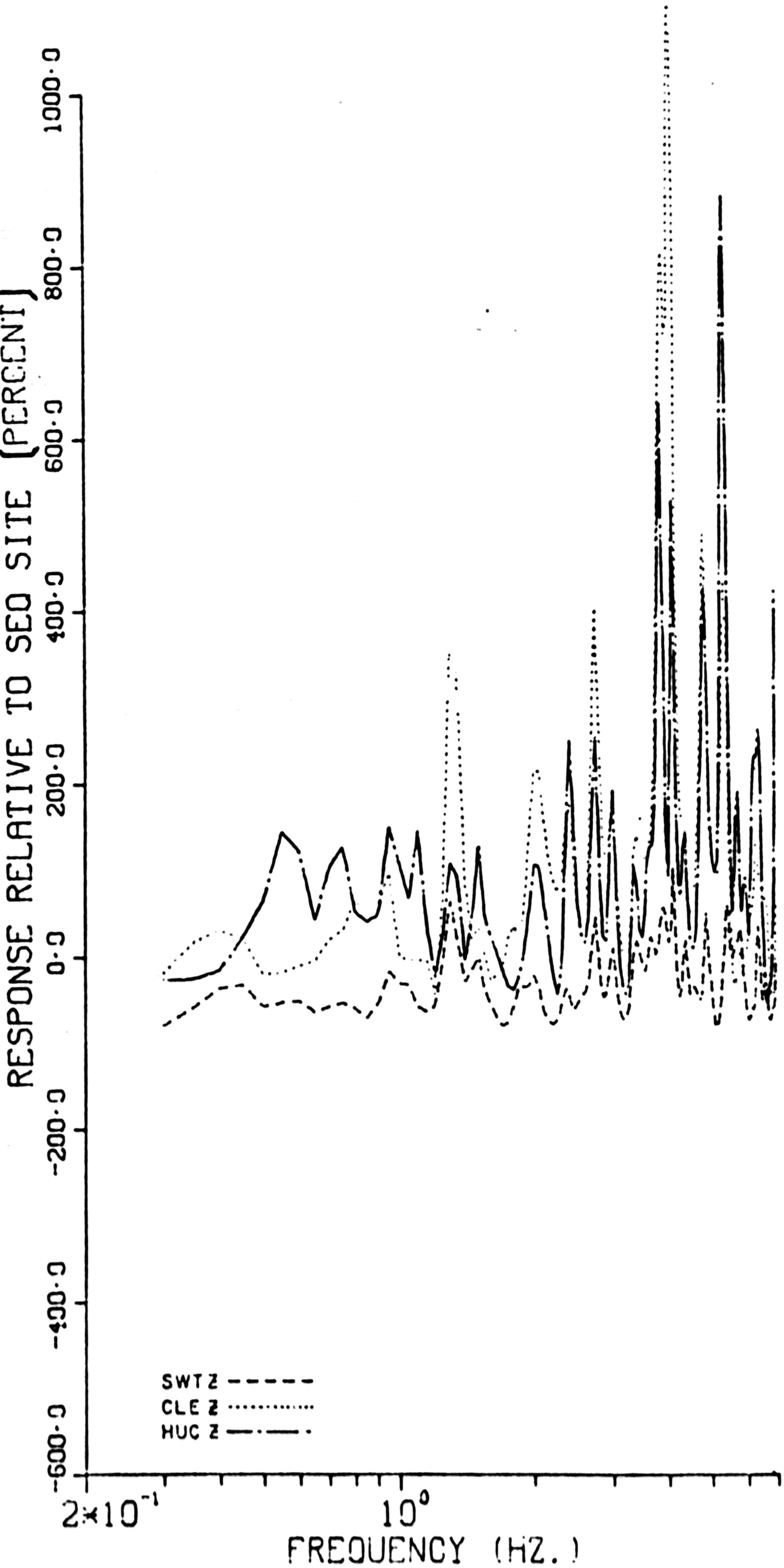

Figure 21

Weston Geophysical

01 JUNE 1978 21 12 (EDT)

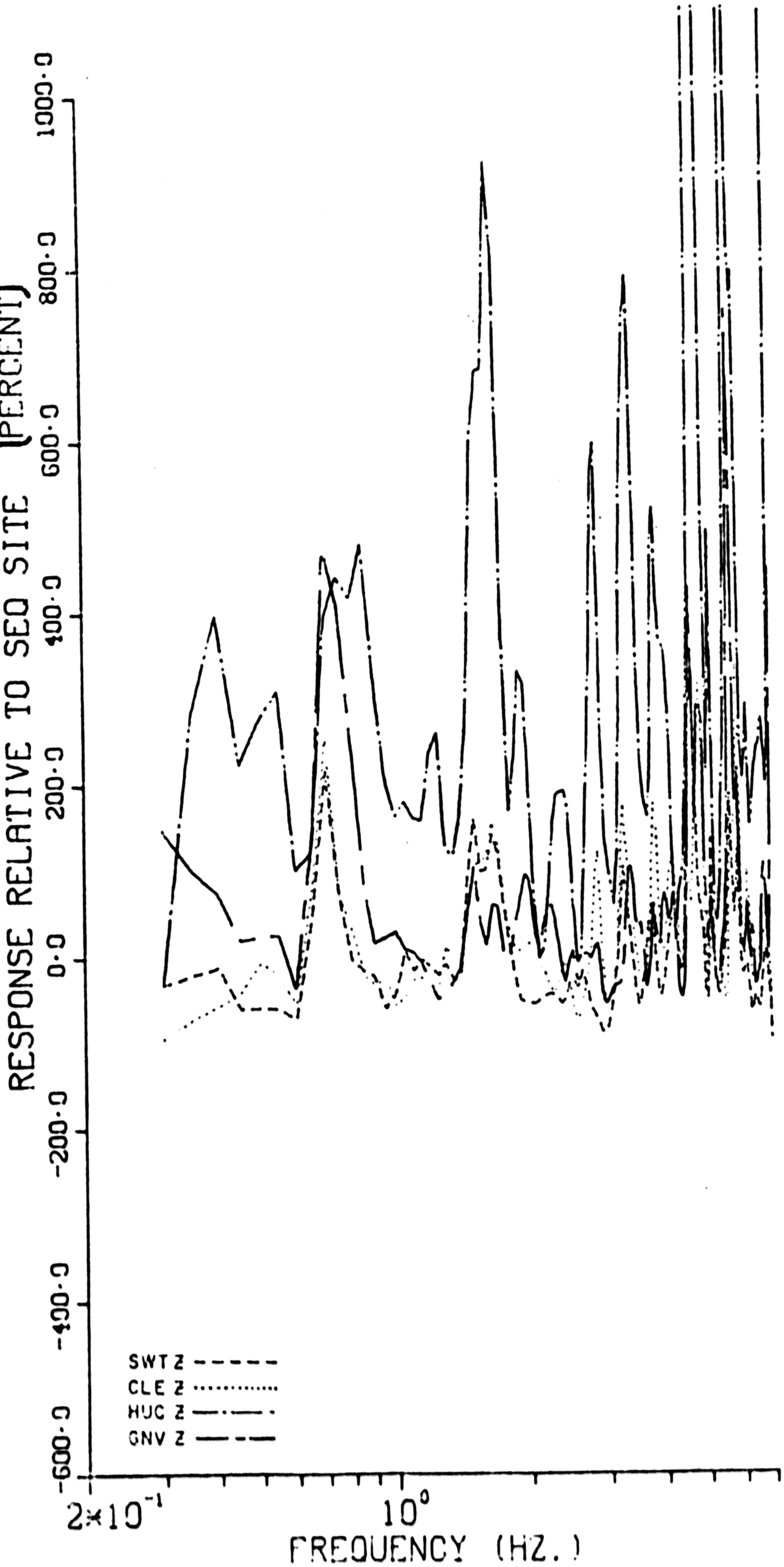

Figure 22

Weston Geophysical

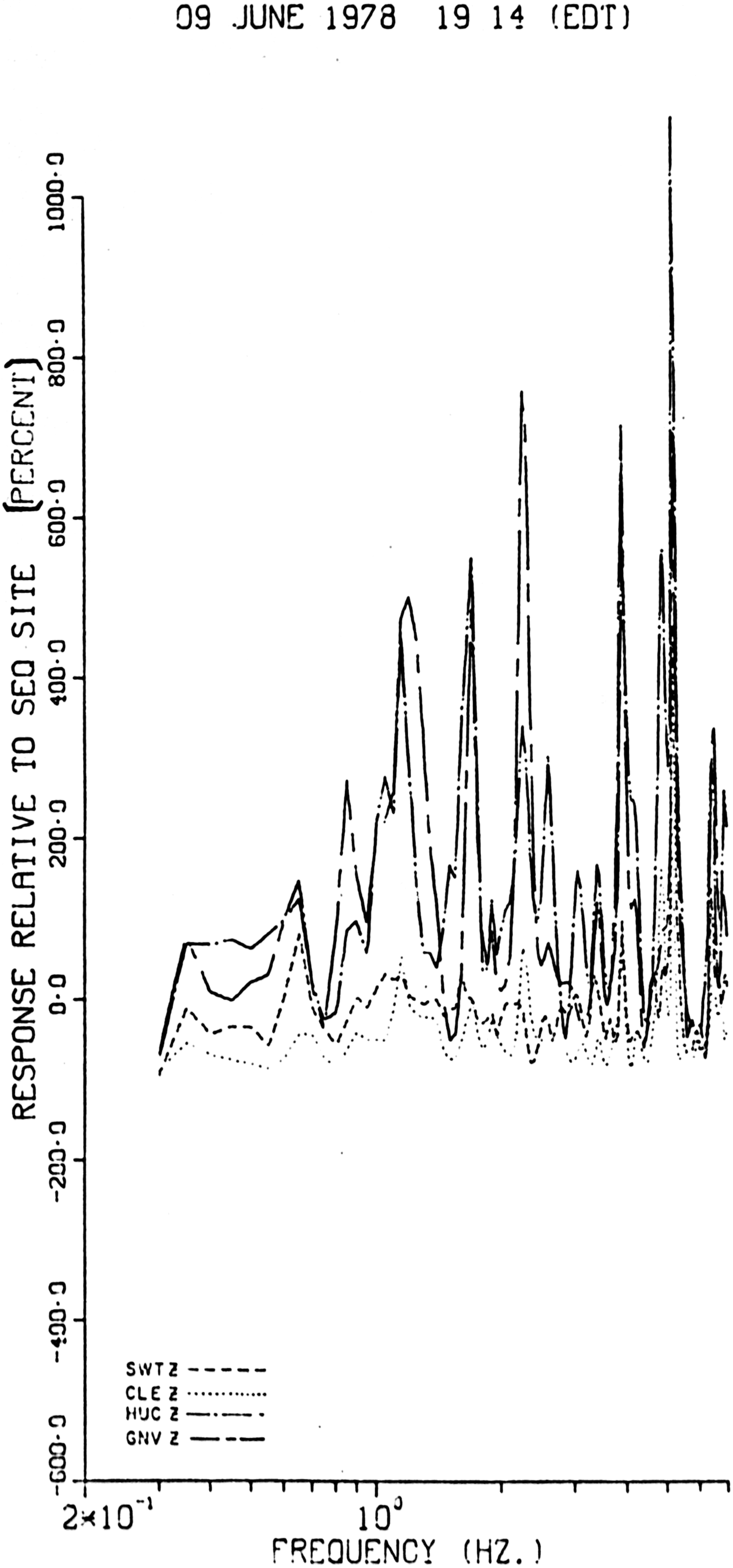

Figure 23

Weston Geophysical

REFERENCES

Ewing, M., W. S. Jardetzky, and F. Press, 1957, "Elastic Waves in Layered Media", McGraw-Hill, New York, p. 358.

Fernandez, L., 1963, "Variations in Amplitudes of Short Period P Waves", The Geochemical Corporation Technical Report, No. 63-106 for Contract AF 49(638)-1150.

Gutenberg, B., 1934, "Periods of the Ground in Southern California Earthquakes", Earthquake Investigation in California, 1934-1935, United States Geological Survey Special Publication 201, pp. 163-225.

Gutenberg, B., 1957, "Effects of Ground on Earthquake Motion", Bulletin of the Seismological Society of America, Vol. 47, pp. 221-249.

Hasegawa, H. S., 1971, "Crustal Transfer Ratios of Short- and Long-Period Body Waves Recorded at Yellowknife", Bulletin of the Seismological Society of America, Vol. 61, No. 5, pp. 1303-1320.

Imamura, A., 1929, "On the Earth Vibrations Induced in Some Localities at the Arrival of Seismic Waves", Bulletin of the Earthquake Research Institute (Tokyo), 7, pp. 489-494.

Ishimoto, M., 1931, "Charactéristiques des ondes Sismiques", Bulletin of the Earthquake Research Institute (Tokyo), 9, pp. 473-484.

Ishimoto, M., 1932, "Comparaison Accélérométrique des Secousses Sismiques dans deux parties de la ville de Tokyo", Bulletin of the Earthquake Research Institute (Tokyo), 10, pp. 171-187.

Ishimoto, M., 1934, "Observations Accélérométriques des Secousses Sismiques dans les villes de Tokyo et Yokohama", Bulletin of the Earthquake Research Institute (Tokyo), 12, pp. 234-248.

Kurita, T., 1973, "Regional Variations in the Structure of the Crust in the Central United States from P-Wave Spectra", Bulletin of the Seismological Society of America, Vol. 63, No. 5, pp. 1663-1687.

Leblanc G., 1967, "Truncated Crustal Transfer Functions and Fine Crustal Structure Determination", Bulletin of the Seismological Society of America, Vol. 57, No. 4, pp. 719-733.

Leblanc, G. and B. F. Howell, Jr., 1967, "Spectral Study of Short Period P Waves", Canadian Journal of Earth Sciences, Vol. 4, pp. 1049-1063.

Morse, P. M., and H. Feshbach, 1953, "Methods of Theoretical Physics", McGraw Hill, New York, 1978 p.

Nuttli, O. W., 1964, "The Determination of S-Wave Polarization Angles for an Earth Model with Crustal Layering", Bulletin of the Seismological Society of America, Vol. 54, pp. 429-440.

Nuttli, O. W., 1973, "Seismic Wave Attenuation and Magnitude Relations for Eastern North America", Journal of Geophysical Research, Vol. 78, No. 5, pp. 876-885.

Nuttli, O. W., 1978, "A Time-Domain Study of the Attenuation of 10 Hz Waves in the New Madrid Seismic Zone", Bulletin of the Seismological Society of America, Vol. 68, No. 2, pp. 343-355.

Nuttli, O. W. and J. D. Whitmore, 1961, "An Observational Determination of the Variation of the Angle of Incidence of P-Waves with Epicentral Distance", Bulletin of the Seismological Society of America, Vol. 51, pp. 269-276.

Phinney, R. A., 1964, "Structure of the Earth's Crust from Spectral Behavior of Long Period Body Waves", Journal of Geophysical Research, Vol. 69, pp. 2997-3017.

Seed, H. B., C. Ugas, and J. Lysmer, 1976, "Site-Dependent Spectra for Earthquake-Resistant Design", Bulletin of the Seismological Society of America, Vol. 66, No. 1, pp. 221-243.

Takahasi, R. and K. Hirano, 1941, "Seismic Vibrations of Soft Ground", Bulletin of the Earthquake Research Institute (Tokyo), 19, p 534.

Trifunac, M. D., 1976, "Preliminary Analysis of the Peaks of Strong Earthquake Ground Motion - Dependence of Peaks on Earthquake Magnitude, Epicentral Distance, and Recording Site Conditions", Bulletin of the Seismological Society of America", Vol. 66, No. 1, pp. 189-219.

APPENDIX A

SEISMOGRAMS OF EVENTS ANALYZED IN THE GROUND MOTION STUDY

23 MAY 1978 06:16(EDT)

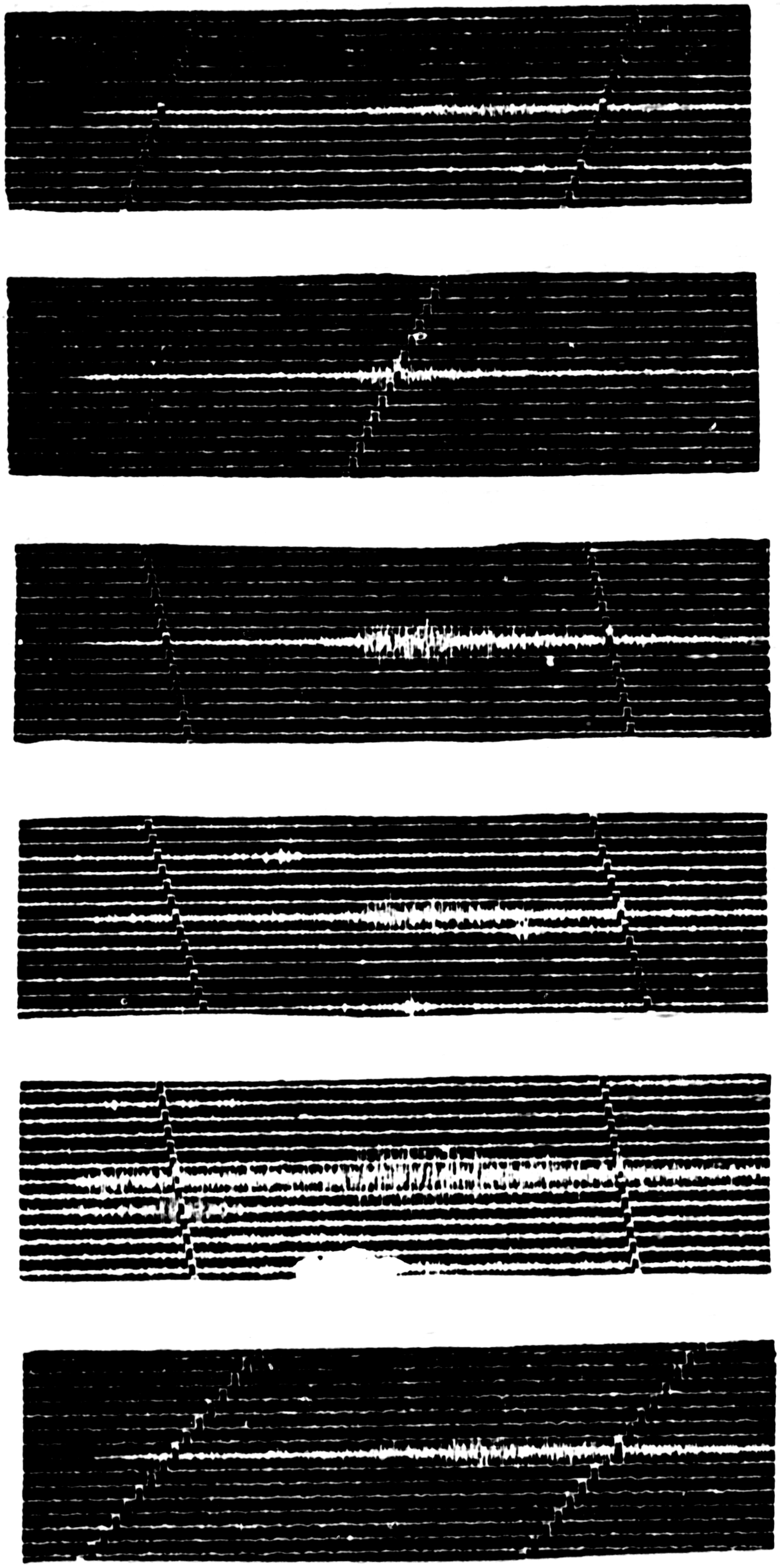

STATION	COMP.	GAIN
CLE	Z	72db
SEQ	Z	72db
SEQ	H	72db
HUC	Z	72db
WAT	Z	72db
SWT	Z	78db

Figure A-1

01 JUNE 1978 22:08 (EDT)

STATION	COMP.	GAIN
GNV	Z	72db
WAT	Z	66db
HUC	Z	72db
SEQ	Z	72db
SWT	Z	72db
CLE	Z	72db

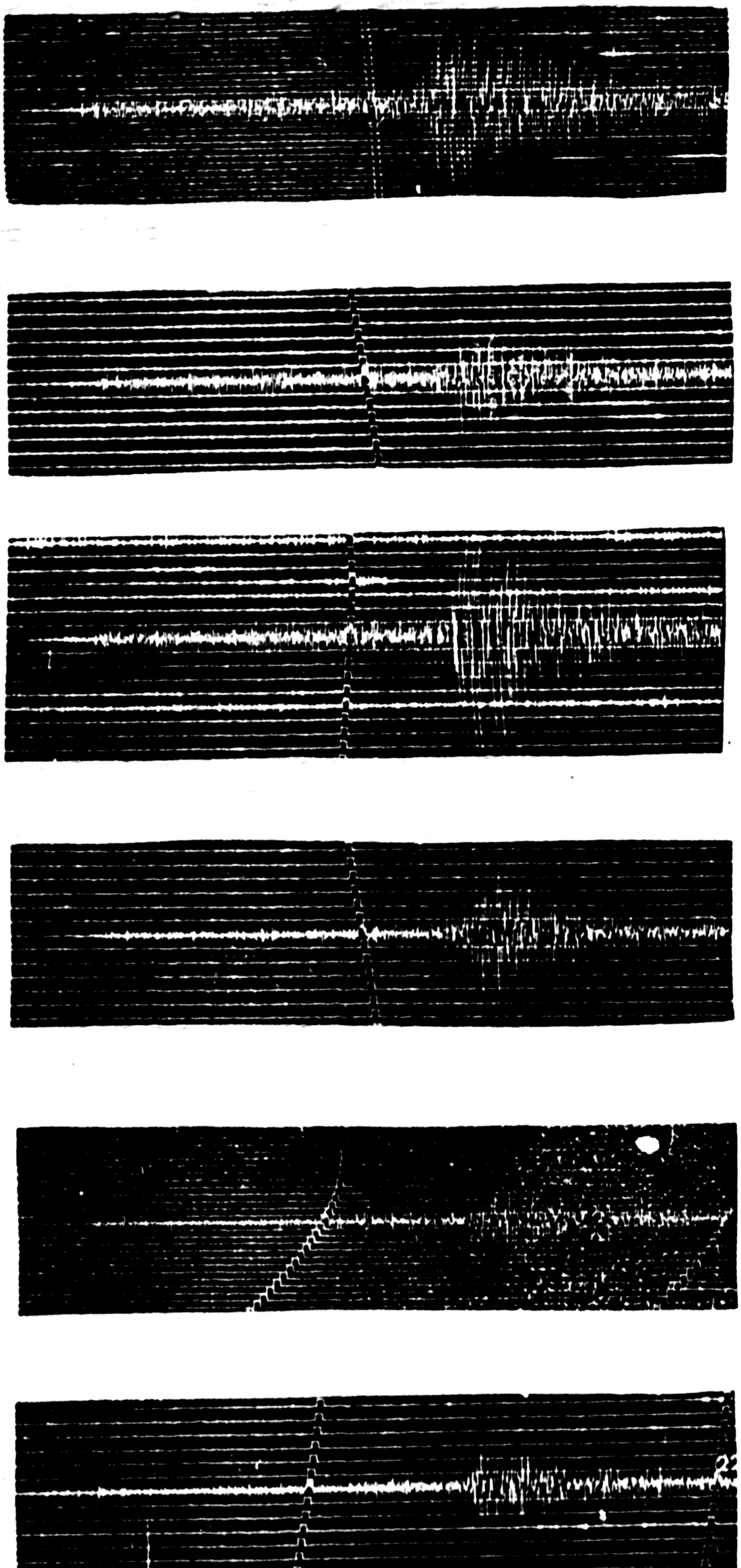

Figure A-2

Weston Geophysical

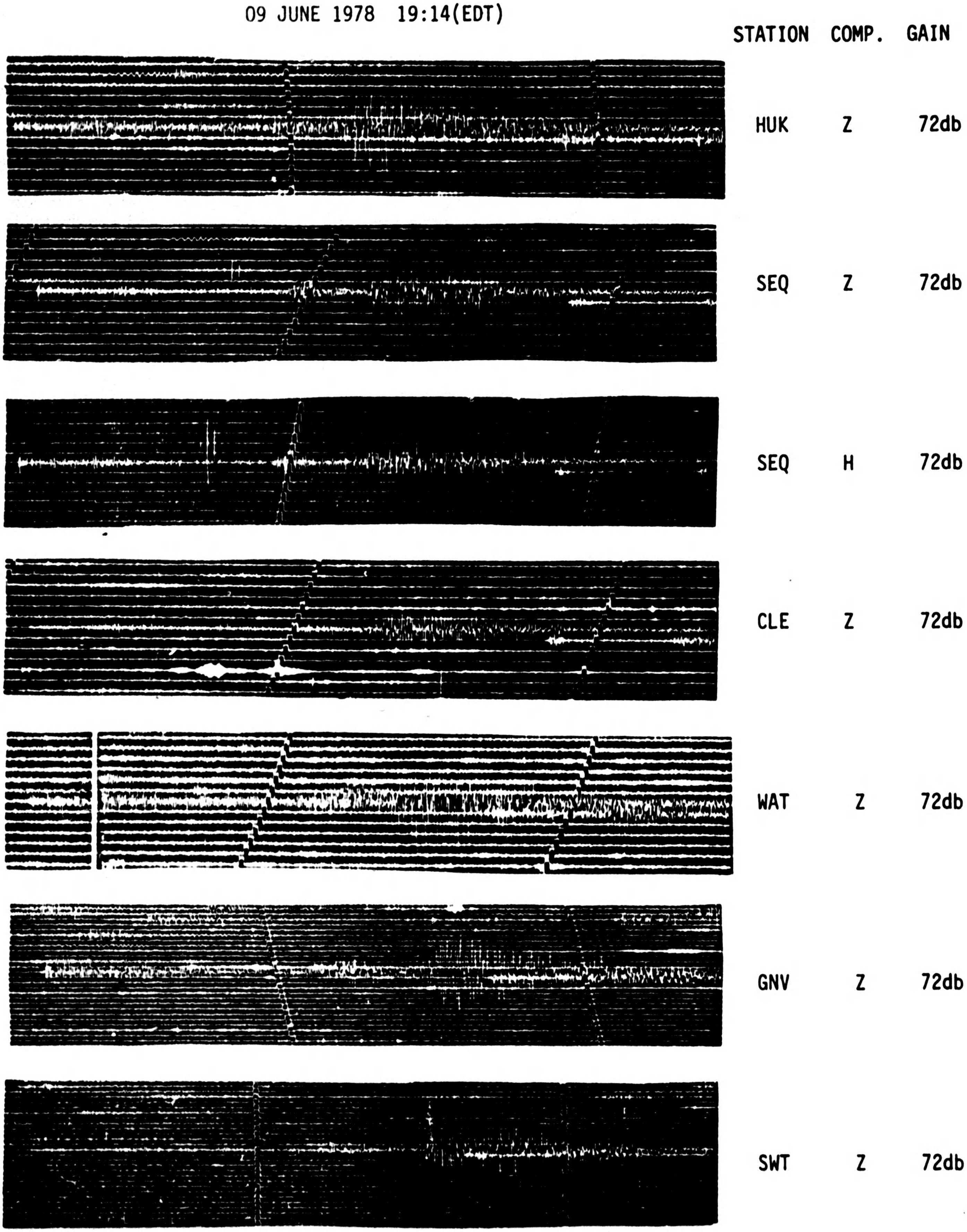

Figure A-3

Weston Geophysical

30 MAY 1978 21:12(EDT)

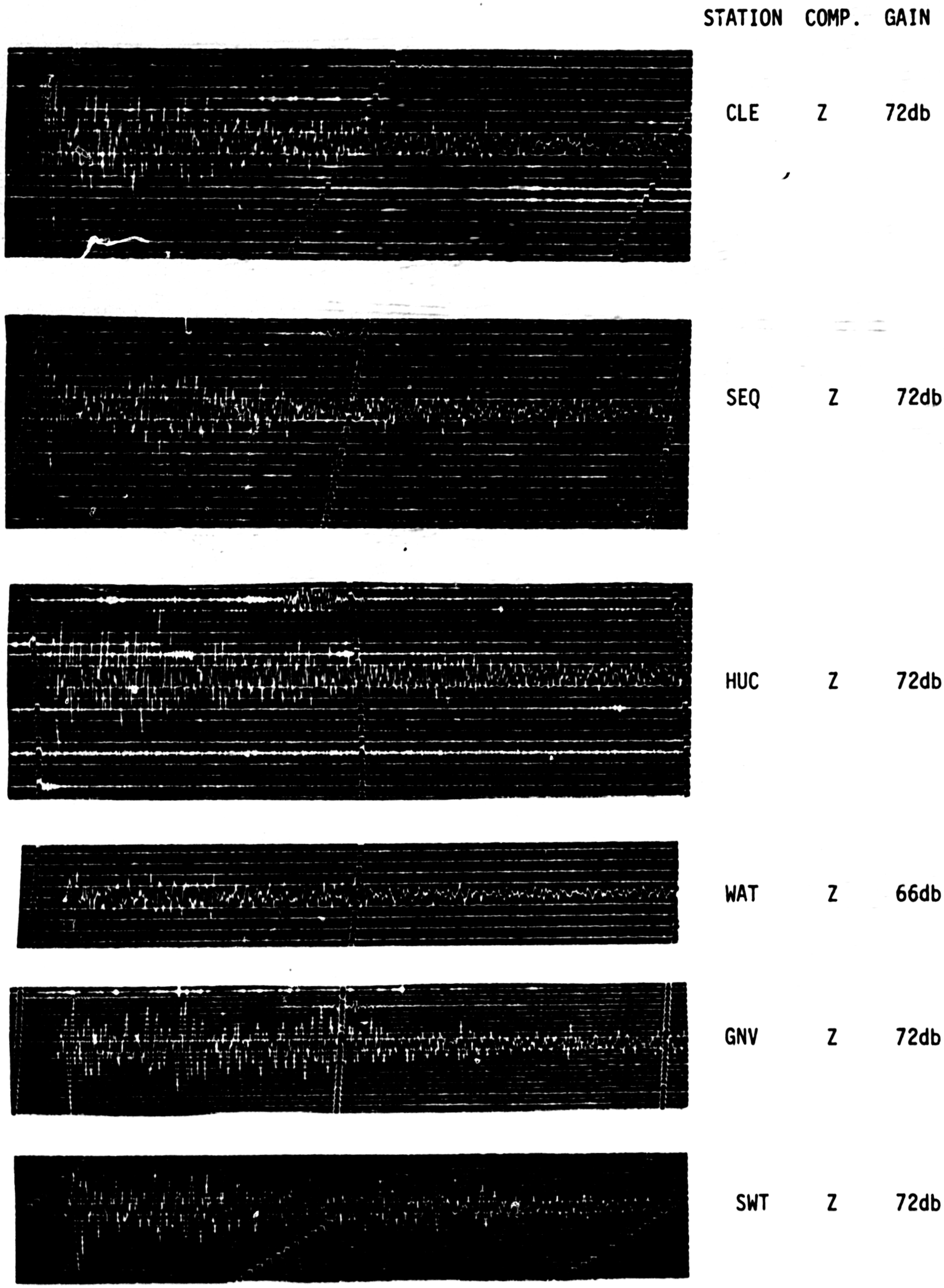

Figure A-4

11 JULY 1978 08:24(EDT)

STATION COMP. GAIN

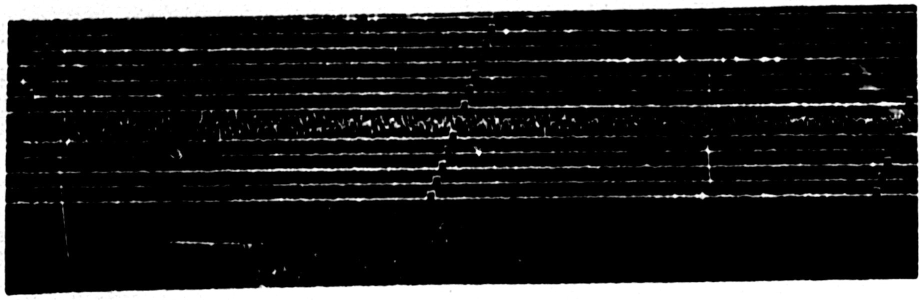

CLE Z 72db

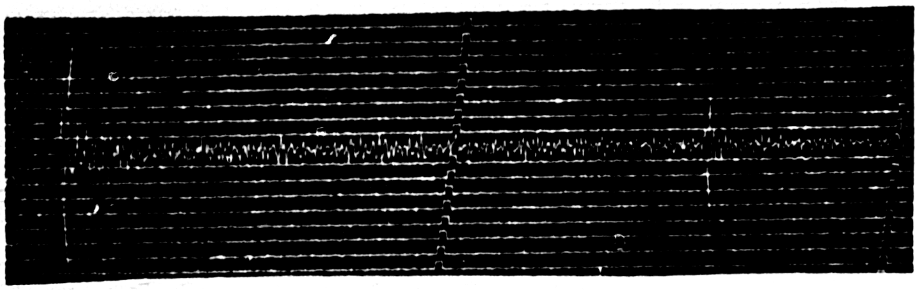

SEQ Z 72db

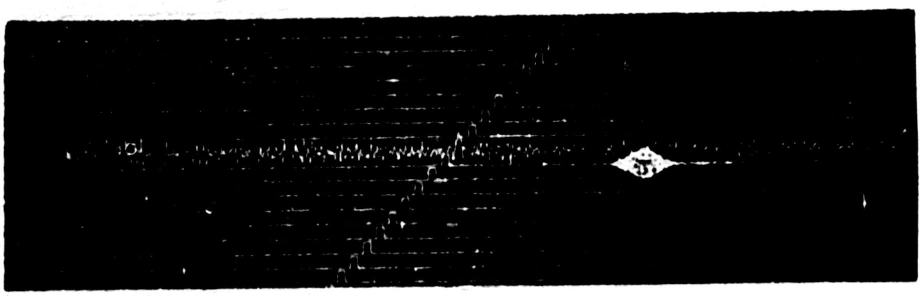

SEQ H (east-west) 72db

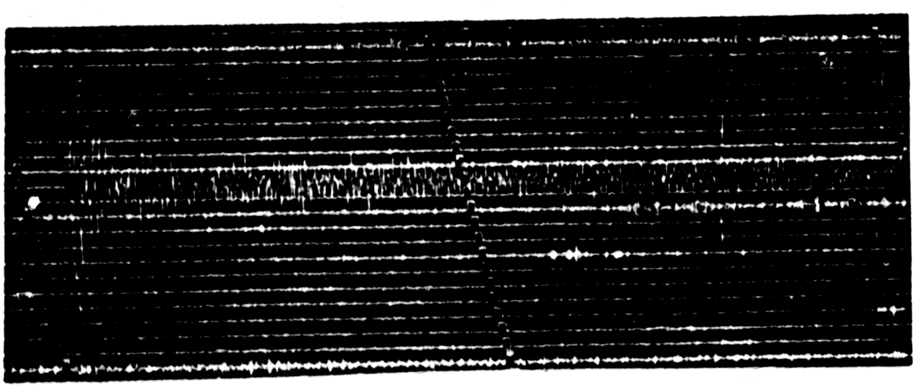

HUK Z 72db

Figure A-5a

11 JULY 1978 08:24(EDT)

STATION	COMP.	GAIN

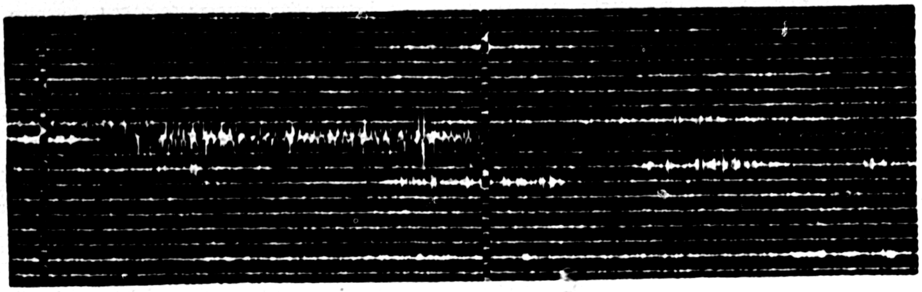

WAT	Z	66db

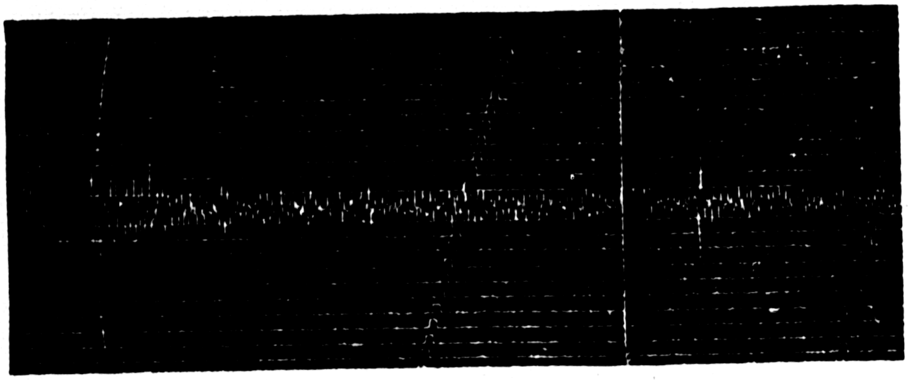

GNV	Z	72db

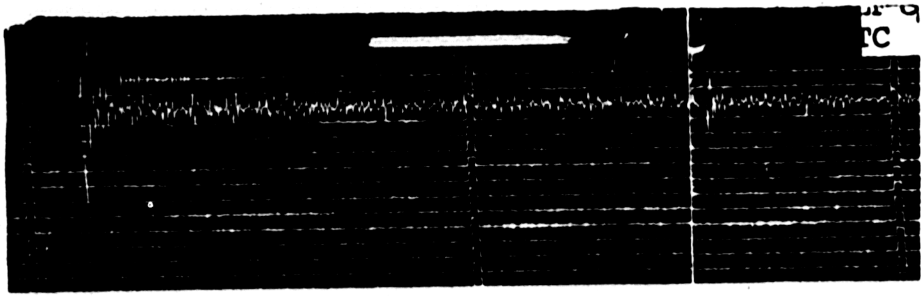

SWT	Z	72db

Figure A-5b

APPENDIX B

DIGITIZED TIME HISTORIES AND CORRECTED SPECTRA FOR EVENTS ANALYZED IN THE GROUND MOTION STUDY

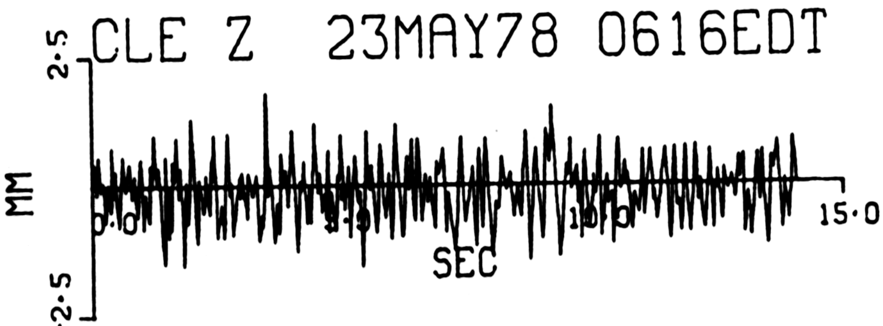

Figure B-1

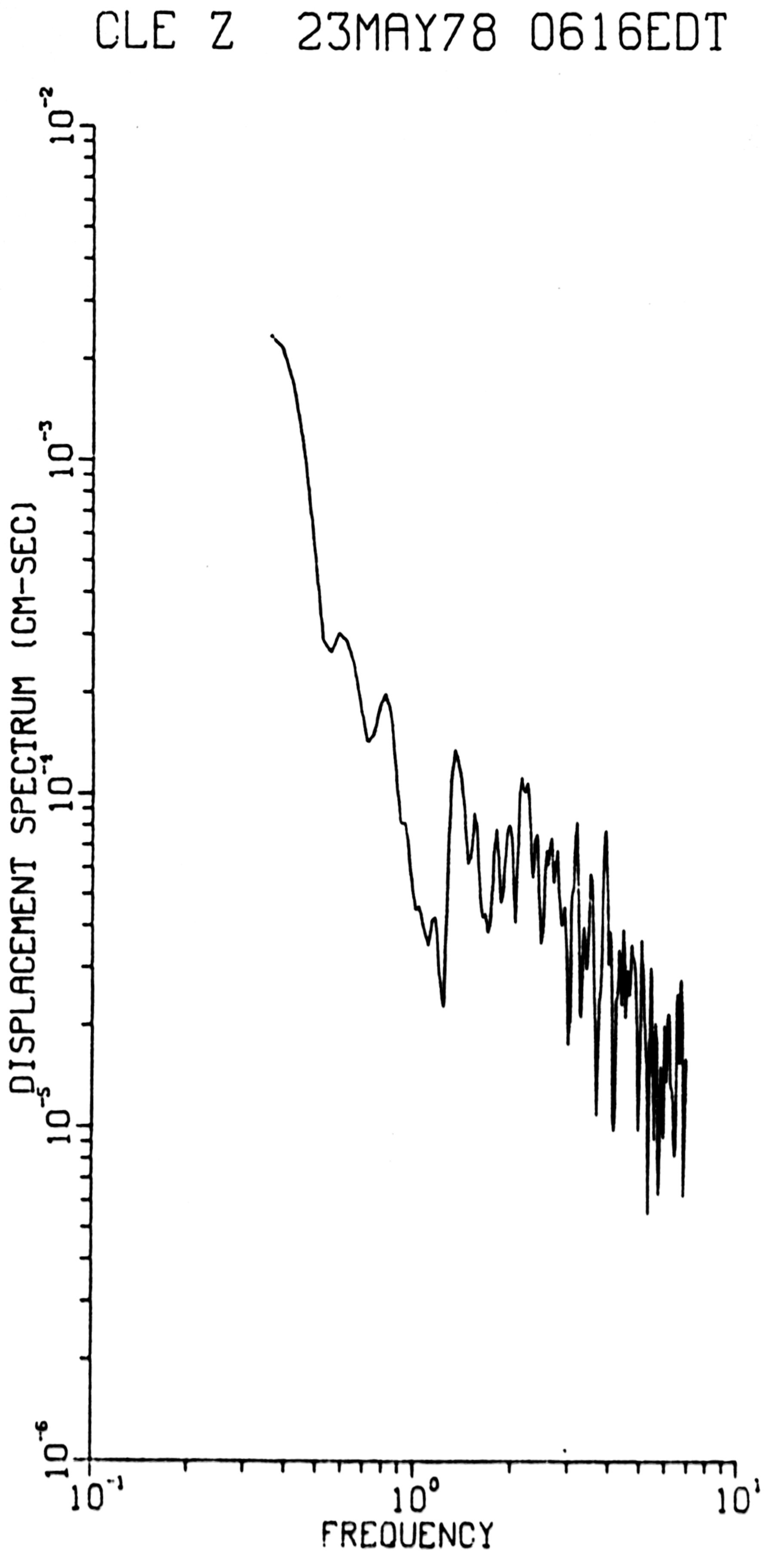

Figure B-2

Weston Geophysical

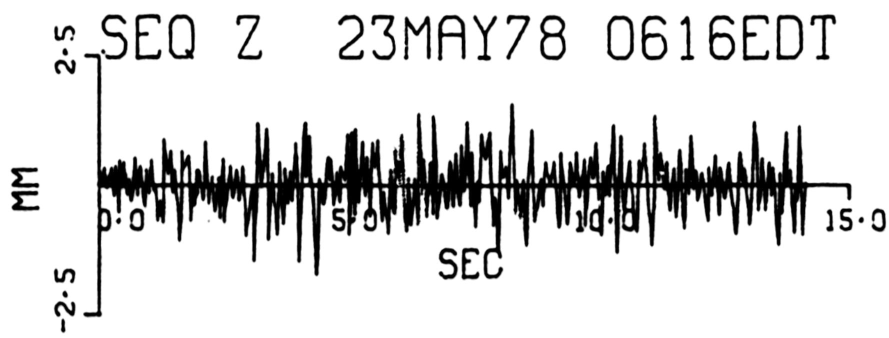

Figure B-3

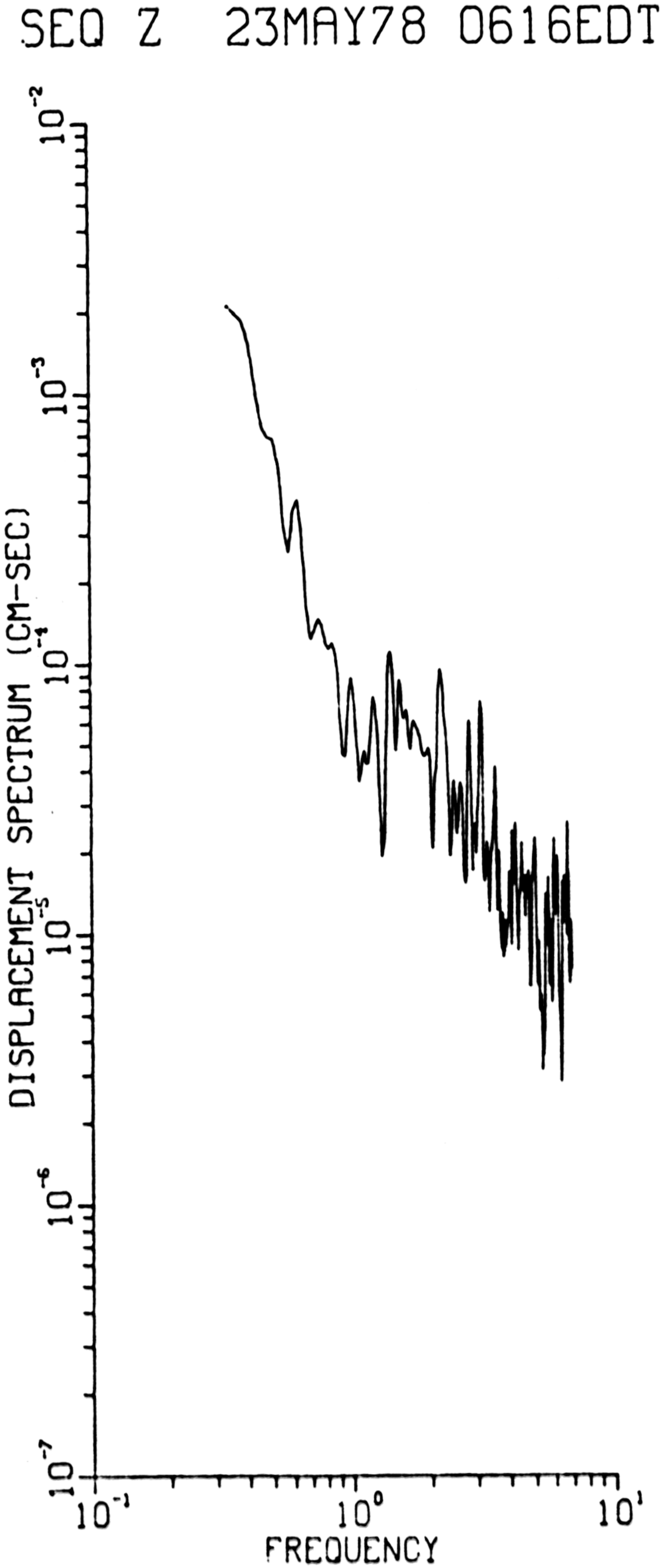

Figure B-4

Weston Geophysical

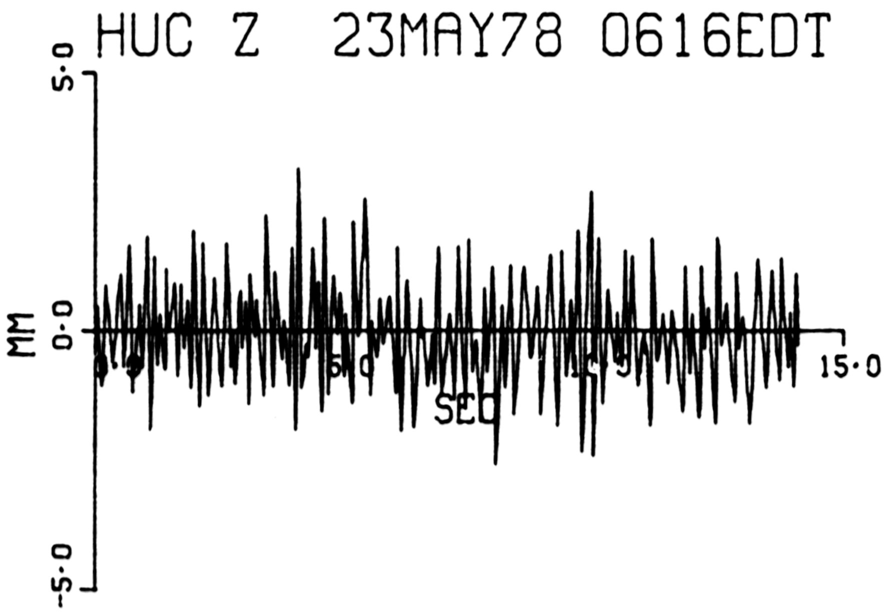

Figure B-5

Weston Geophysical

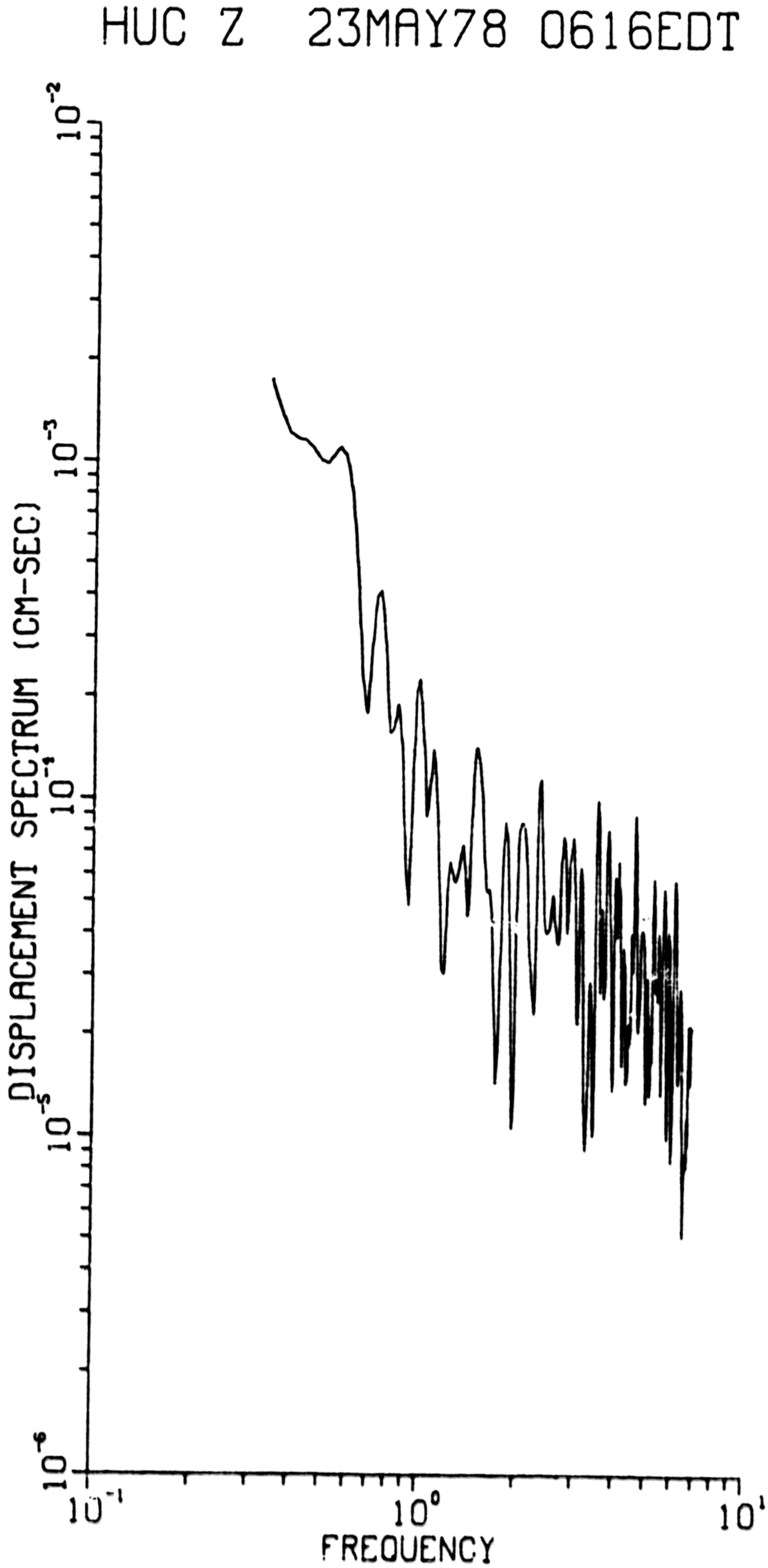

Figure B-6

Weston Geophysical

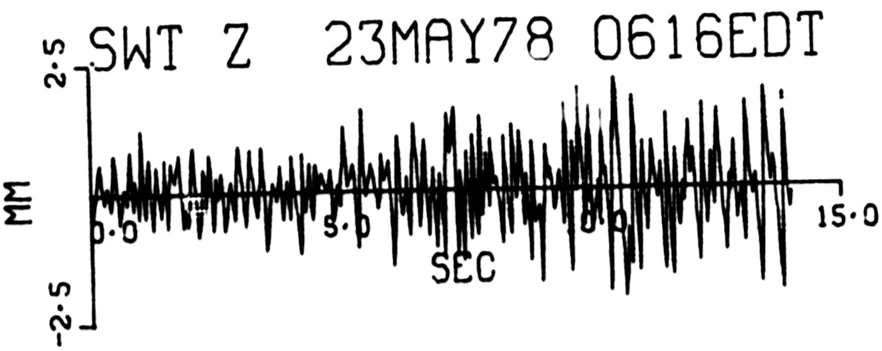

Figure B-7

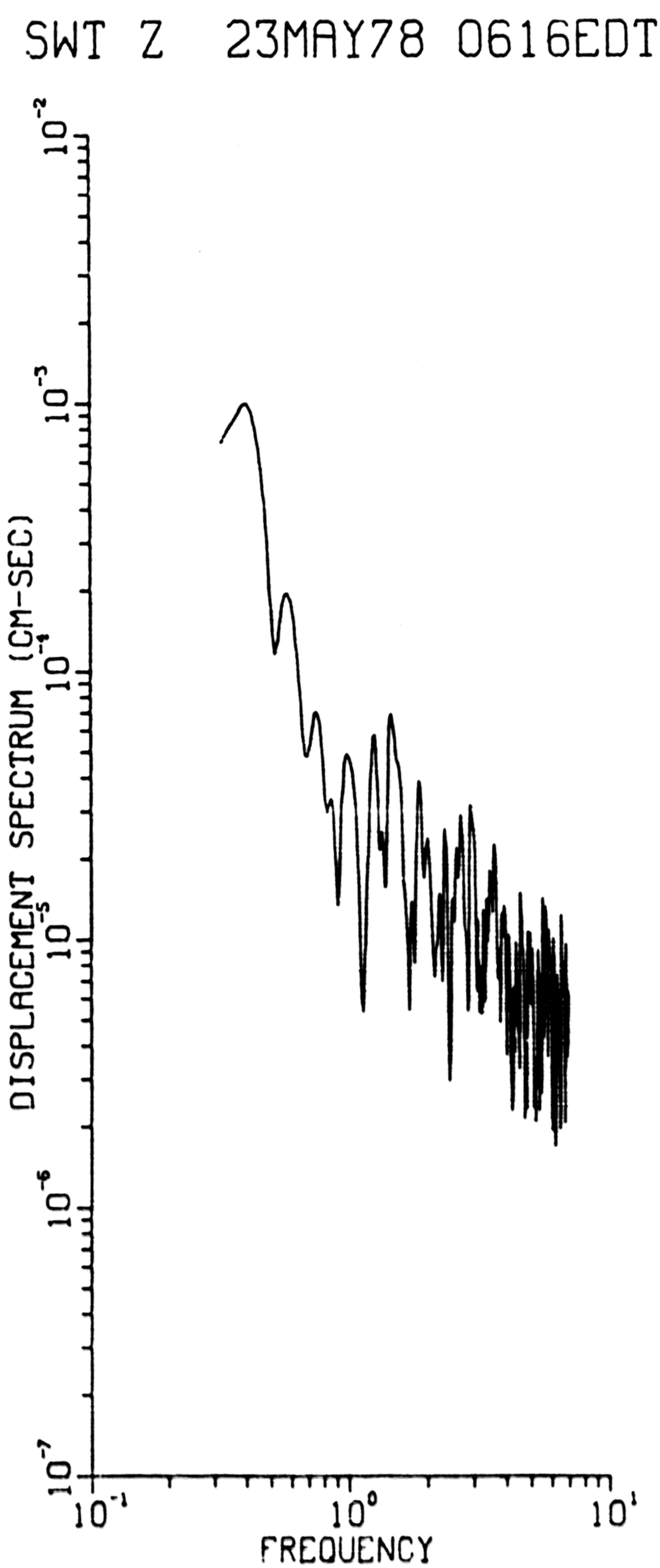

Figure B-8

Weston Geophysical

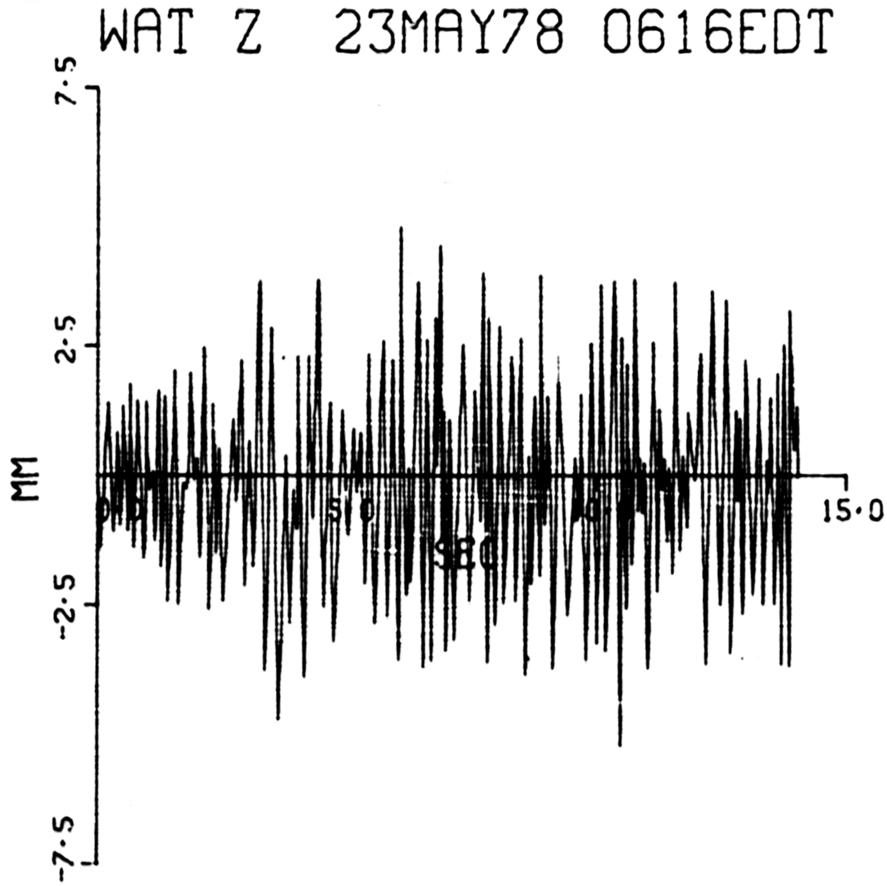

Figure B-9

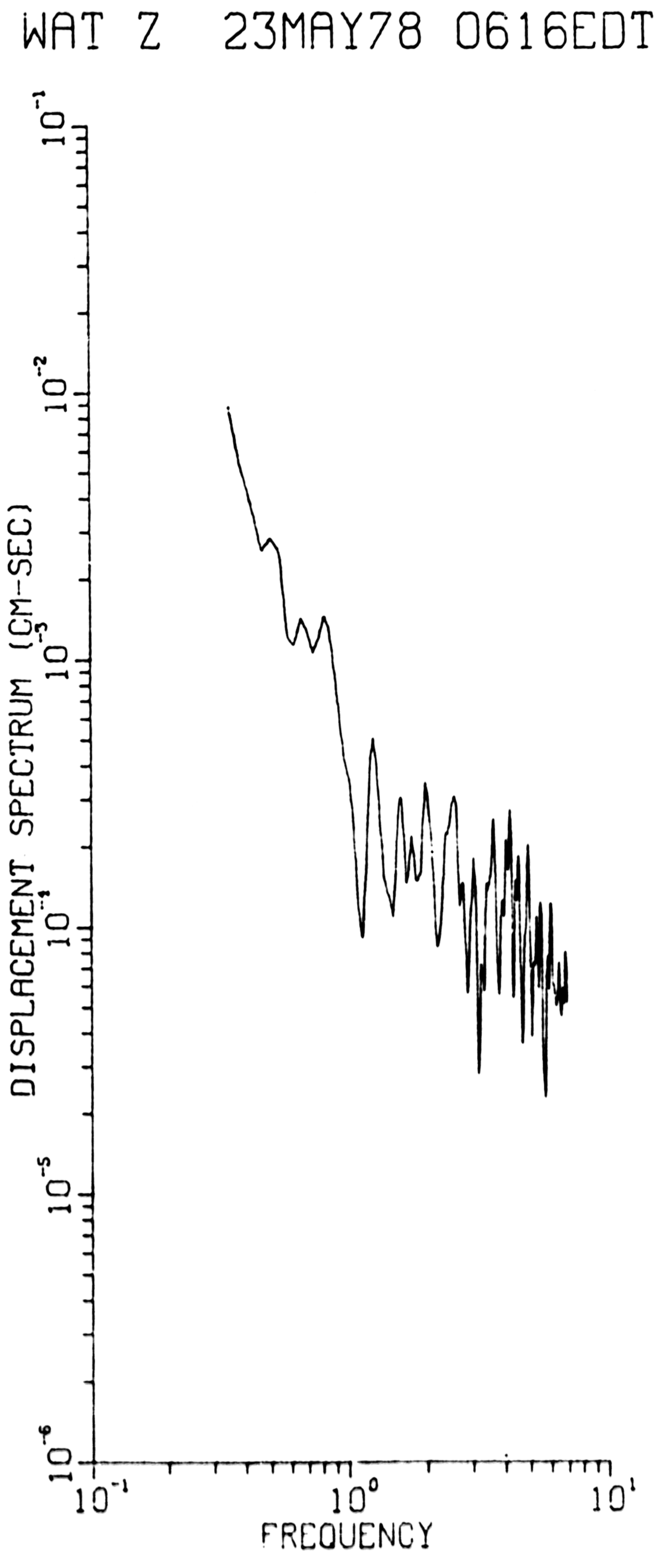

Figure B-10

Weston Geophysical

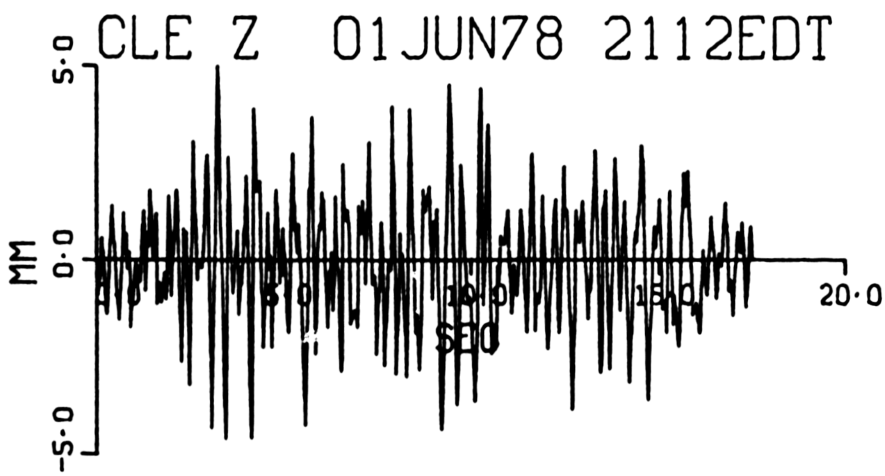

Figure B-11

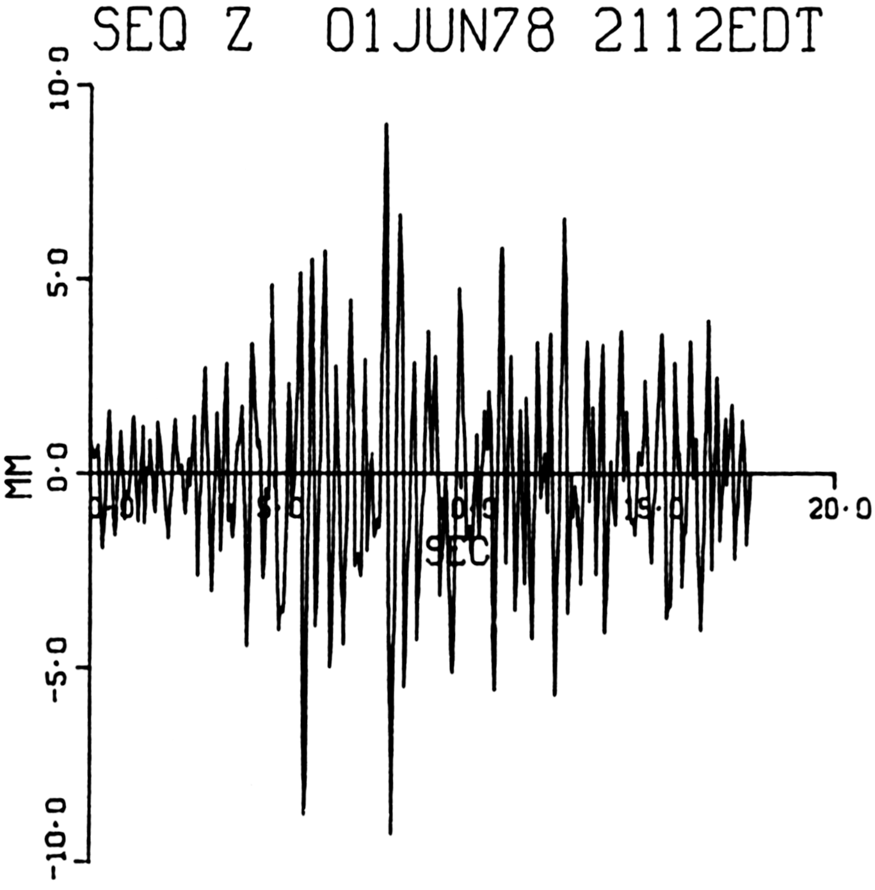

Figure B-13

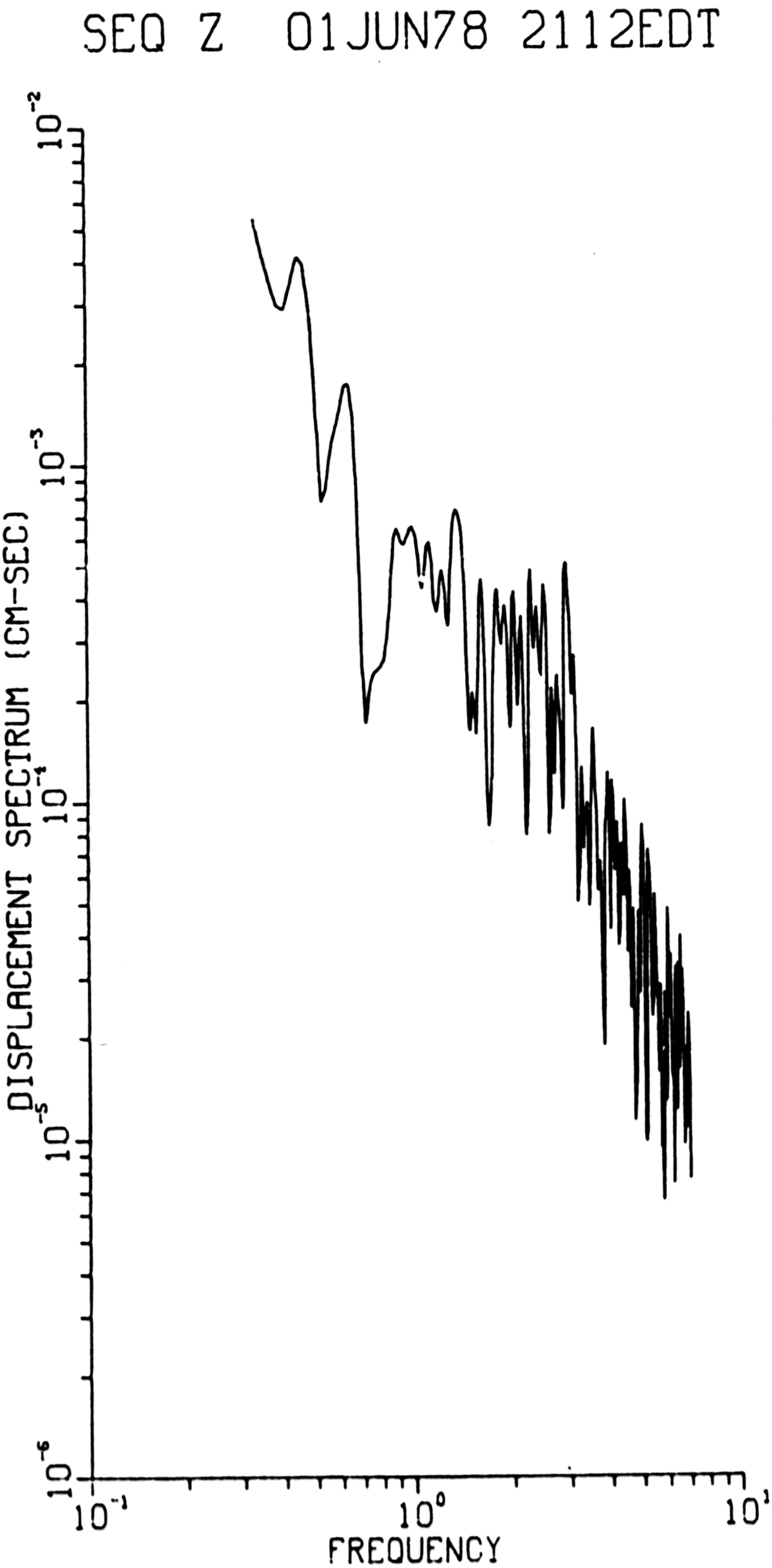

Figure B-14

Weston Geophysical

HUC Z 01JUN78 2112EDT

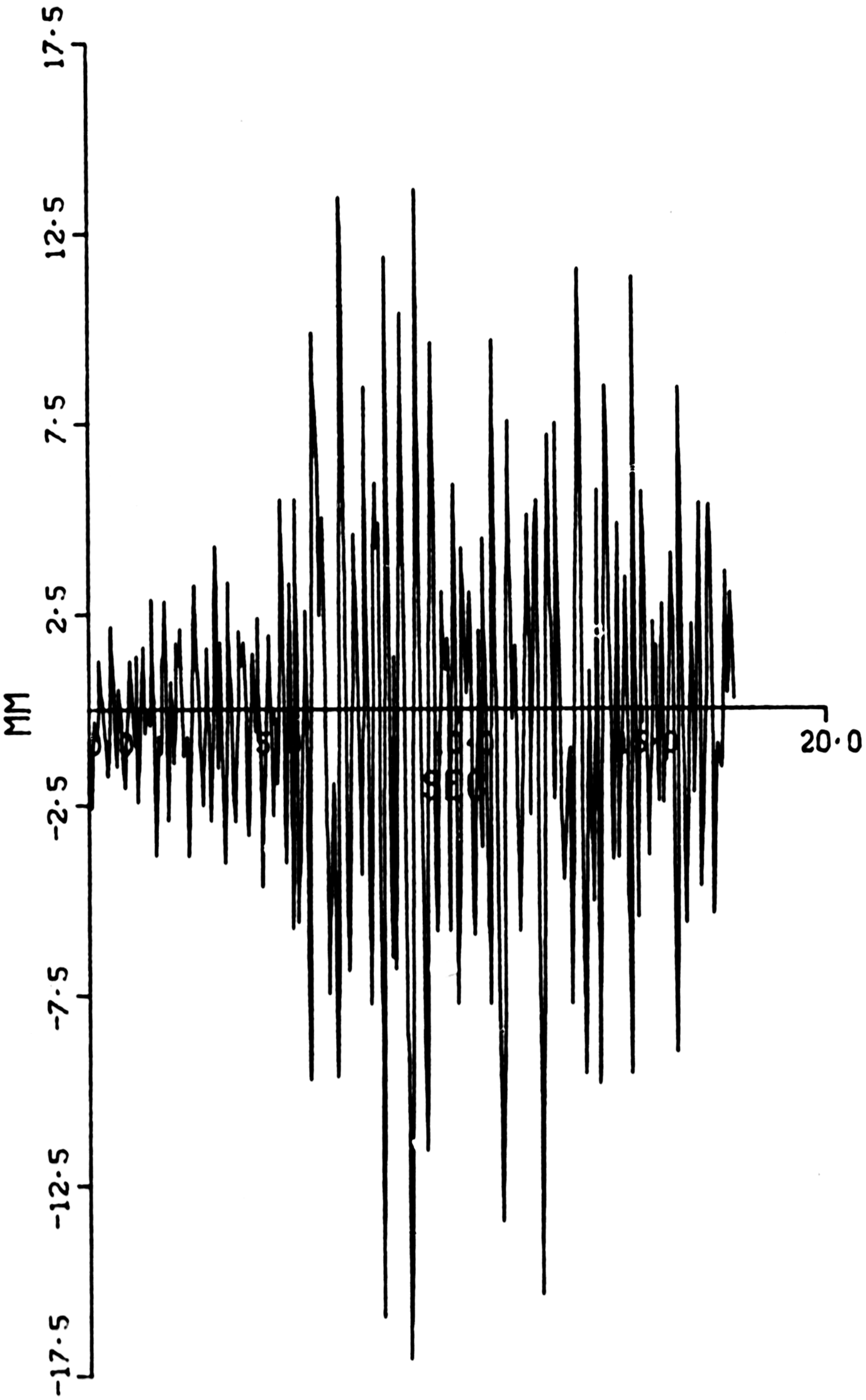

Figure B-15

Weston Geophysical

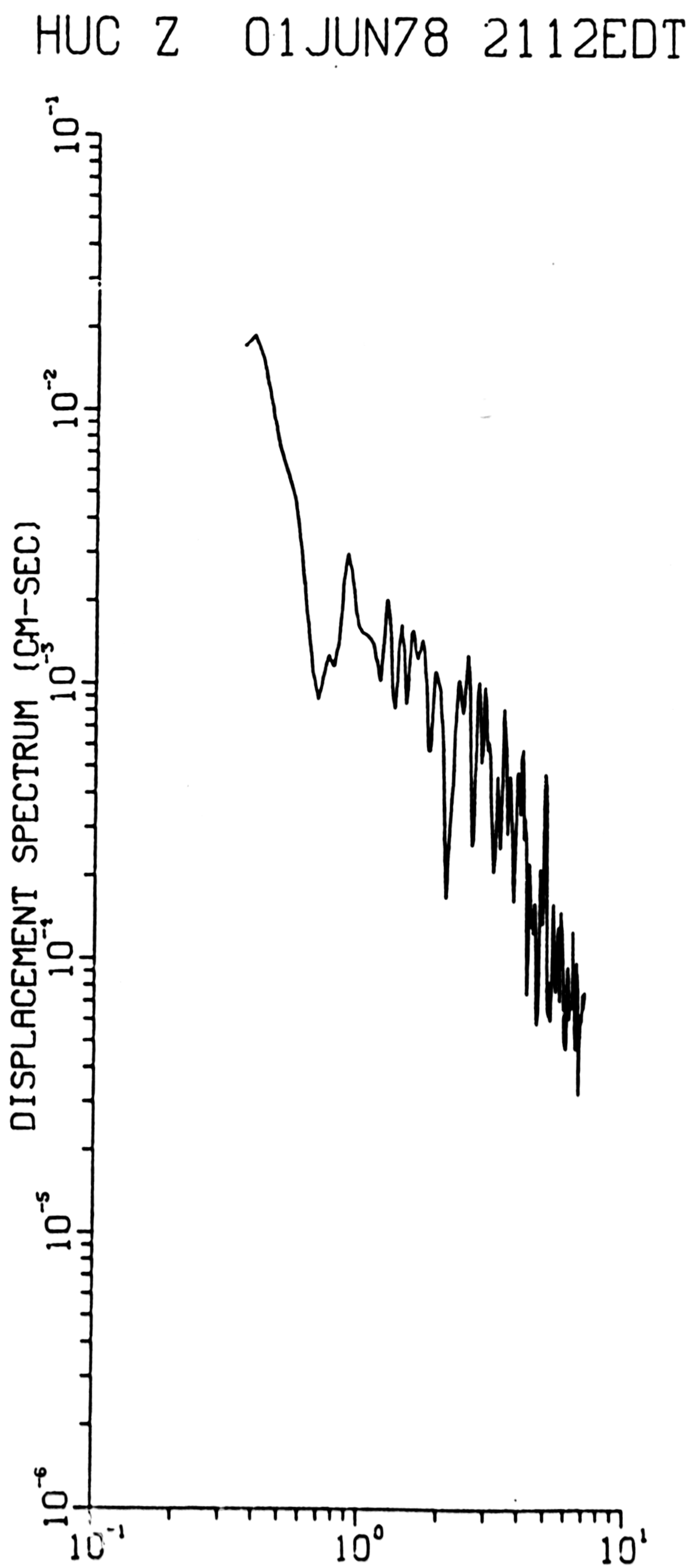

Figure B-16

Weston Geophysical

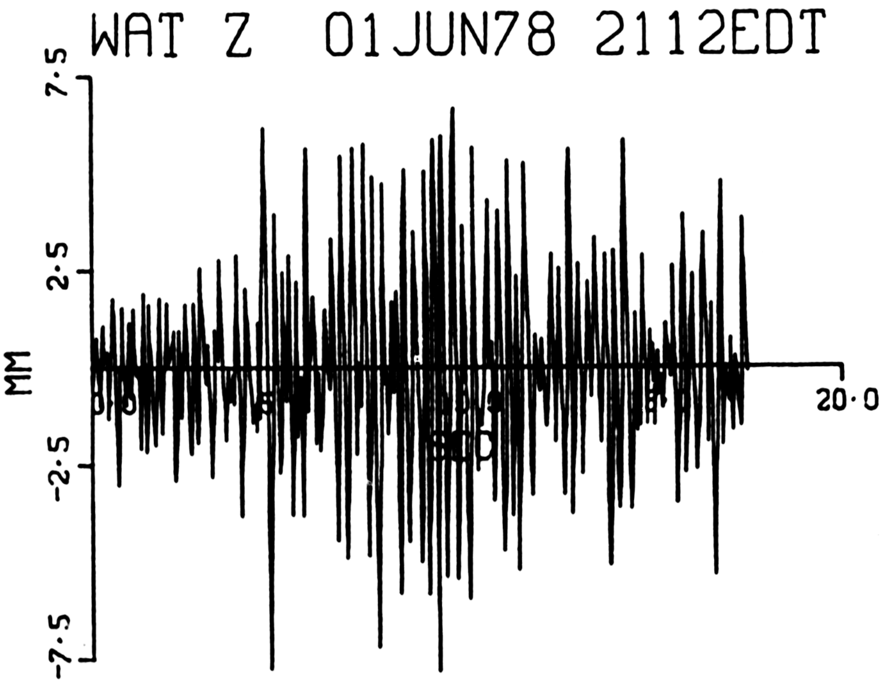

Figure B-17

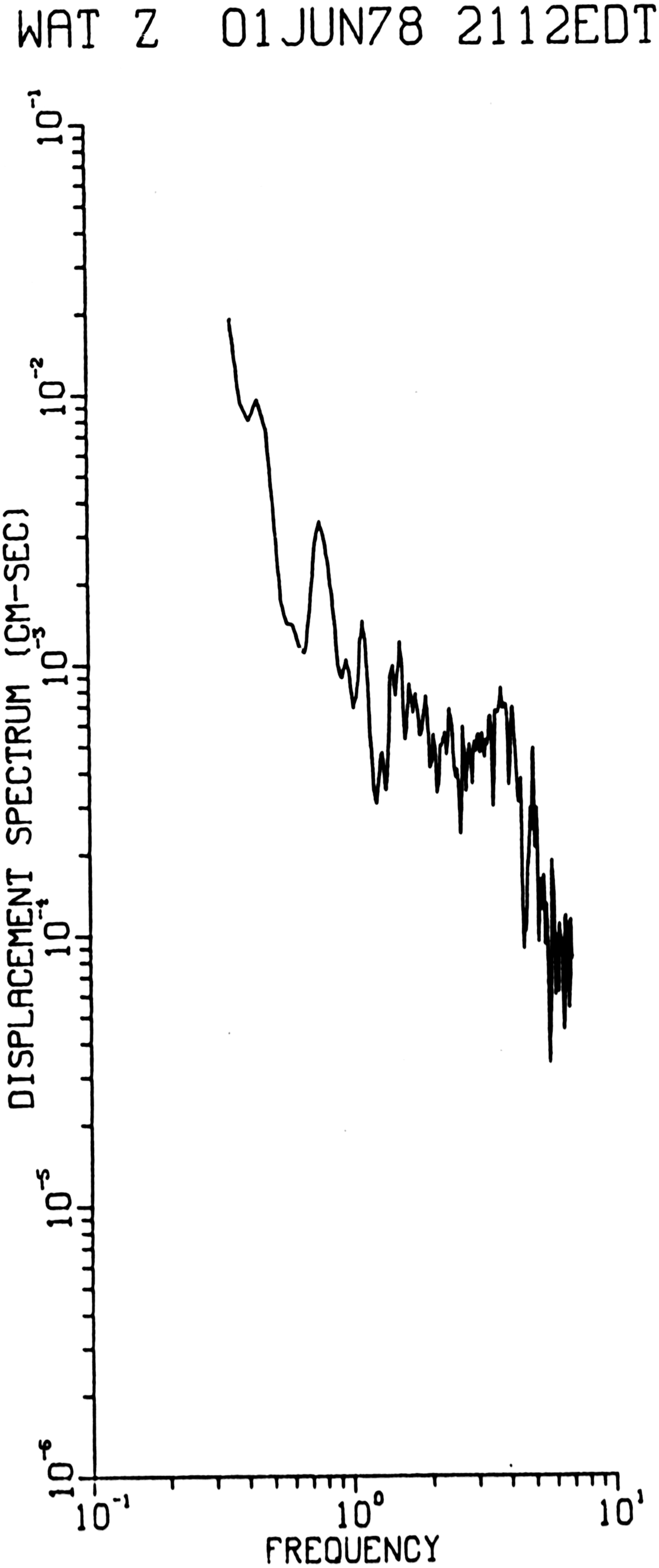

Figure B-18

Weston Geophysical

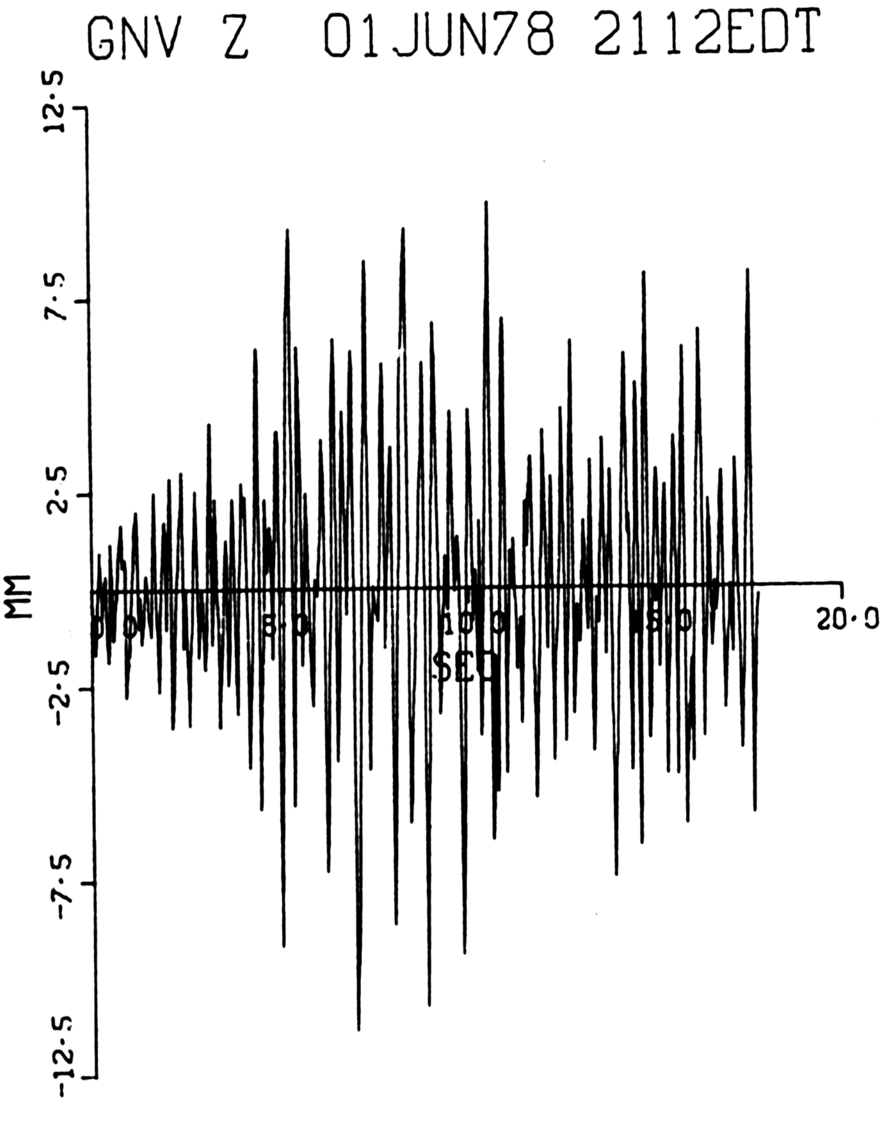

Figure B-19

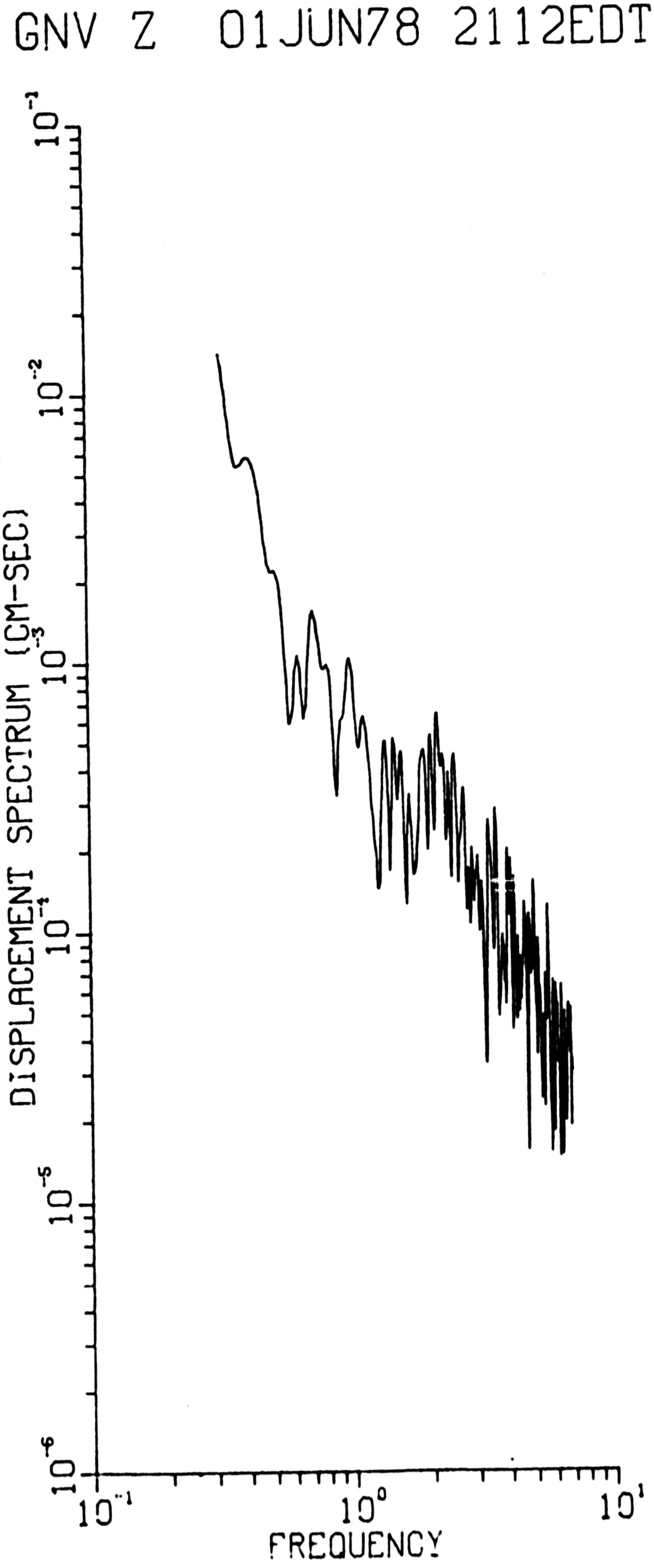

Figure B-20

Weston Geophysical

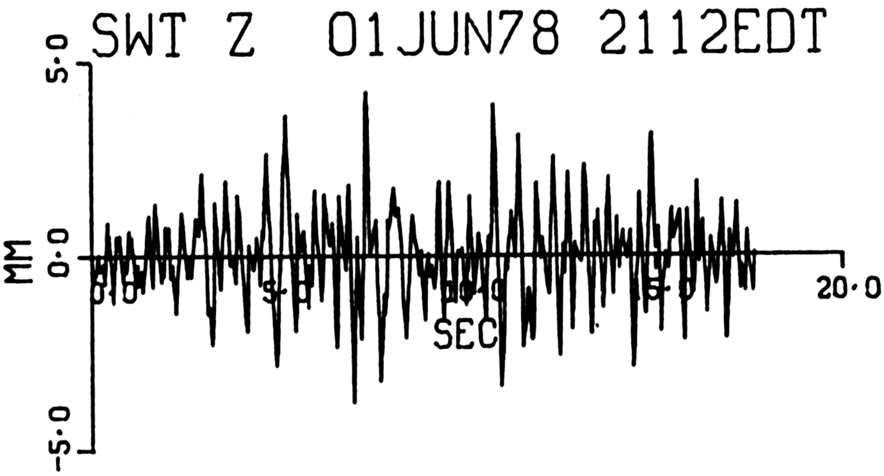

Figure B-21

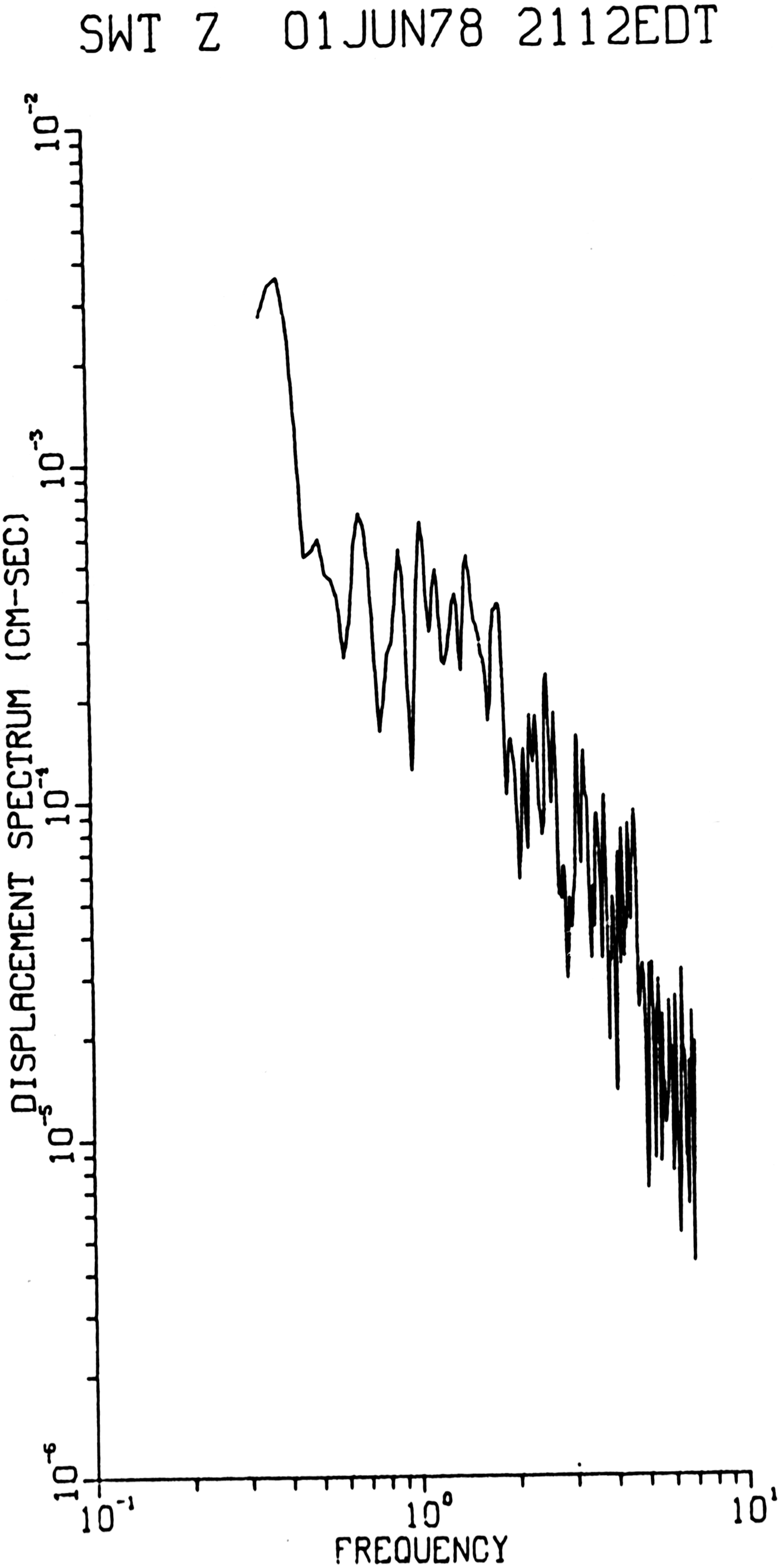

Figure B-22

Weston Geophysical

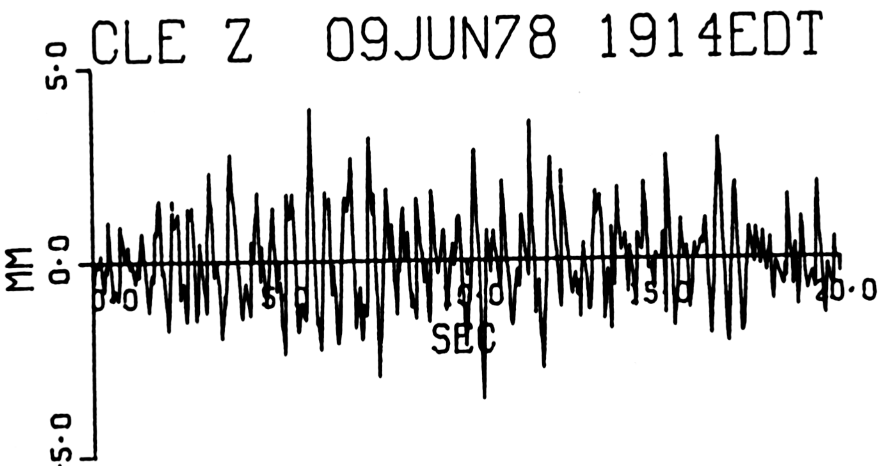

Figure B-23

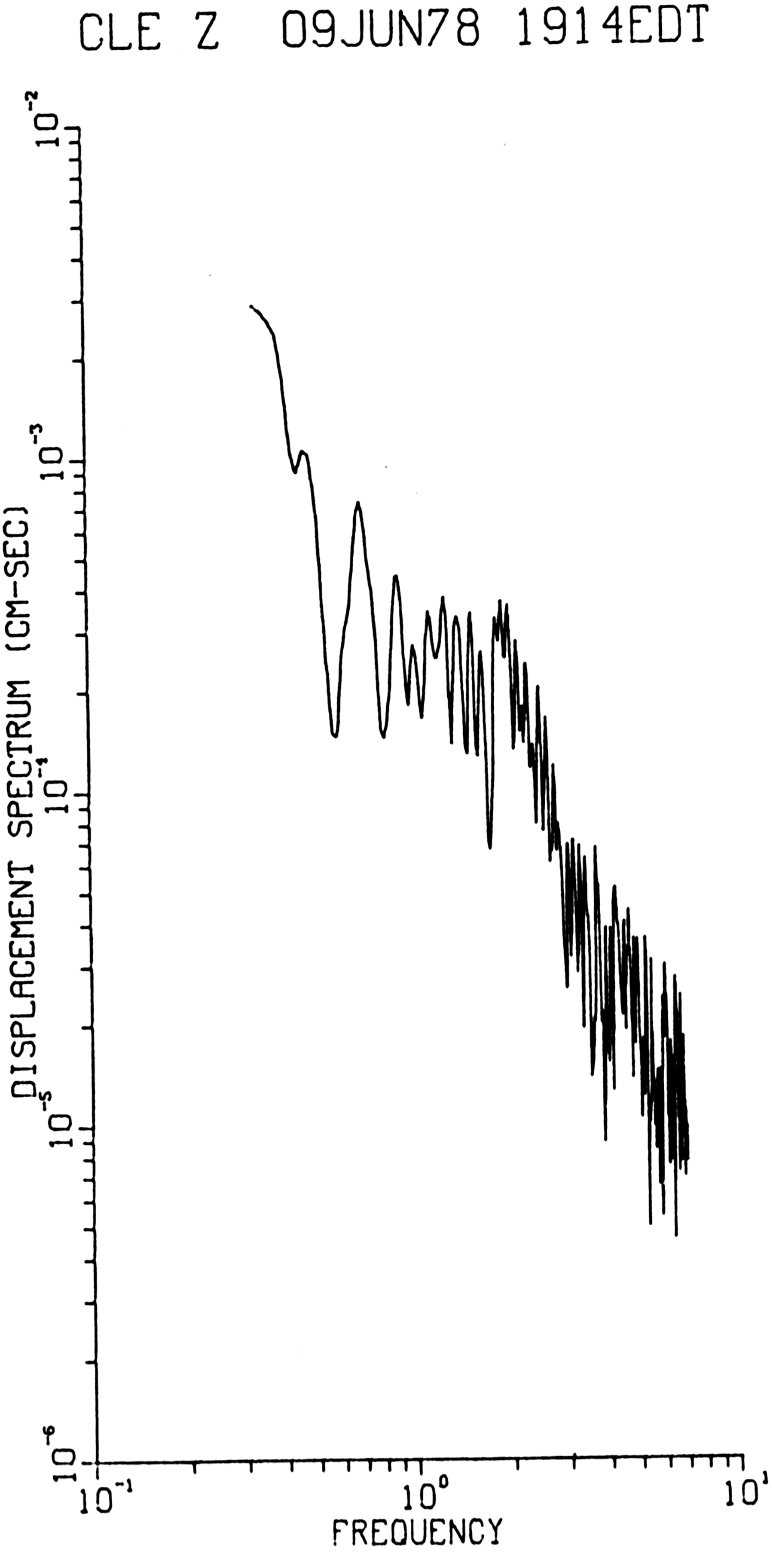

Figure B-24

Weston Geophysical

Figure B-25

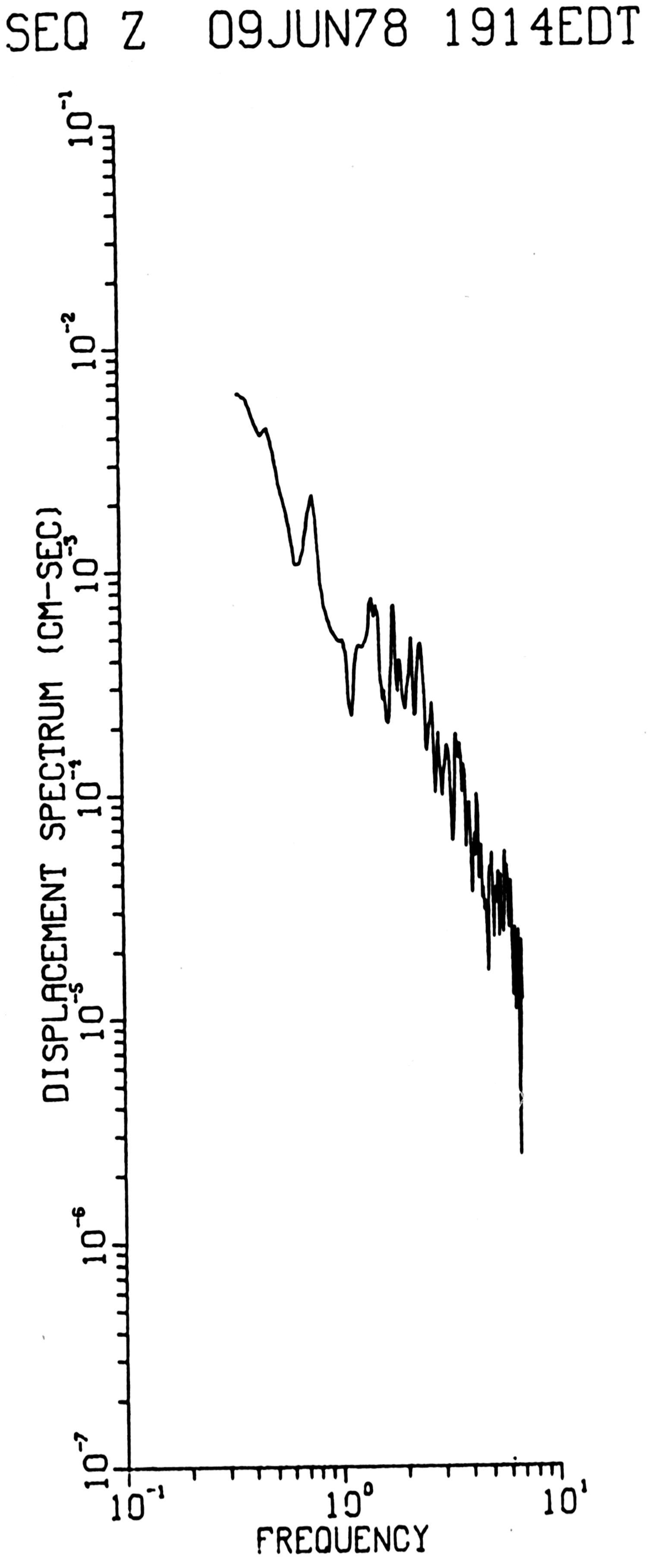

Figure B-26

Weston Geophysical

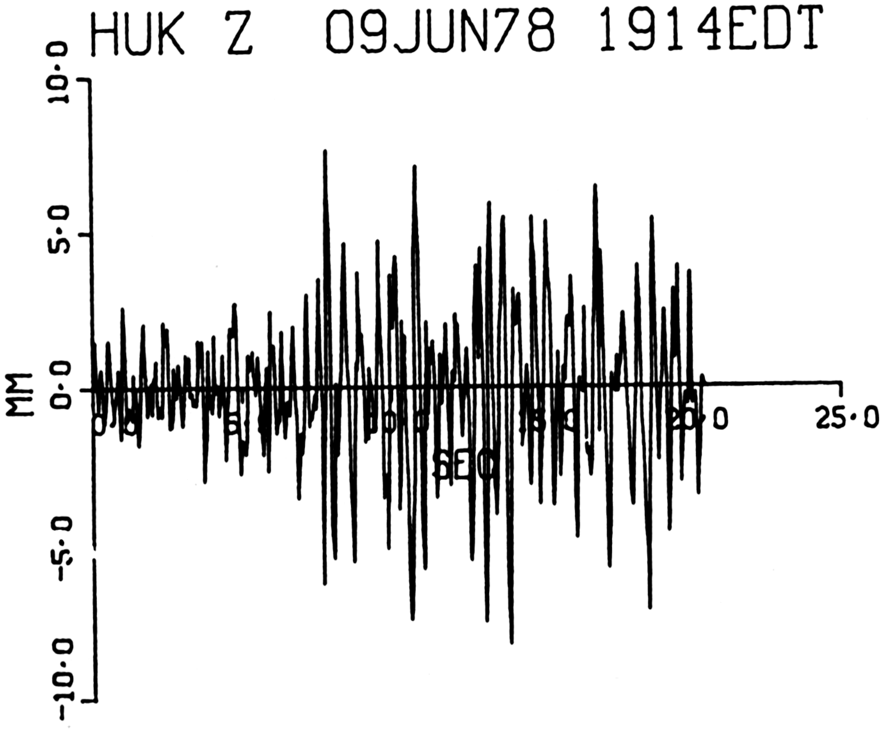
HUK Z 09JUN78 1914EDT
10.0
5.0
0.0
-5.0
-10.0
MM
0.0
5.0
10.0
15.0
20.0
25.0
SEC

Figure B-27

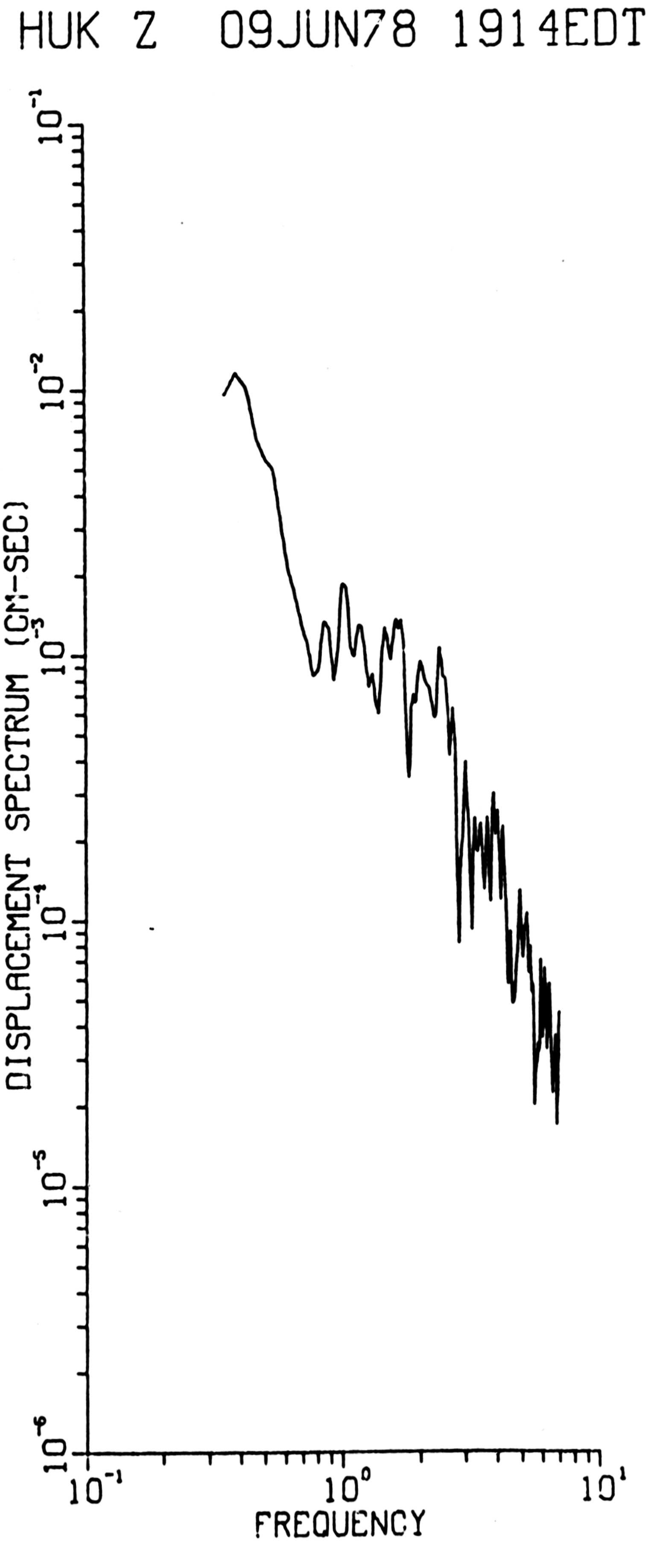

Figure B-28

Weston Geophysical

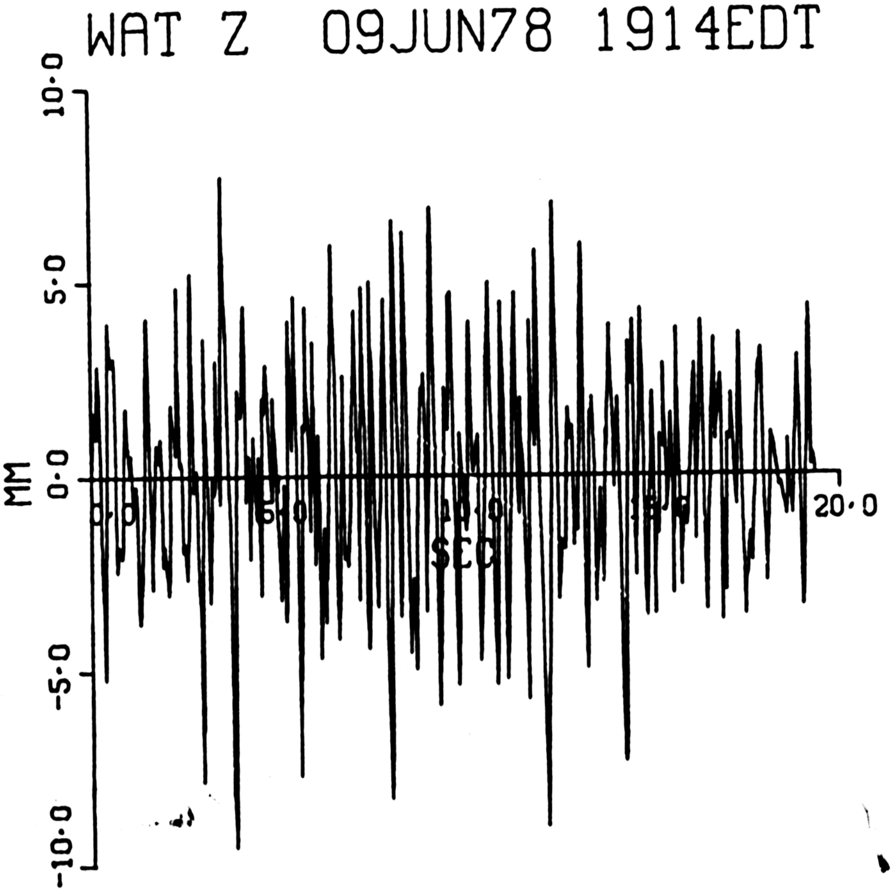

Figure B-29

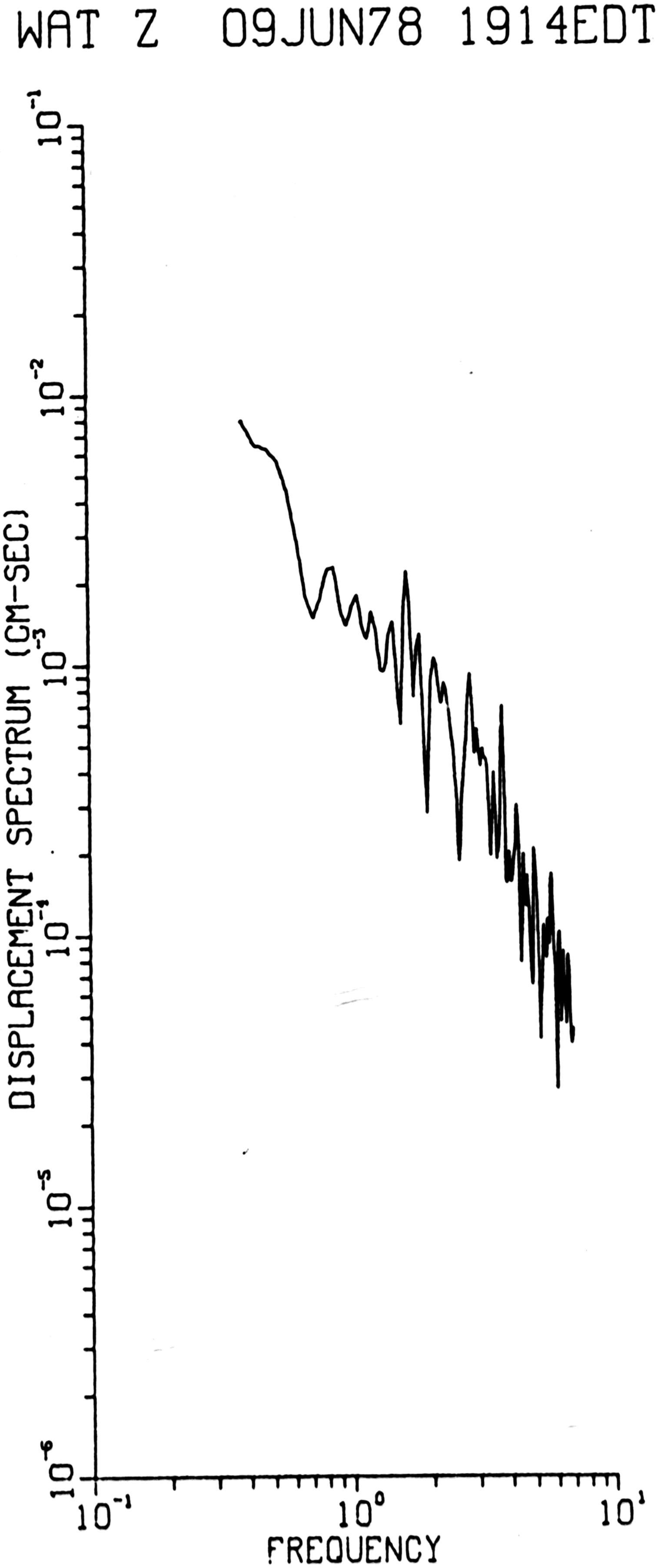

Figure B-30
Weston Geophysical

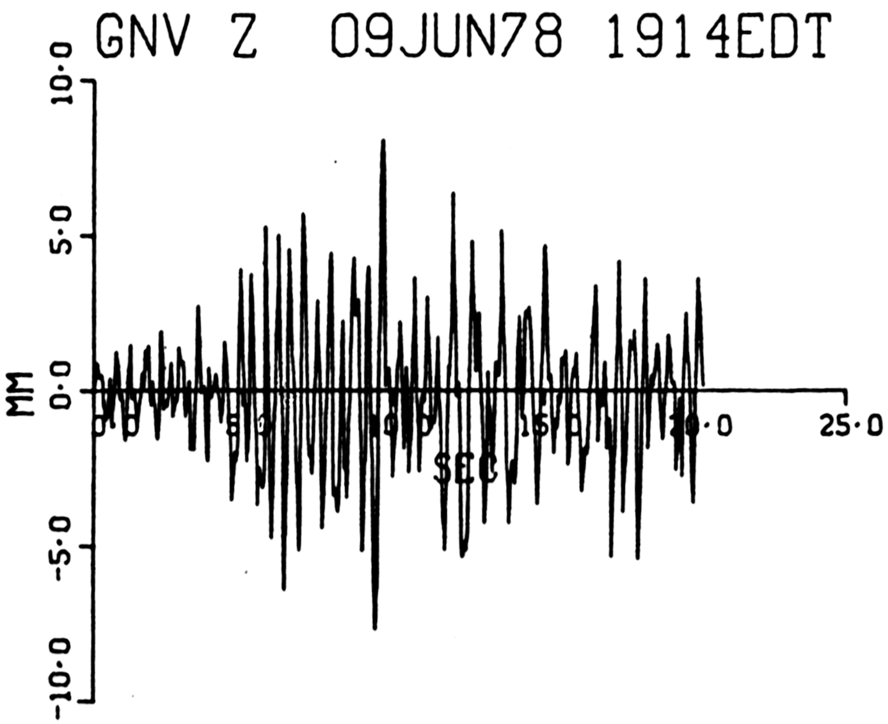
GNV Z 09JUN78 1914EDT
10.0
5.0
0.0
-5.0
-10.0
MM
0.0
5.0
10.0
15.0
20.0
25.0
SEC

Figure B-31

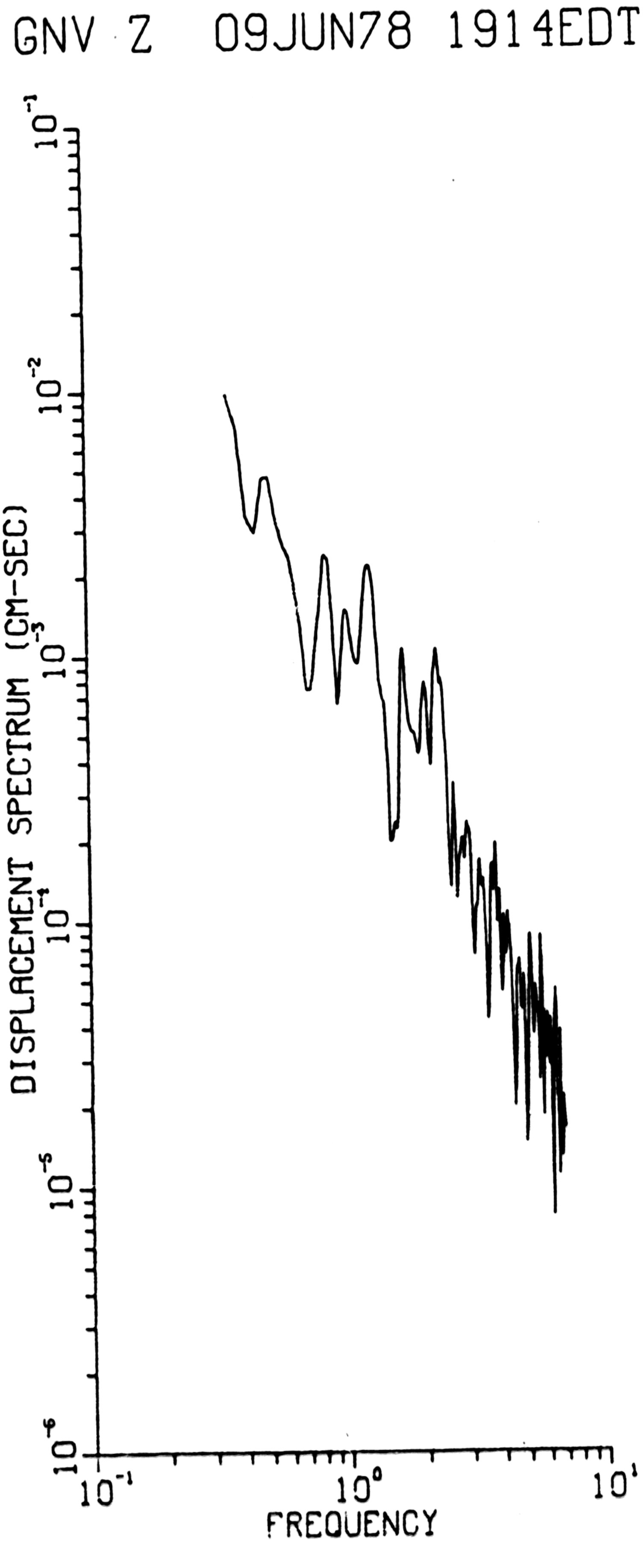

Figure B-32

Weston Geophysical

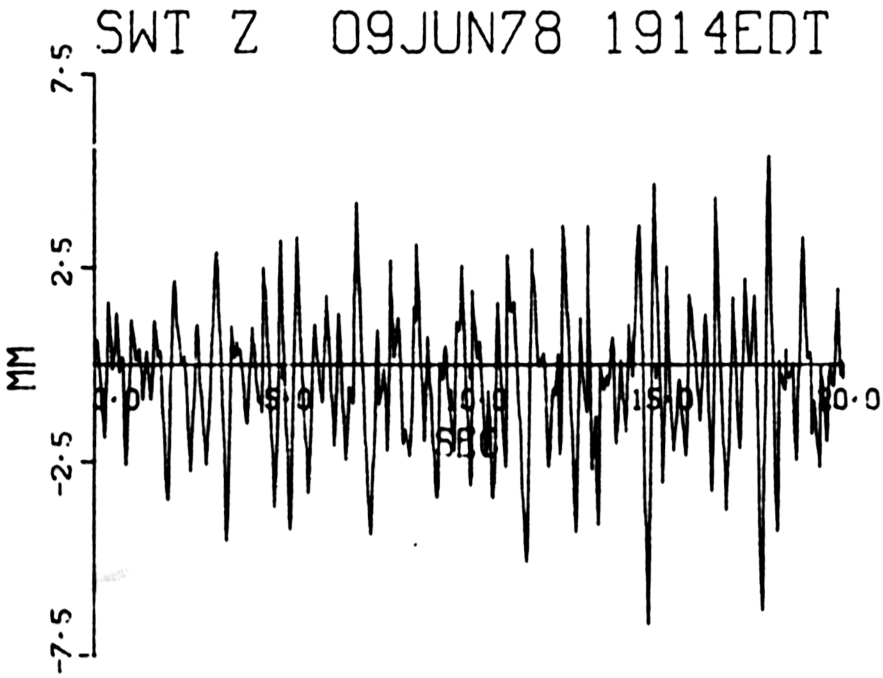

Figure B-33

SWT Z 09JUN78 1914EDT

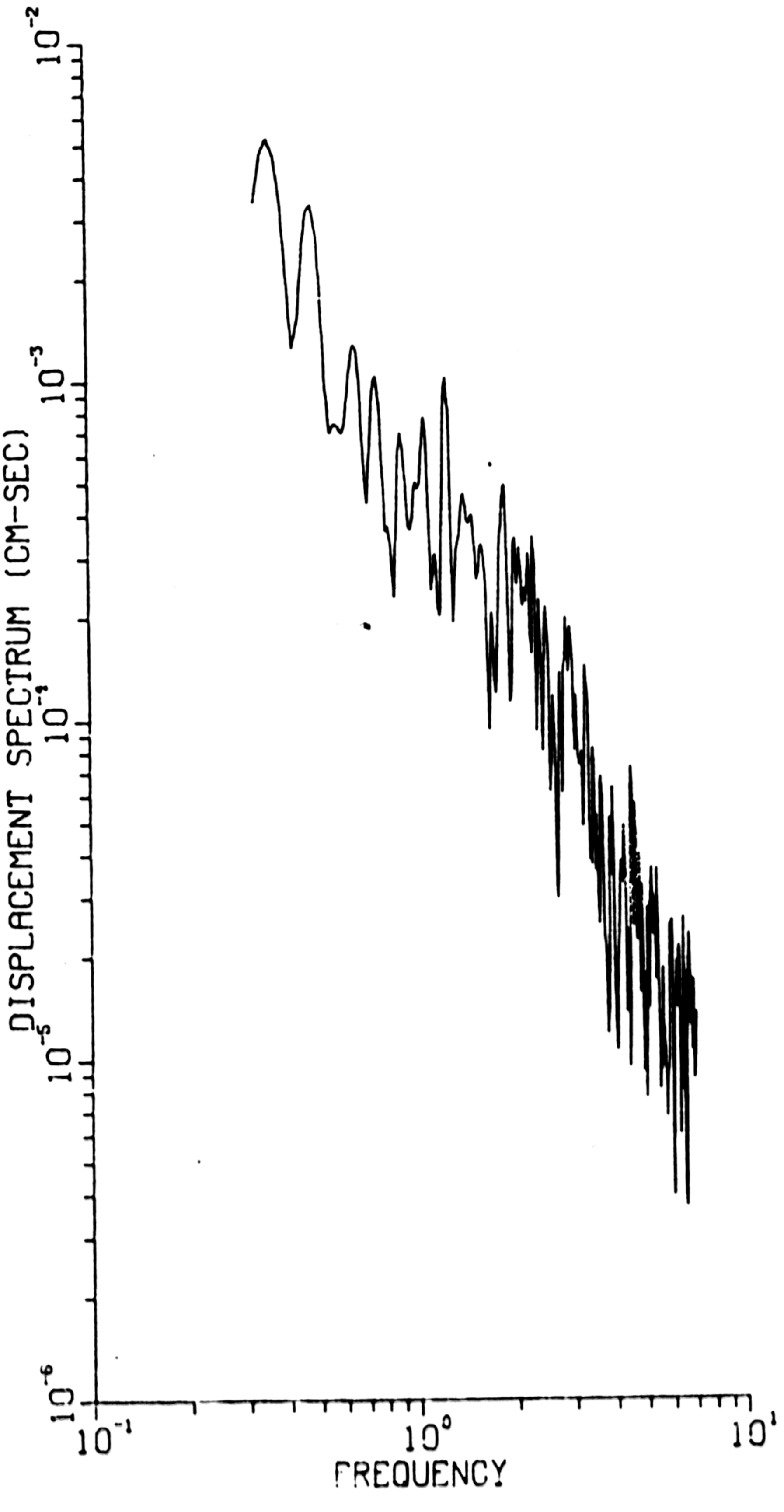

Figure B-34

Weston Geophysical

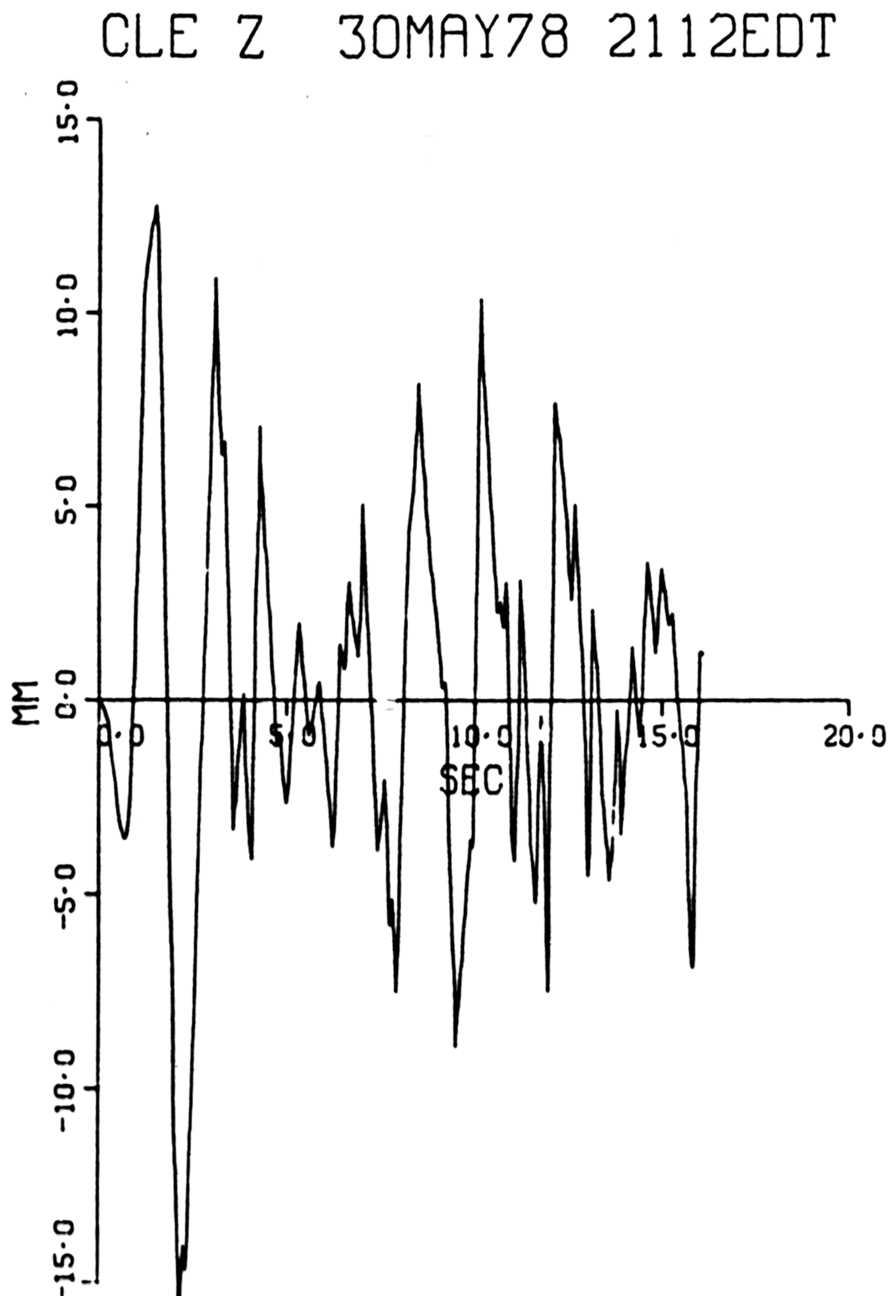
CLE Z 30MAY78 2112EDT
15.0
10.0
5.0
0.0
-5.0
-10.0
-15.0
MM
0.0
5.0
10.0
15.0
20.0
SEC

Figure B-35

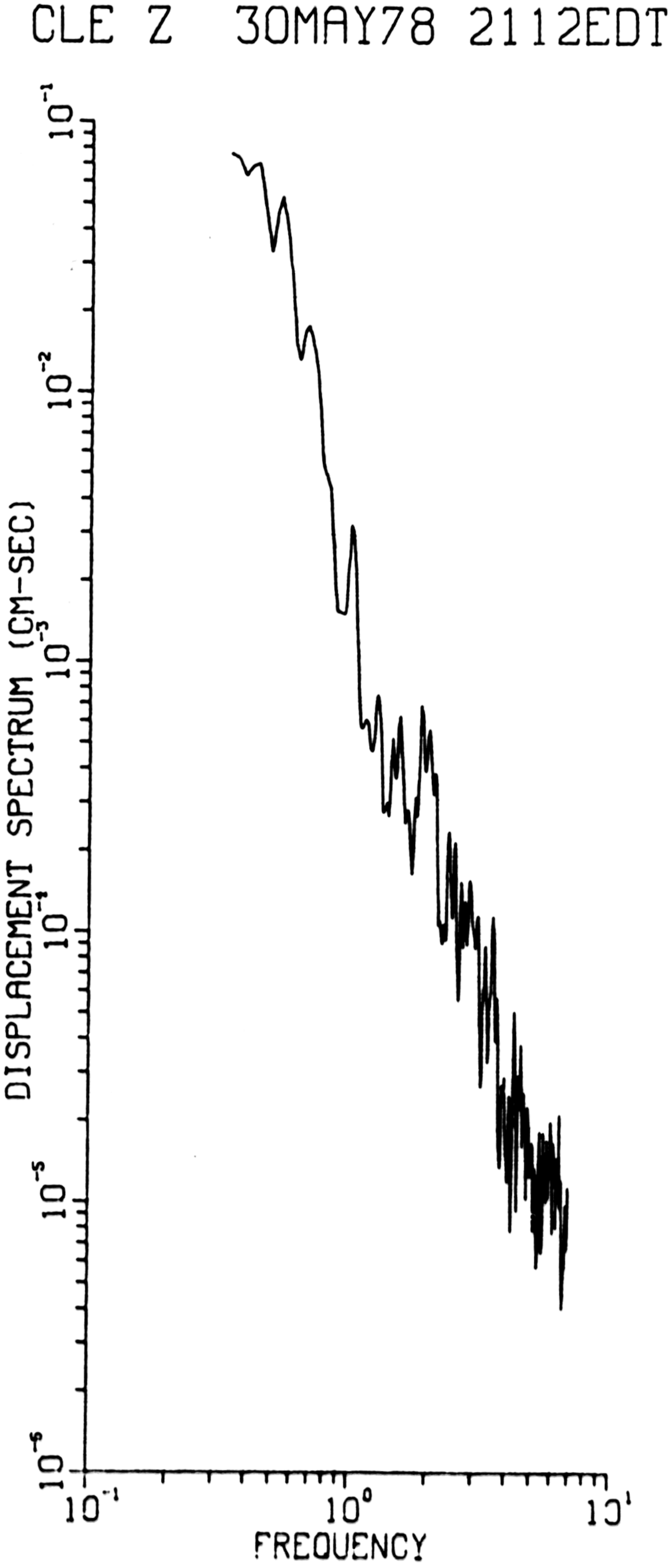

Figure B-36

Weston Geophysical

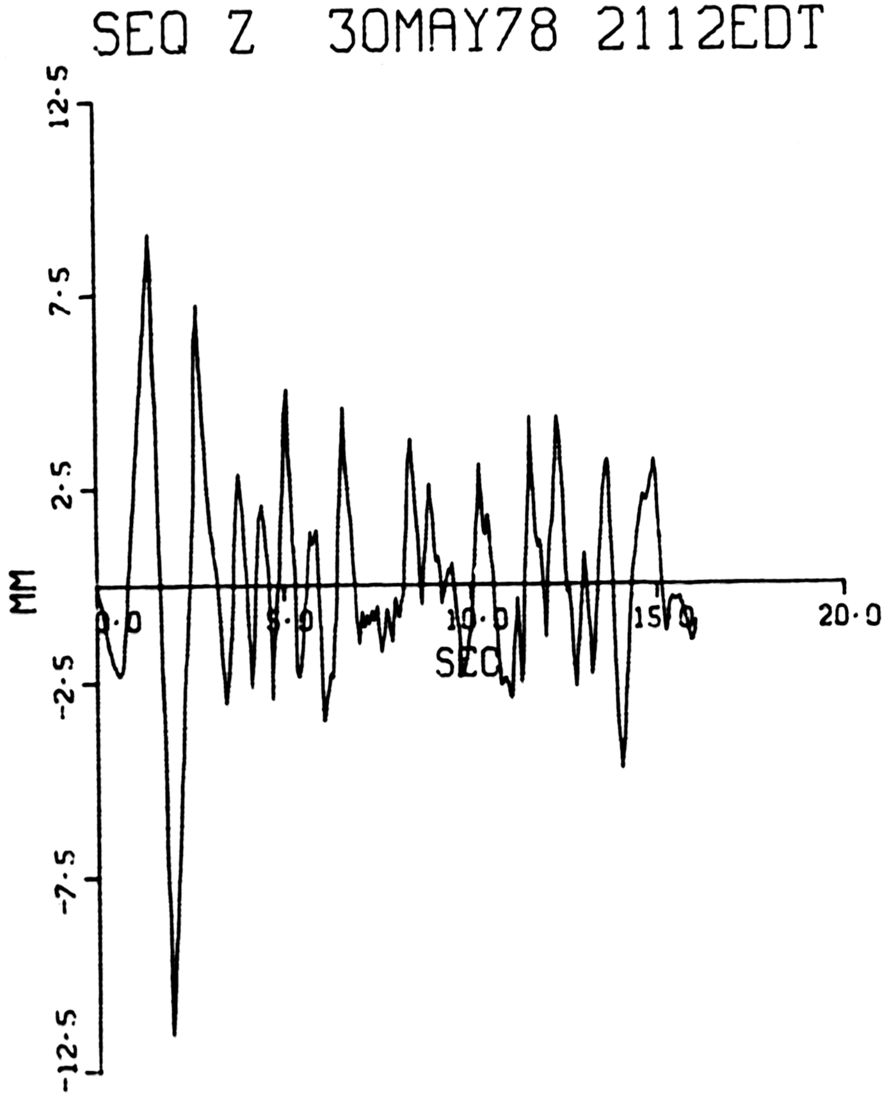
SEQ Z 30MAY78 2112EDT
12·5
7·5
2·5
-2·5
-7·5
-12·5
MM
0·0
5·0
10·0
15·0
20·0
SEC

Figure B-37

SEQ Z 30MAY78 2112EDT

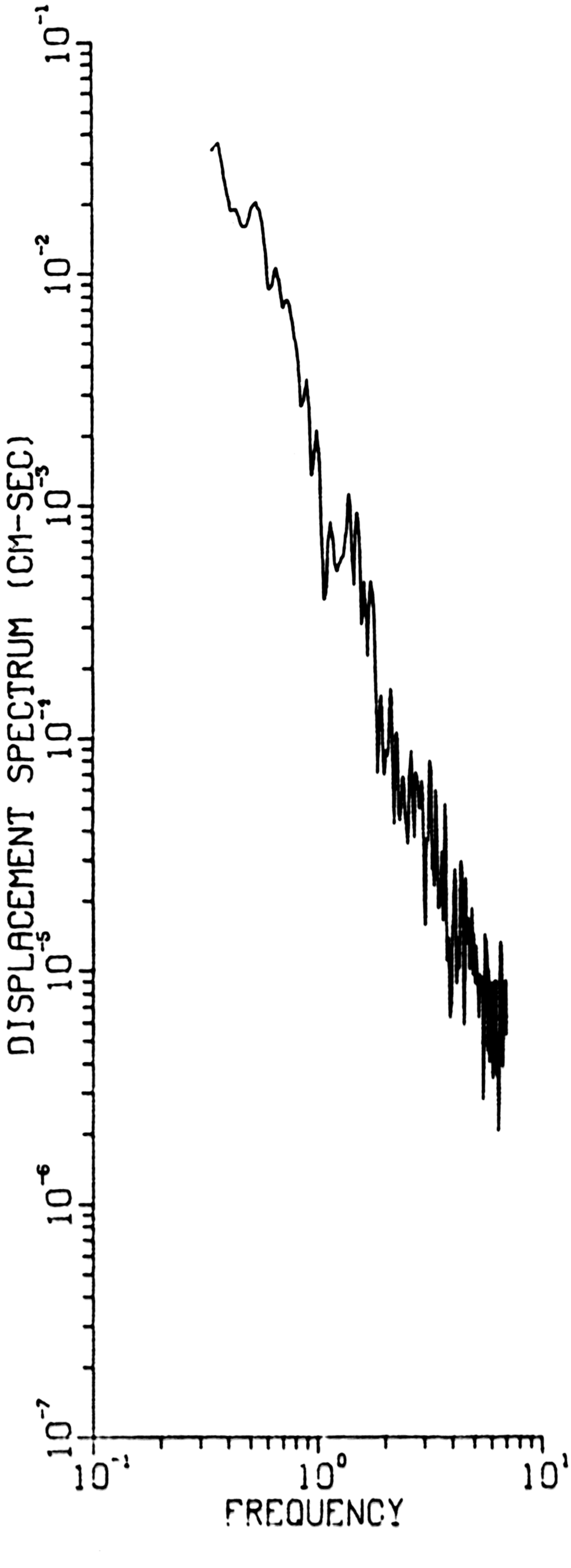

Figure B-38

Weston Geophysical

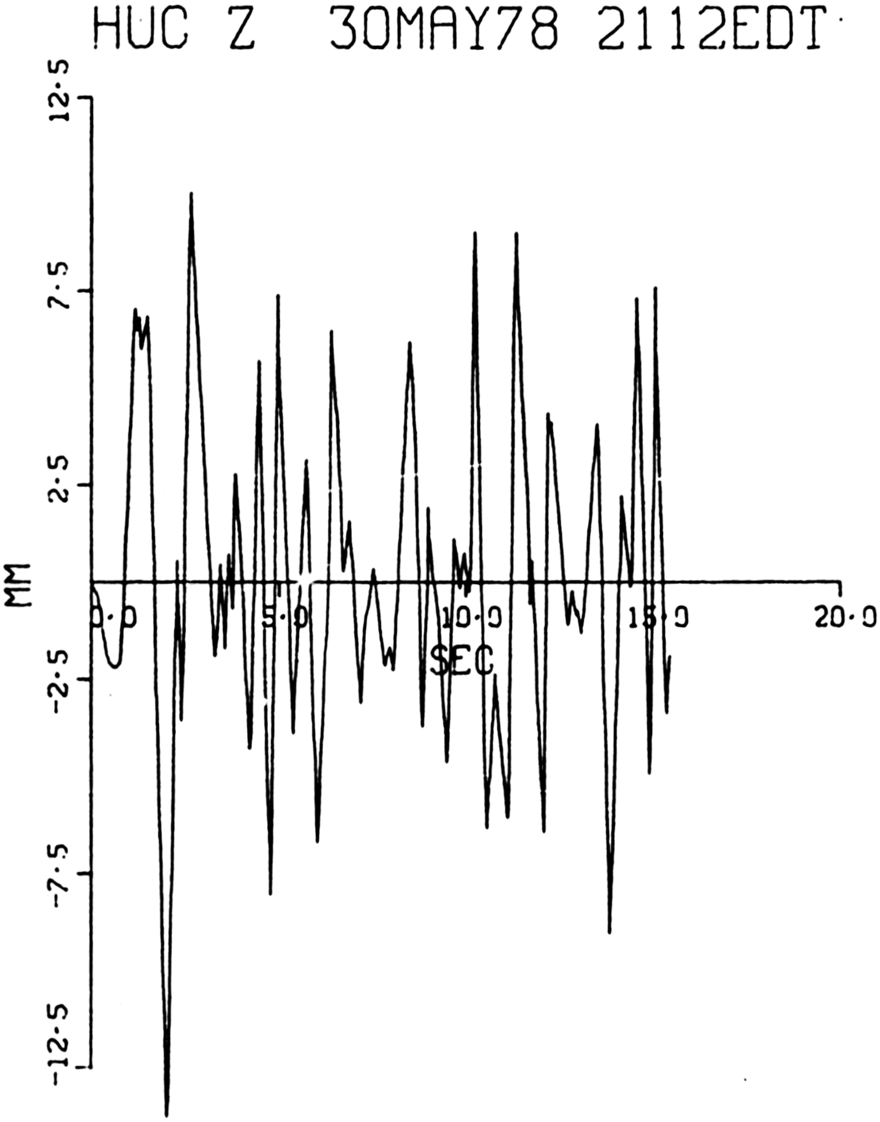
HUC Z 30MAY78 2112EDT
12.5
7.5
2.5
-2.5
-7.5
-12.5
MM
0.0
5.0
10.0
15.0
20.0
SEC

Figure B-39

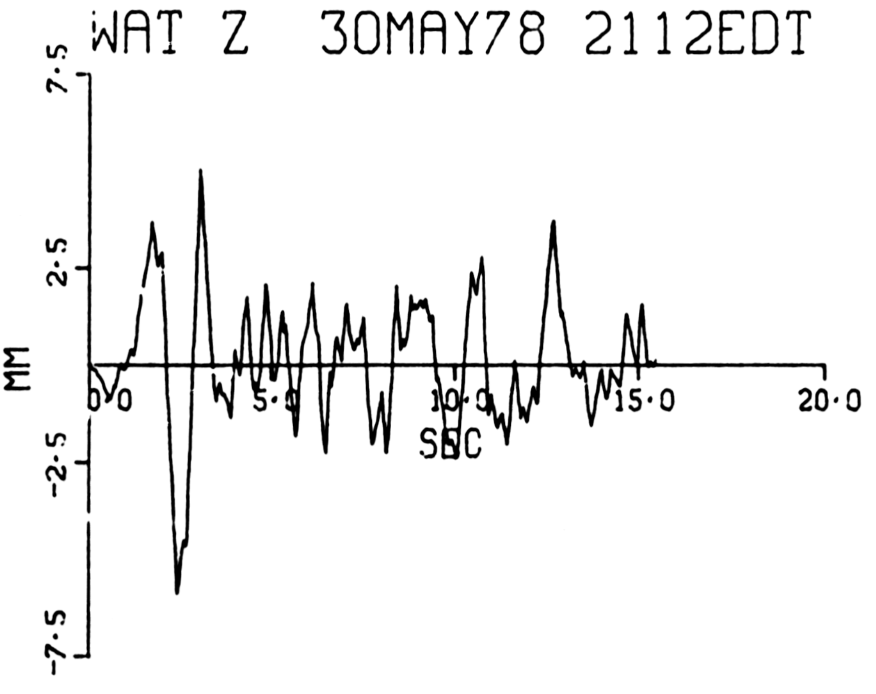

Figure B-41

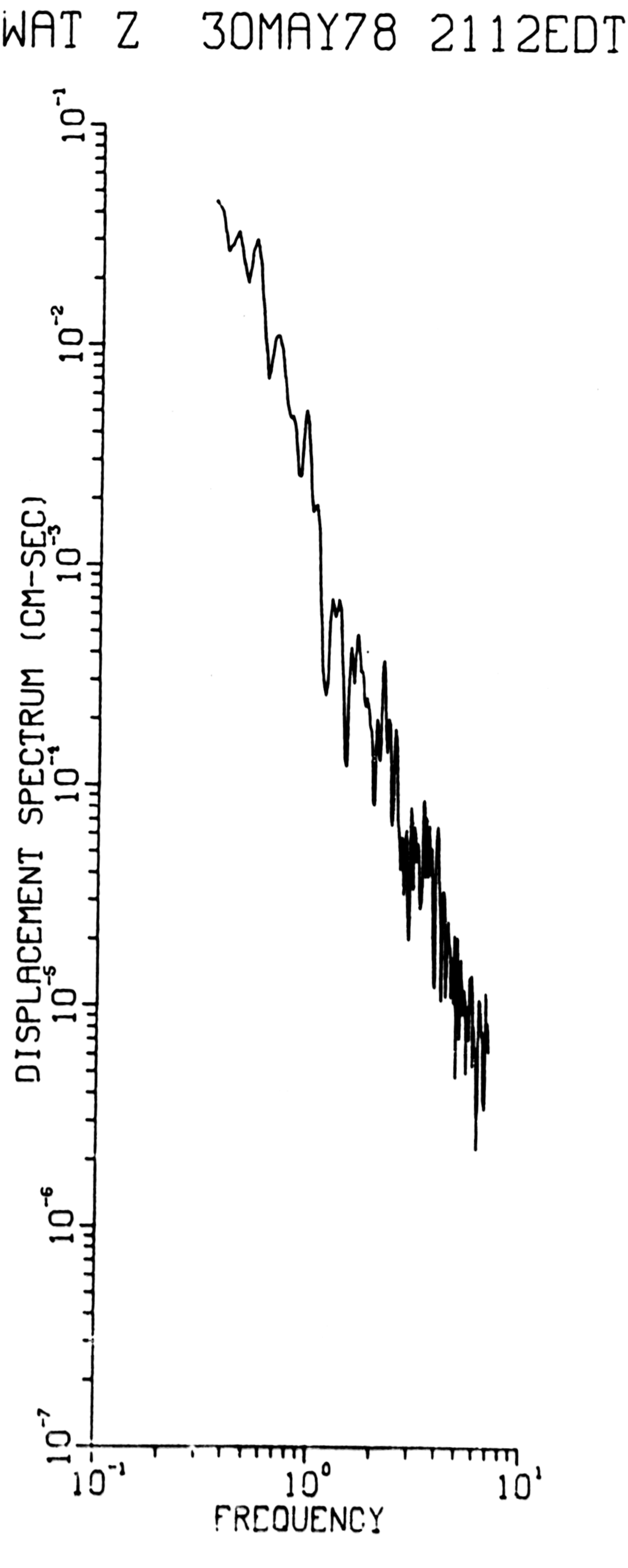

Figure B-42

Weston Geophysical

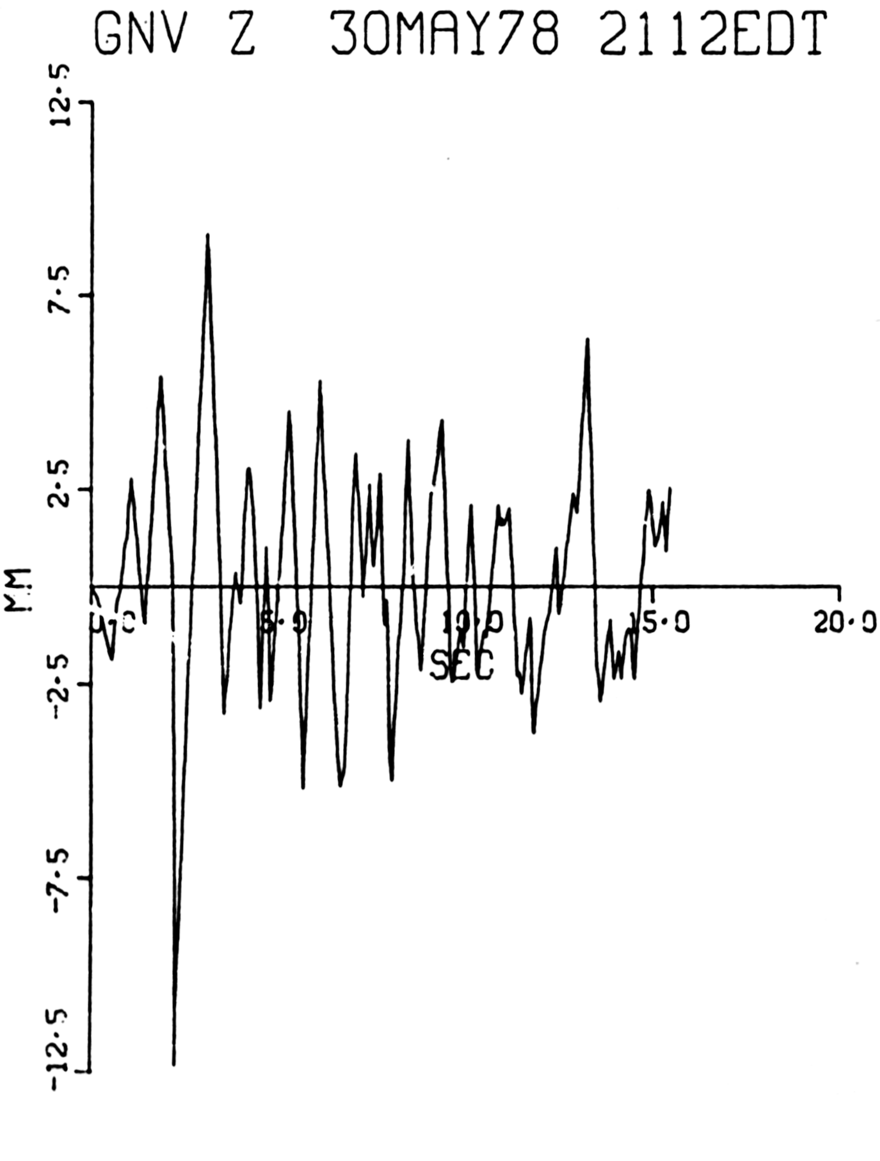
GNV Z 30MAY78 2112EDT
12.5
7.5
2.5
-2.5
-7.5
-12.5
MM
0.0
5.0
10.0
15.0
20.0
SEC

Figure B-43

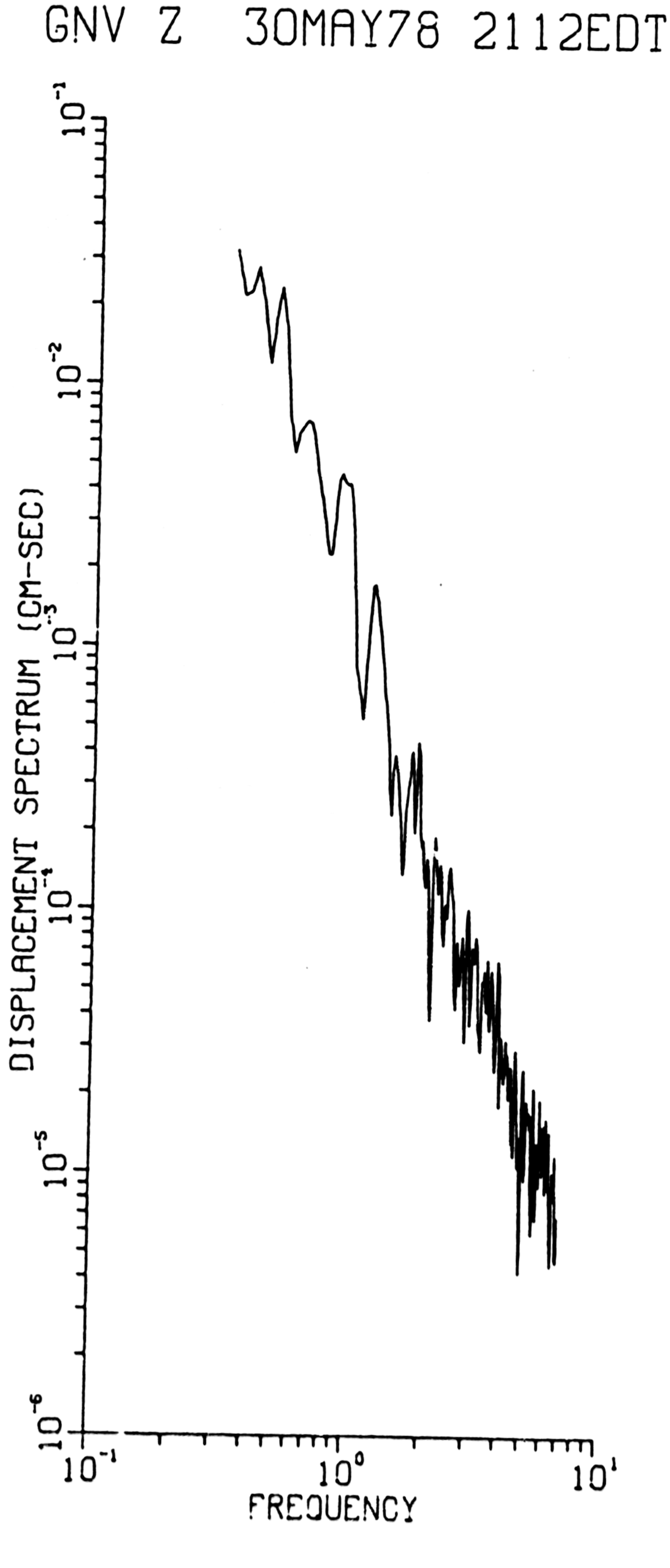

Figure B-44

Weston Geophysical

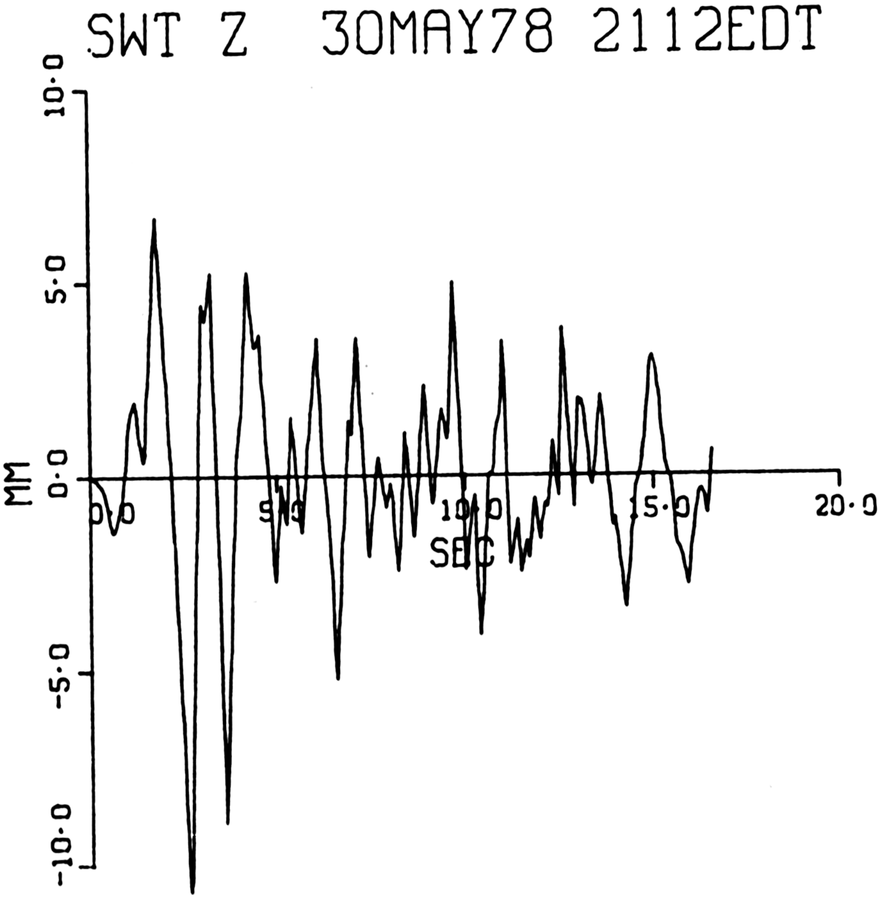

Figure B-45

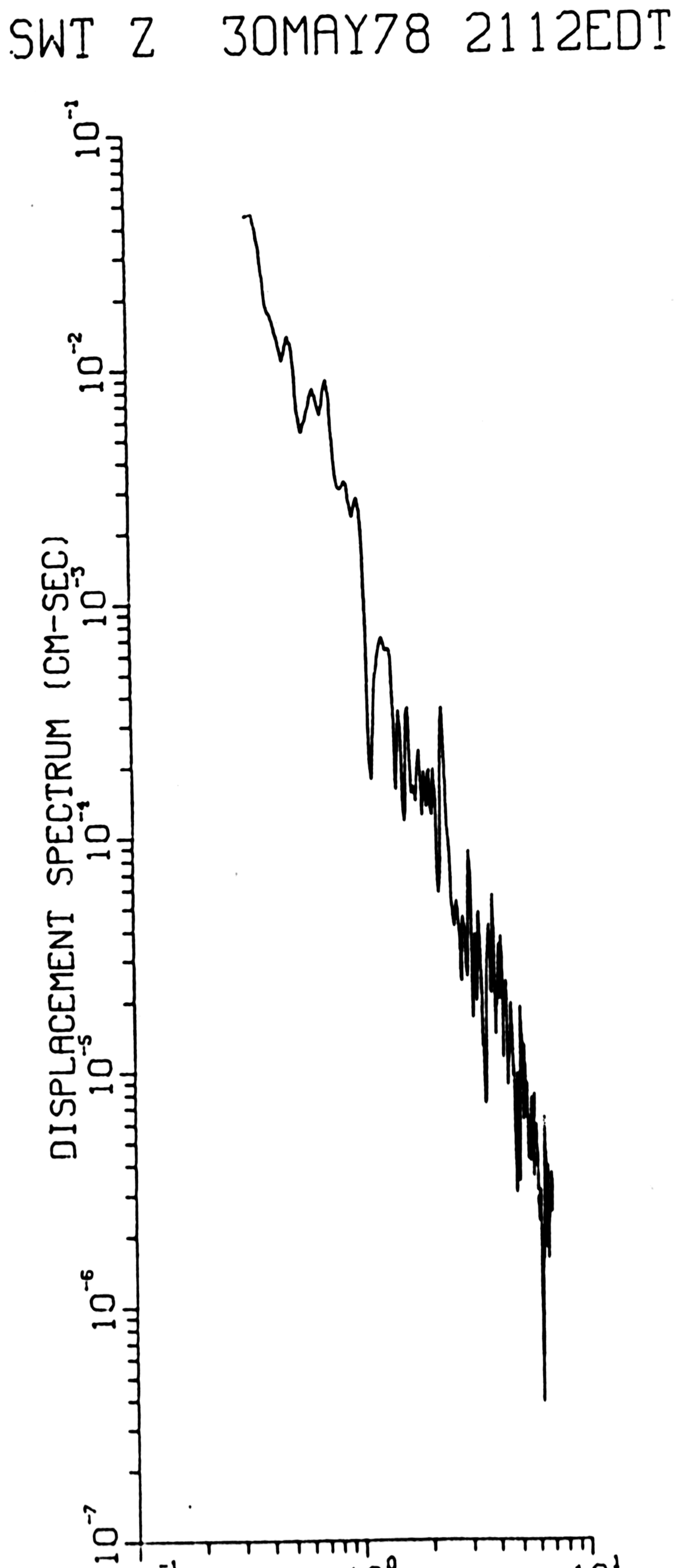

Figure B-46

Weston Geophysical

CLE Z 11JUL78 0824EDT

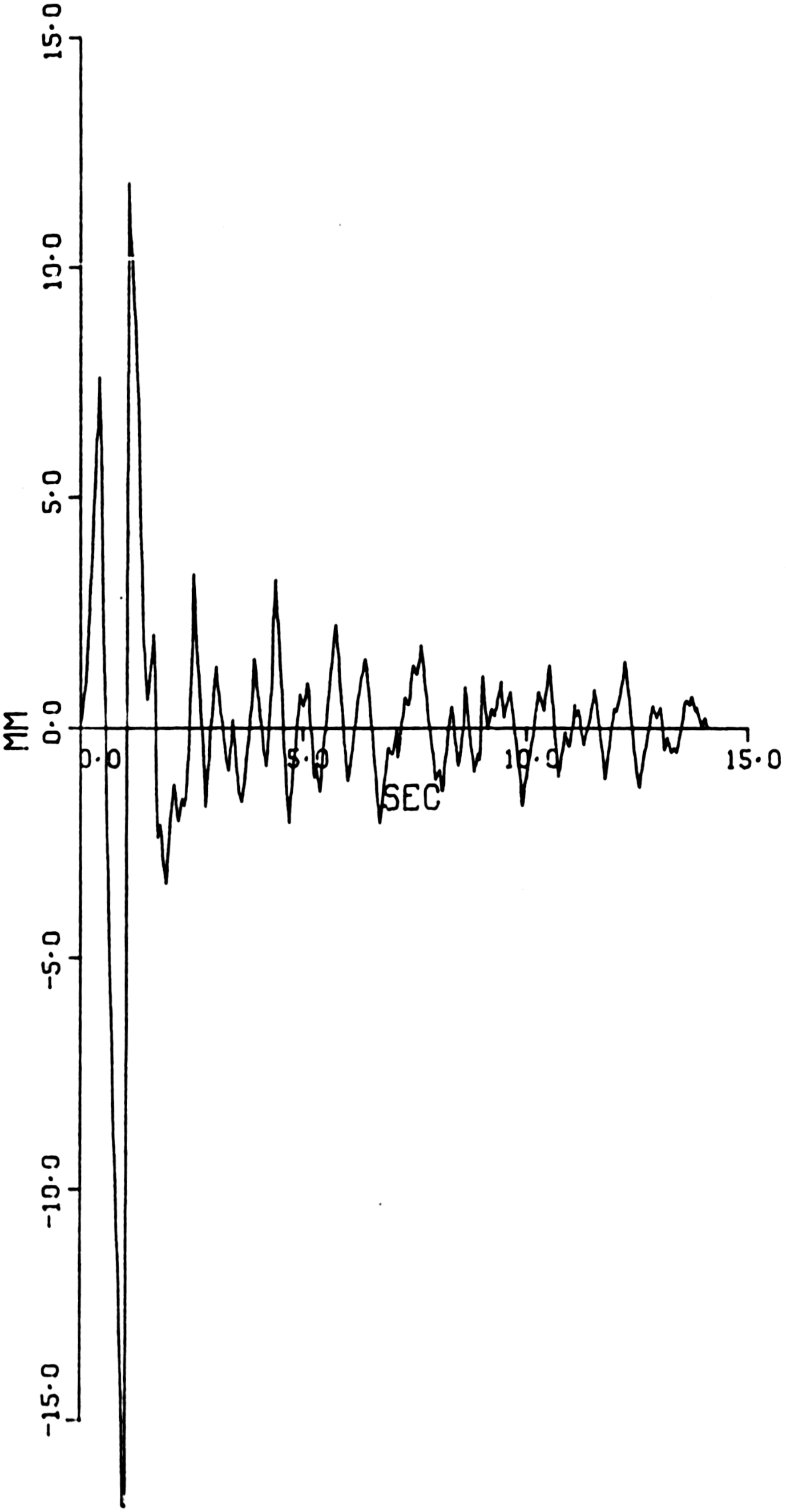

Figure B-47

Weston Geophysical

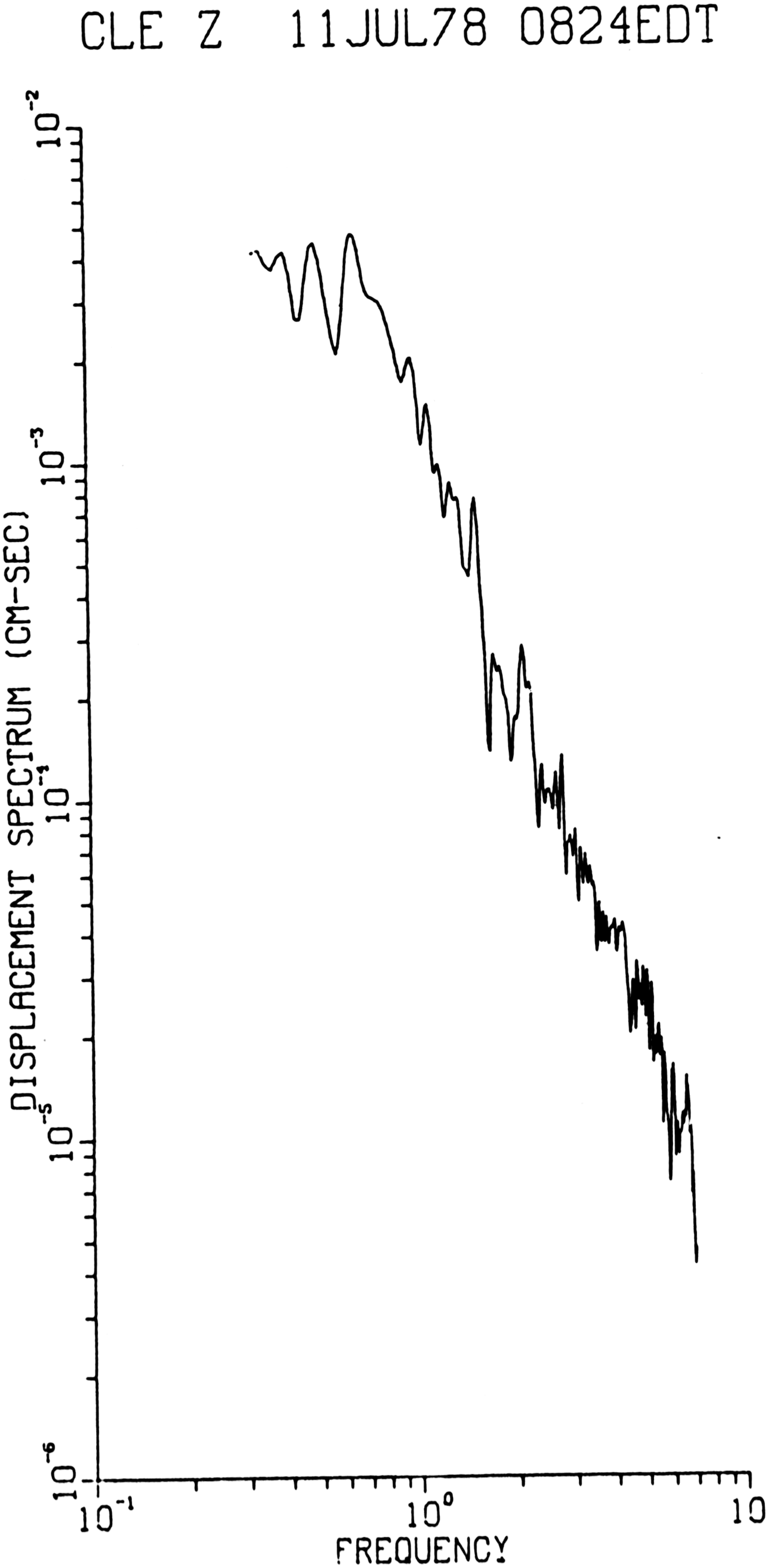

Figure B-48

Weston Geophysical

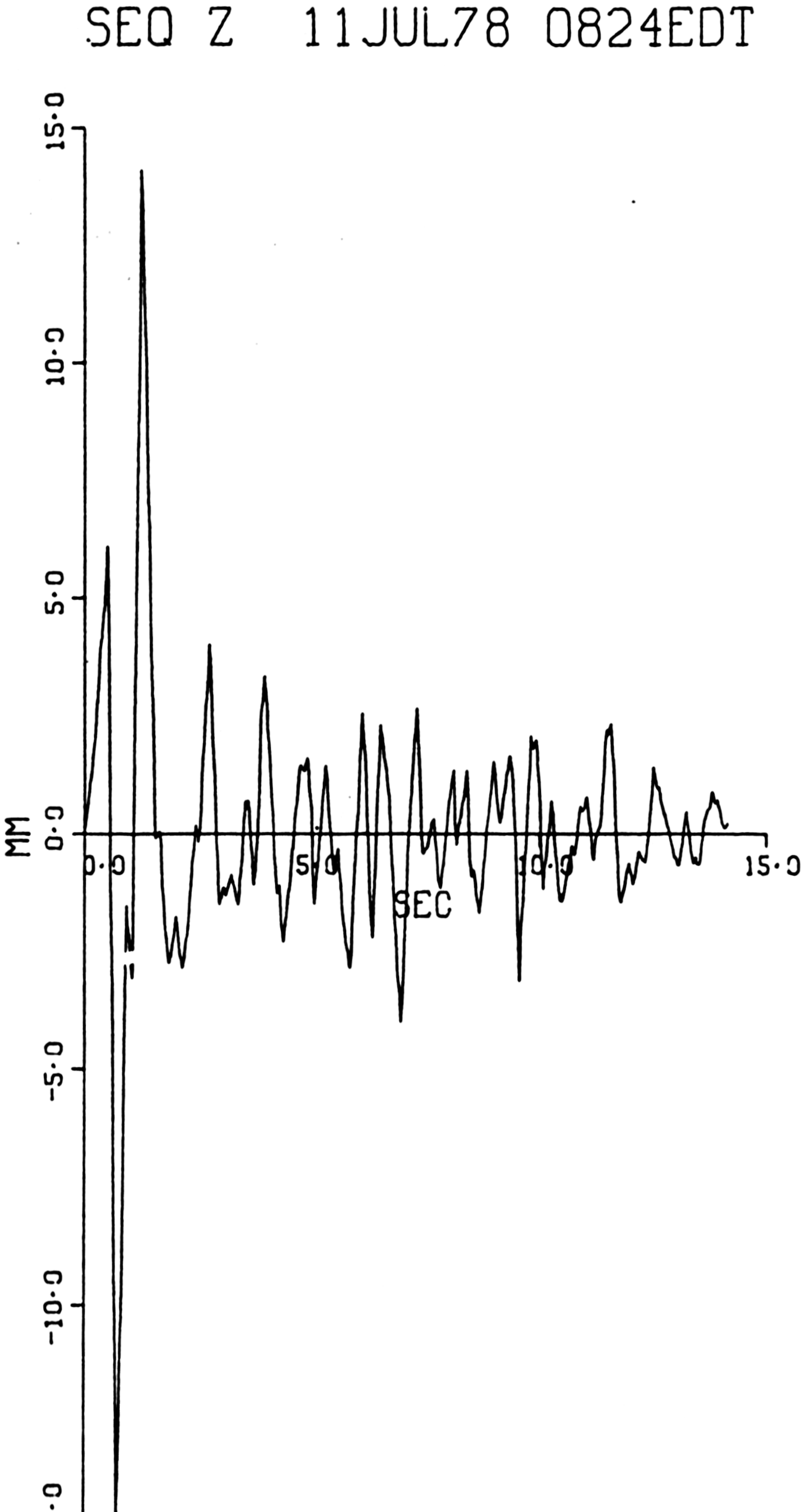
SEQ Z 11JUL78 0824EDT
15.0
10.0
5.0
0.0
-5.0
-10.0
-15.0
MM
0.0
5.0
10.0
15.0
SEC

Figure B-49

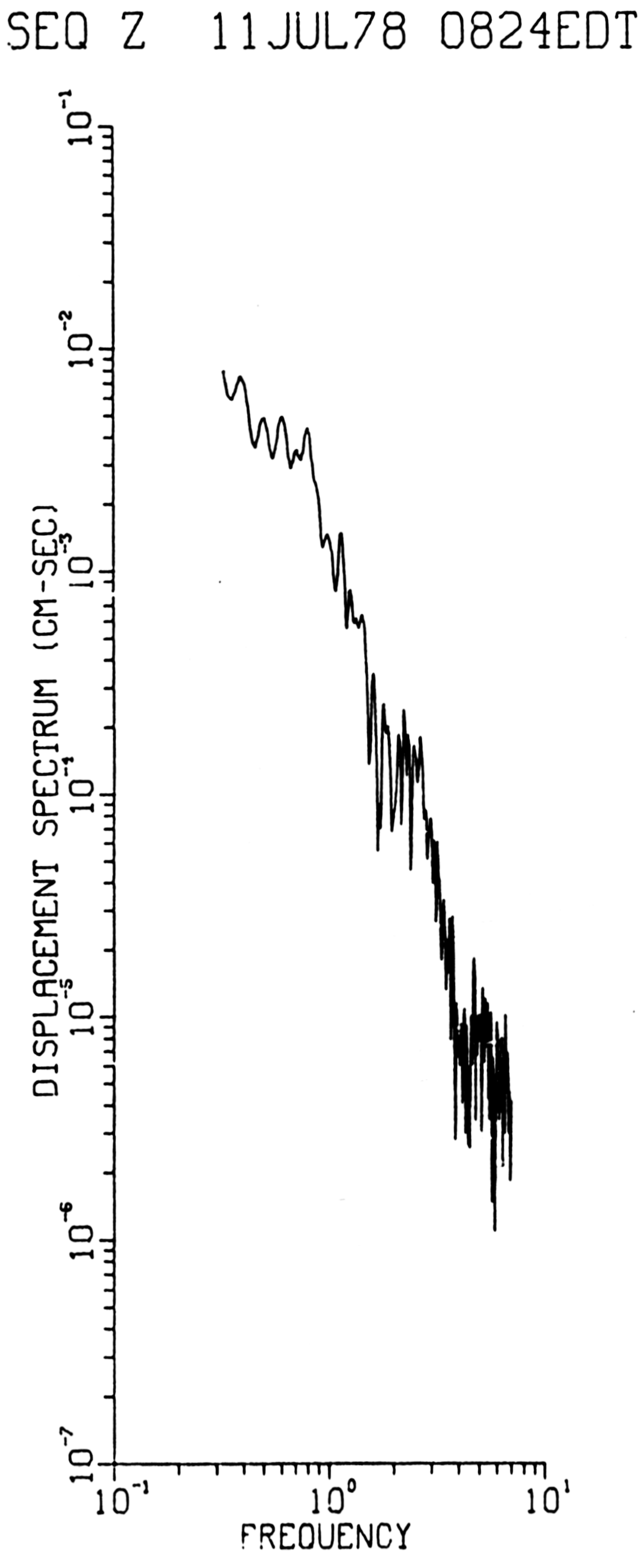

Figure B-50

Weston Geophysical

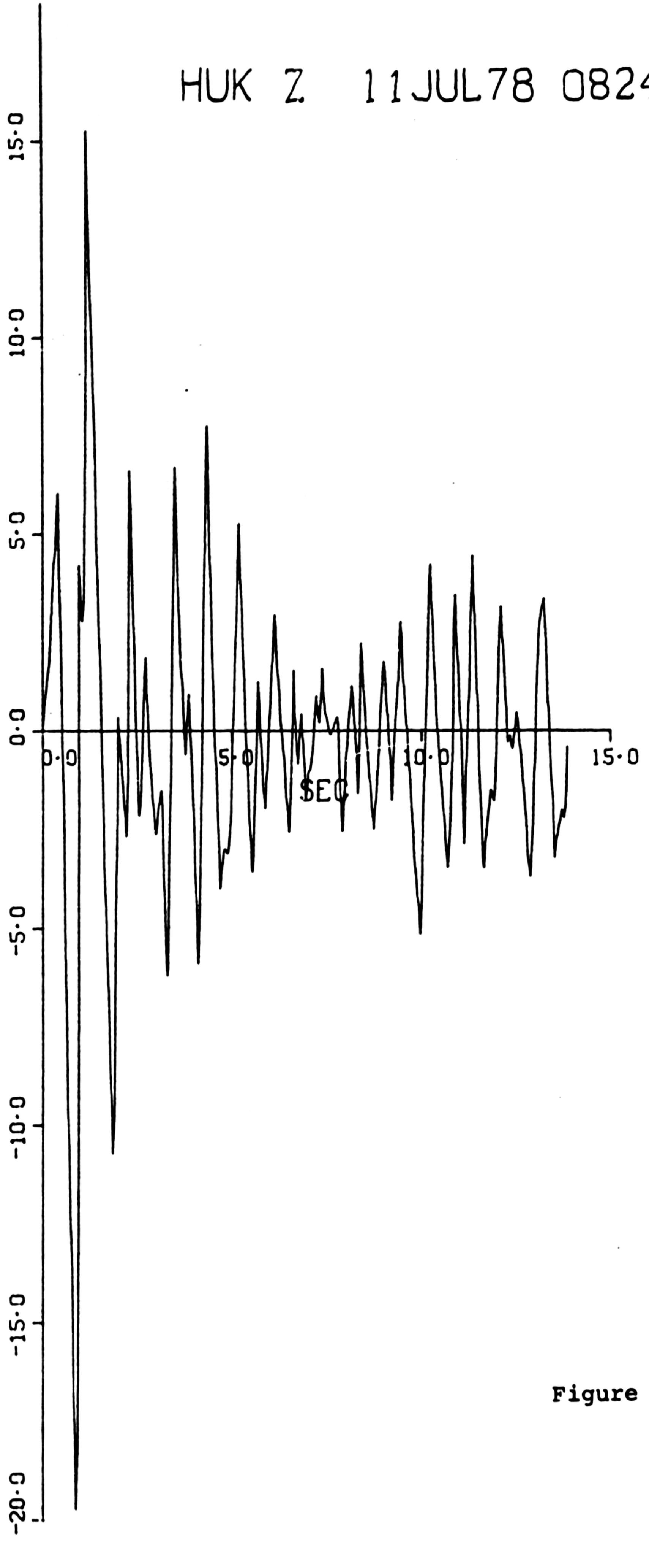
HUK Z 11JUL78 0824EDT
15.0
10.0
5.0
0.0
-5.0
-10.0
-15.0
-20.0
MM
0.0
5.0
10.0
15.0
SEC

Figure B-51

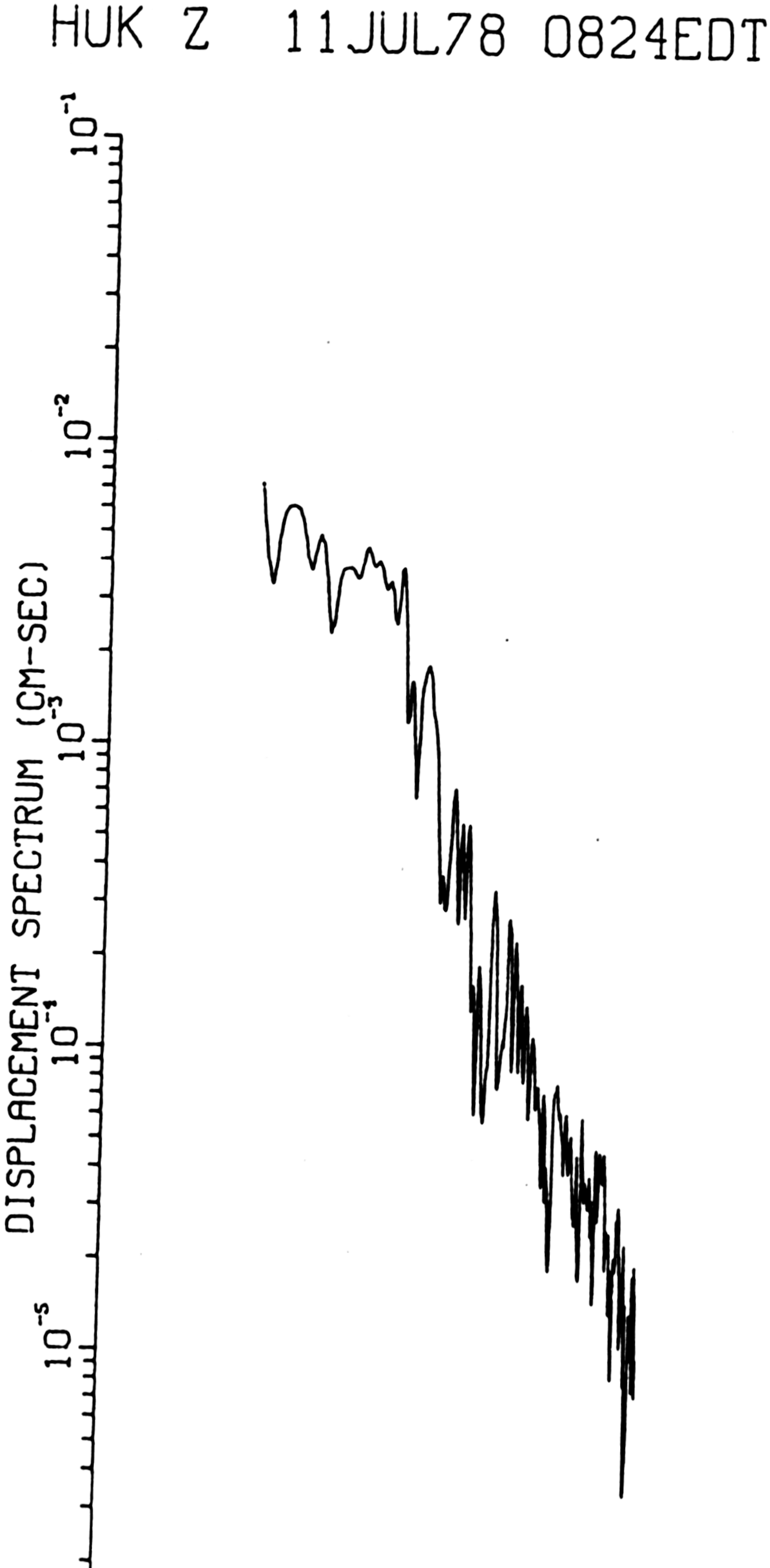

Figure B-52

Weston Geophysical

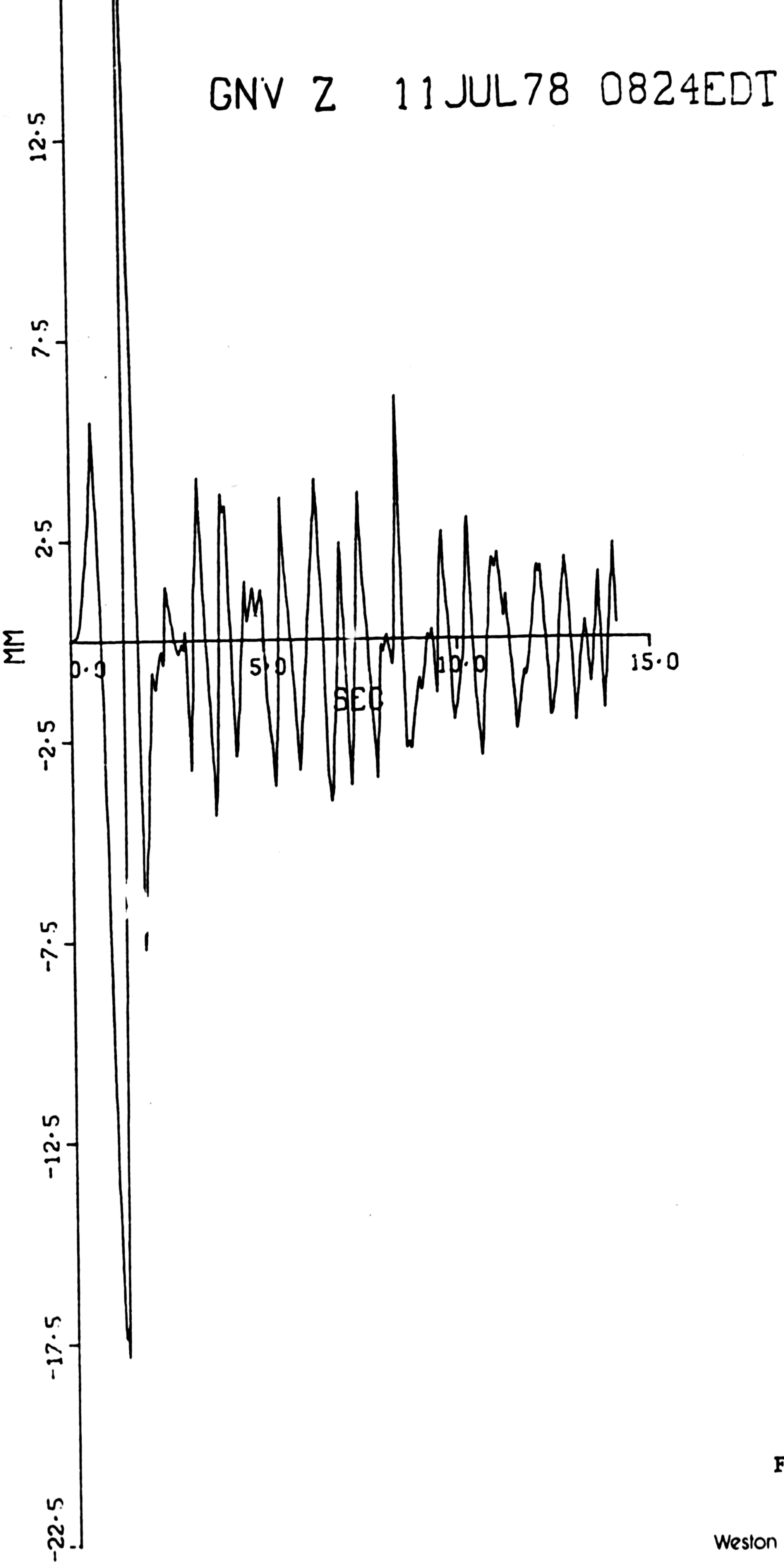

Figure B-53

Weston Geophysical

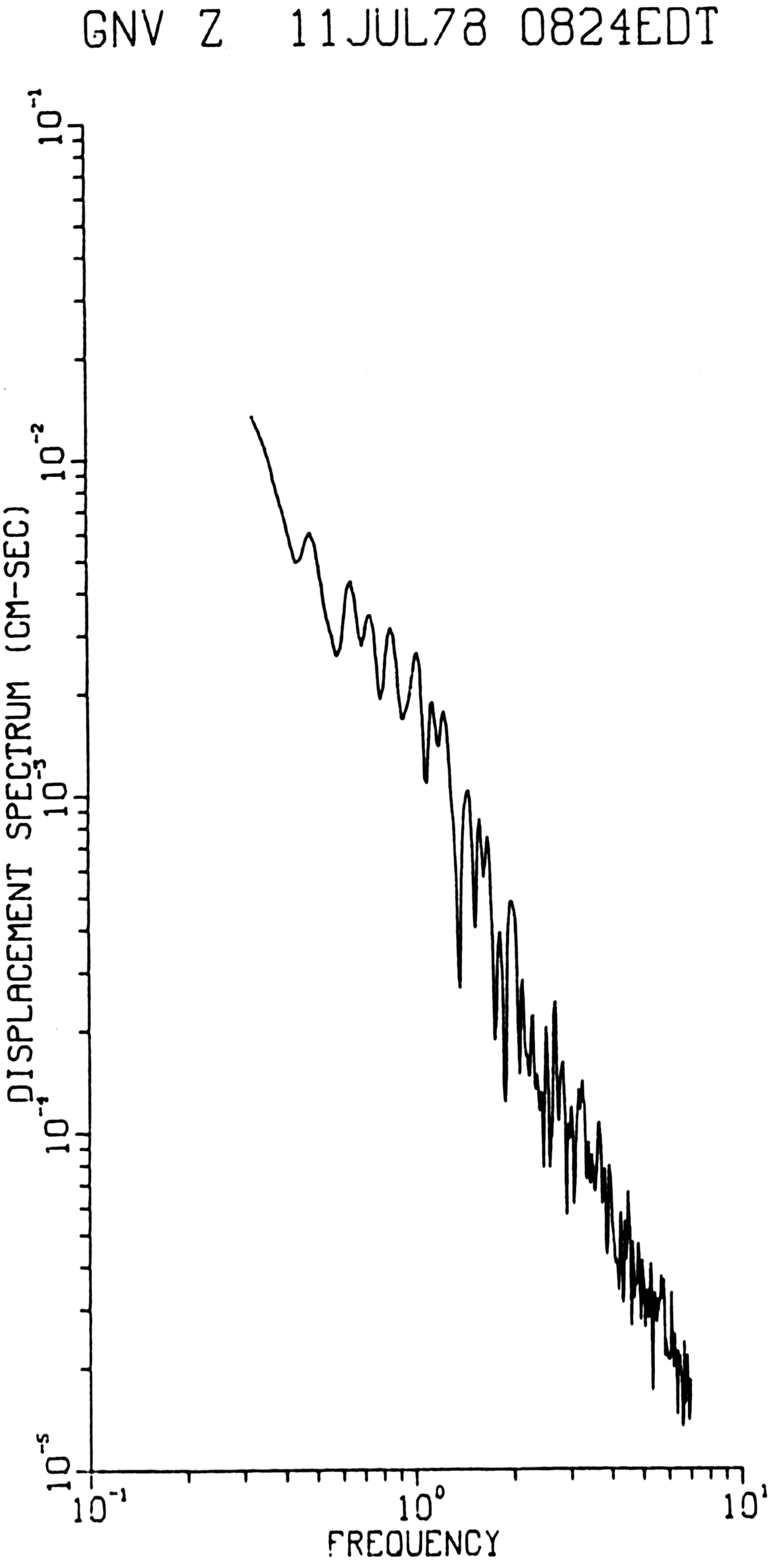

Figure B-54
Weston Geophysical

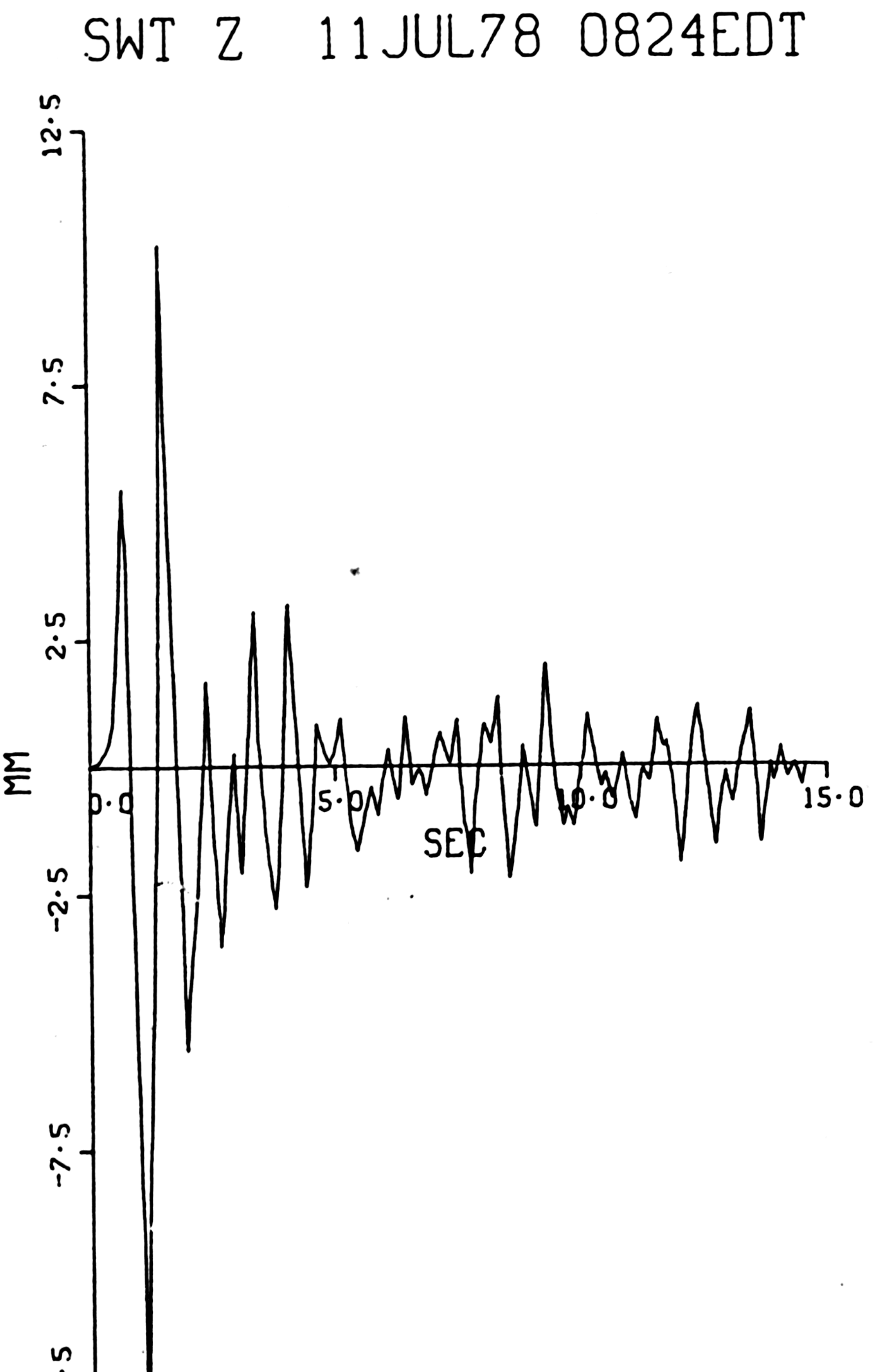

Figure B-55

In the time domain, the seismogram is the result of a series of convolutions:

$$r(t) = b(t) * az(t) * d(t) * h(t) * s(t). \quad (2)$$

In the frequency domain, the mathematical equivalence is a series of multiplied Fourier Transforms:

$$R(f) = B(f) \cdot AZ(f) \cdot D(f) \cdot H(f) \cdot S(f). \quad (3)$$

See Morse and Feshbach (1953) for relationships of time and frequency domains through Fourier Transformation. Considering that the instrumental response (S(f)) is known and can be corrected for, and that <u>for selected conditions</u>, azimuthal and attenuation effects, K(f), can be considered relatively constant or can be calculated, the source obviously being the same, it can be seen that seismograms recorded at various sites become representative of crustal effects at the respective sites, and that differences between site spectra are proportional to, and indicative of, the crustal effect:

$$R(f)_i \simeq H(f)_i \cdot B(f) \cdot K(f). \quad (4)$$

This explains why a spectral comparison of recorded signals can yield information on the local crustal response.

SITE SELECTION

The experimental procedure developed to study the relative ground motion response of six rock sites in eastern Tennessee included, as a primary step, the deployment of instruments at or near the Sequoyah nuclear power plant site. Ideally, seismic monitoring should have taken place on the actual rock foundation of the reactor site. Due to

09 JUNE 1978 19 14 (EDT)

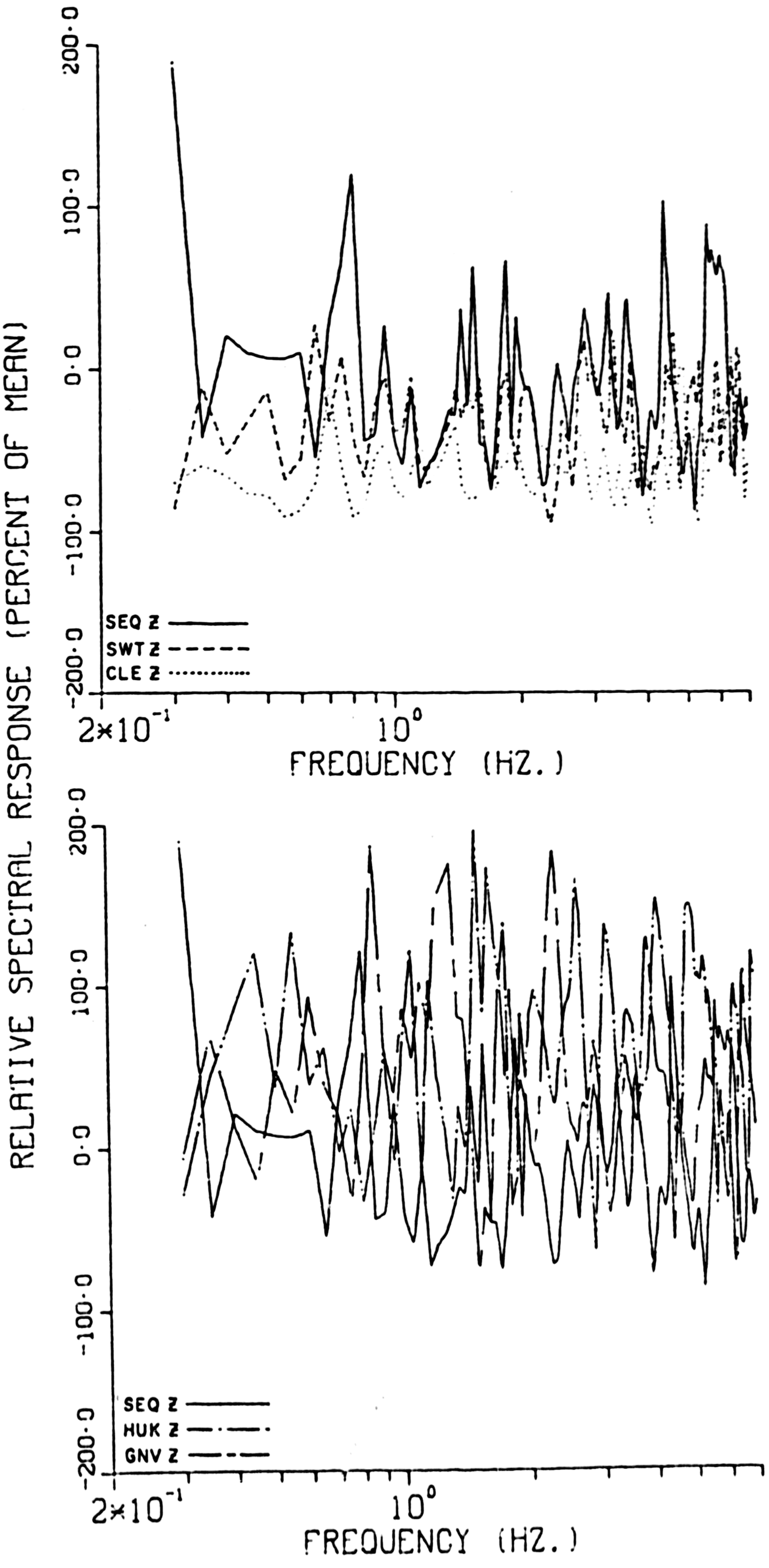

Figure 17

Weston Geophysical

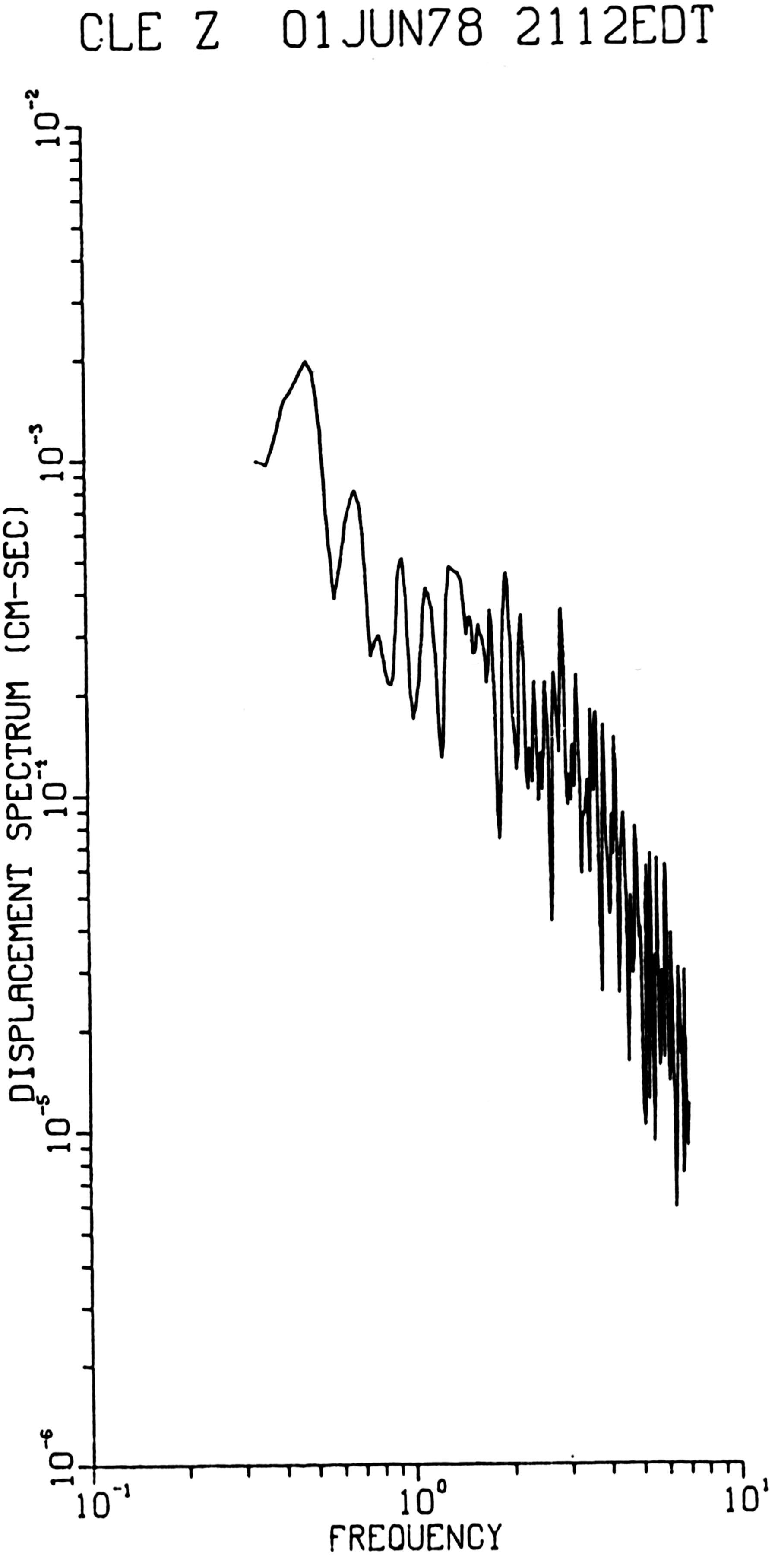

Figure B-12

Weston Geophysical

HUC Z 30MAY78 2112EDT

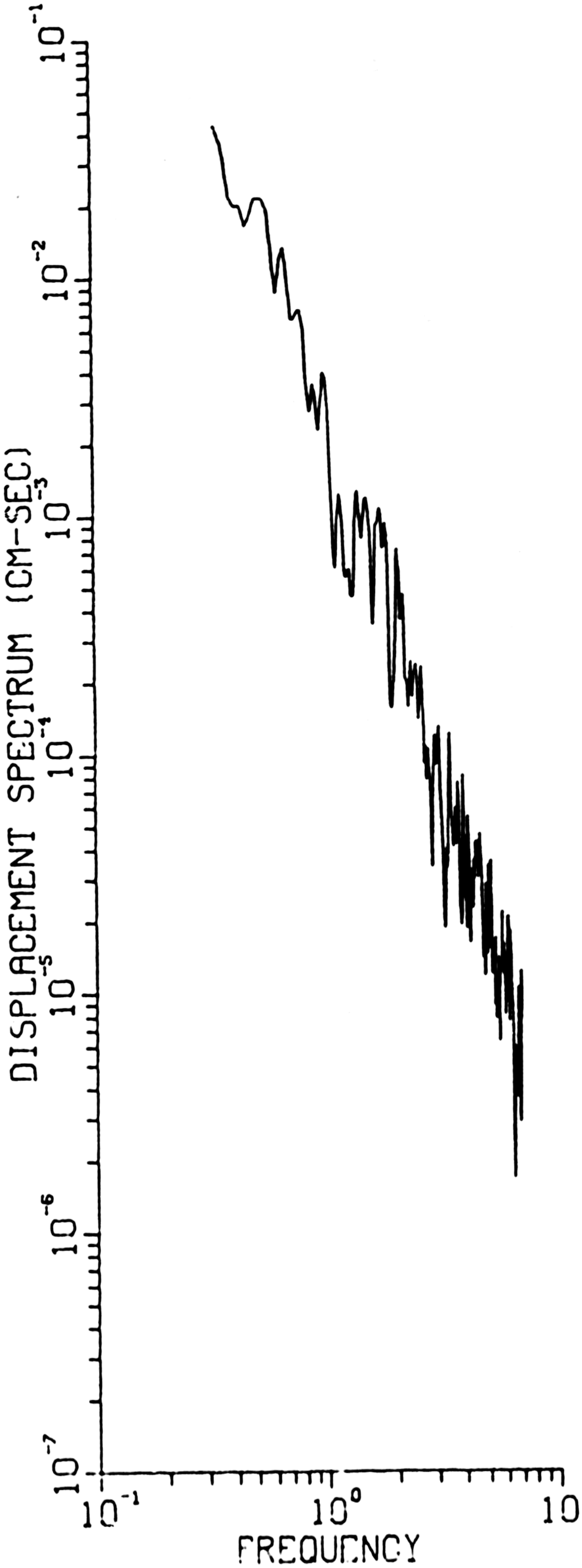

Figure B-40

Weston Geophysical

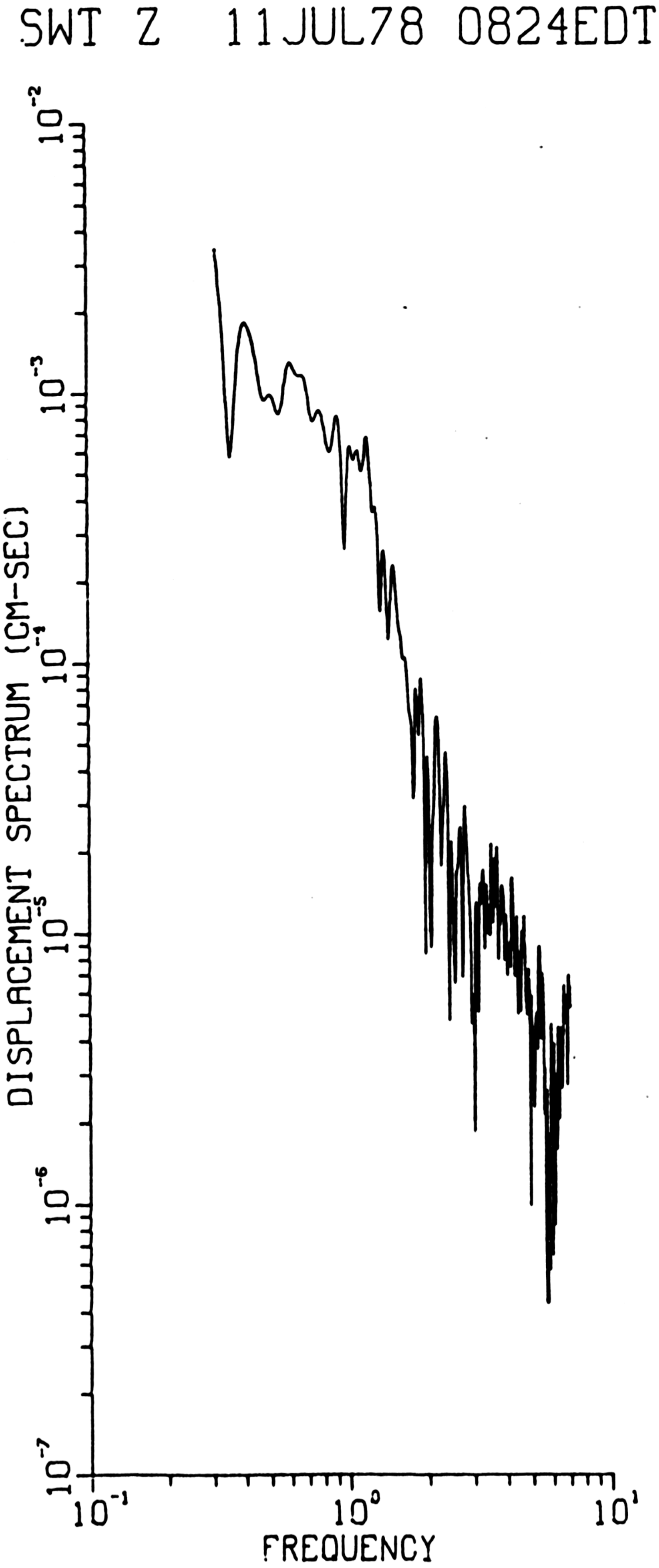

Figure B-56

Weston Geophysical